The first 3D structural model of an eukaryotic heteromeric aminoacid transporter

Primer model estructural en 3D d' un transportador heteromèric d'aminoàcids eucariota

Meritxell Costa i Torres

Departament de Bioquímica i Biologia Molecular
Facultat de Biologia
Universitat de Barcelona

Programa de Doctorat en Biomedicina
Bienni 2009-2011

"The first 3D structural model of an eukaryotic heteromeric aminoacid transporter"

"Primer model structural en 3D d' un transportador heteromèric d' aminoàcids eucariota"

Meritxell Costa i Torres

Barcelona, 2012

Departament de Bioquímica i Biologia Molecular
Facultat de Biologia
Universitat de Barcelona

Programa de Doctorat en Biomedicina
Bienni 2009-2011

Tesi realitzada als laboratoris del Parc Científic de Barcelona (IRB)

Memòria per a optar al grau de
Doctora per la Universitat de Barcelona

Presentada per
Meritxell Costa i Torres

Vist i plau dels directors,

Dr. Manuel Palacín Prieto Dr. Albert Rosell Febres

L´interessada,

Meritxell Costa Torres

Barcelona, 2012

PhD “The first structural model of an eukaryotic heteromeric aminoacid transporter”

by Meritxell Costa Torres, Barcelona 2012.

Covert “When science meets art”. Created and designed by Meritxell Costa Torres (MEP).

Original idea by Prof. Manuel Palacín Prieto.

A Jose David Gallardo García,

Por siempre apoyarme,

Escucharme

Y permanecer a mi lado pase lo que pase

Gracias

and…

Joaquima
Jordi

Els meus "papas científics". Vosaltres hem vau ensenyar la ciència quan jo acabava de sortir de la carrera

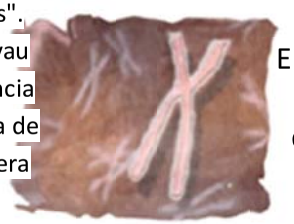

Maria (la primera FISH de la meva vida)
Javier (geni de photoshop), Ana, Pedro,
Cristina (mapaches... help!), Jorge, Angels...

Mai oblidaré tot el que vaig aprendre a Reprogenetics

Elsa
Albert
Lidia

Els quatre vam viure una aventura a la ciutat dels gratacels...Elsa, recuerdas las incursiones al Western beef y a la tienda de Lindt ?

Santi
Mercedes

…y familia gracias por hacernos reir tantas veces y ser nuestra familia en Nueva York

Tim (the number one),
Piedad
Pere (ese Monster Sushi!!)

Gracias todos!

Montse

Mi padawan que superó a la maestra... cuantos cromosomas hemos contado tu y yo. Ahora tienes una carrera impresionante y una bebé preciosa!

Manel

Quantes Nawrotades tenim per explicar! Gràcies a tu, vaig descobrir el que es treballar en un sincrotró i menjar fondie (també alguna pita) a Grenoble.

Esteve (genials les classes de logopèdia)
Pep (sempre ensenyant "la pota")
Nuria (les incorruptibles al SAF)
Merce C (compañera sincrotronera)
Ramon (el senyor dels liposomes)
Joan (aquesta senyoreta ja es doctora!)
Elodia (que harian sin ti!)
Mercedes Y (super-organizadora!)
David (parlant de joc de trons...)
Meritxell (WoW! XD)
Julia (històries simplement increibles!)
Mireia, Montse, Meritxell, David, Guio...

Pierrick

What a moments in "La momie folie" and runing away from "the crazy rabbits", just unforgettable

Alberto, Geraldine, Raph/Marie
Thank you for all

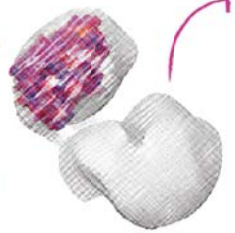

Manuel Palacin Jamás había conocido antes a nadie como tu. Siempre cinco pasos por delante... Para mi siempre vas a ser mi referencia científica. Gracias por haberme dado la oportunidad de aprender y disfrutar en tu laboratorio!

Albert
albertus, mi "veterano miniboss". Tengo tanto que agradecerte que no podría hacerlo en un folio tan pequeño. Por suerte tu ya lo sabes. Siempre has apostado por mi, y lo mejor es que puedo tener el orgullo de llamarte AMIGO. Gracias nen!

Dimitri Gracias por esos tres meses y el modelo! Una nueva etapa me espera en Berna. Thank you for all.

David "el becari"
Ens fem cantants tu i jo? Ja ja
Gràcies per ser tan macu i bon amic
Edi... ahora i siempre, el adorable chulito number 1

Lukasz the hero! Now in Asutralia

Monas chulito 2 jaja

Montse
doctora romero, que decirte..
gracias por aconsejarme en este laaaargo camino
y gracias por protegernos del.. MICOPLASMA!

Nachete
tus historias siempre hacen que la hora de la comida sea una fiesta! Gracias por todo tu apoyo!

Elena la meva compi in "the yeast team". sempre cuidant de tots, llargs experiments de purificació i compenetració perfecte. Quin equip! Vals moltíssim guapa.

Miriam
Boliwood, cata de vinos, danza del vientre...
Eres una artista toda tu y además una maravillosa persona! Gracias por todo Mirims!

Paola
mi valiente y maravillosa italiana. Porque tú siempre has estado ahí "transportando" y ayudandome. Muchísimas gracias

Merce
La noia que va estar a Bassel i va domesticar AdiC en 2D
Ets un "coco" noia! Les teves idees sempre m´han maravillat. Merci!

Gonzalo
Yo ya se que lo tuyo es hacer cerveza!
Si en el fondo trabajar con levaduras es lo mejor! Gracias por tus enseñanzas!

Susana Bodoy
encara pensarà la gent que som germanes? jeje gràcies per tot

Susana Bial
La reina dels clonatges!

Jordi
sempre tocant a trompeta. Visca el nostre Music Man!

Aike cloning heterodimers? in Pichia? Brave!

Natalia M
competent i divertida!
Gracies guapa!

Jessica
Gràcies per ser tan bona
Jess. Treballadora i dispossada a donar-ho tot. Para mi brillas como una estrella!

Judith "la Ju"
Mi fiestera e inquieta amiga,
contigo me lo paso siempre pipa
y se que eso no cambiará estemos en el país que estemos! gracias linda!

Maribel
esas conversaciones sobre "atravesar el charco"... inolvidable

Dr. Sebas
He disfrutado mucho robándote la silla, el boli... sobretodo
gracias por tus chistes increibles

M Angels Sigue siempre así por favor! Divertida y resalá
Cualquier día aparece un... bombero!

Juan Pablo "el JP"
científco brillante y... lector de comics!
la mejor combinación del mundo

Txell Anims nena! que tot acava.

Natalia "Natimaus"
Siempre animandome y con un caramelillo cerca para devolverme la energía!

Manu
gràcies per ser tan dolça. No canviïs mai!

Arturo cada vez más desbocado ya ha entrado en el grupo "chulito"
gracias por ser el mejor compi de ordenador! suerte Arturito!

Laia incorregible! ets la mijor!

seLuis
acias por los brain stromings!

Eva
Illuitadora i a més a més...
rolera! ay! si ho hagués sabut ja ja

Ekaitz pescador y"caçador de bolets" algo mejor?
a ti te va a salir cualquier cristal que se ponga delante
Y si no, se va atener que enfrentar a las consecuencias! Gracias por todo neng!

Ana O Hacer mariposas de cristal es más que especial. Y de colores! Sigue así!
Con constancia todo acaba saliendo!

Olga tant glamour junt... a veure si al final vindrà el Cloney de veritat!

Yuliana
seguidora de series... tu si que sabes lo que vale la pena!

Xevi gràcies per les converses socio-polítiques-revolucionaries
encara tinc llibres que et podria deixar!

Joana nena! escrius com els angels, agafa la ploma i vinga! Merci per tot!

Marcel
thank you for make me laught in the lab and all the coffees in the canteen!
I never will forget the time in Bern!

Ana la más rápida del laboooo
Saska nuestra glamurosa eslovena... fan del deporte! sigue así!
Jana suerte en todo!!

Antonio Zorzano nunca dejarás de sorprenderme con tus ideas!
Gracias Antonio

Pero como podemos ser tantos? Espero no haber olvidado a nadie, y si lo he hecho espero que me perdone… simplemente GRACIAS A TODOS!!!

Ricardo, Victoria y Ricardo Jr.

Que largo ha sido verdad? pero al fin acabo esta etapa.
Quiero que sepais que hubiera sido imposible sin vosotros.
gracias por acompañarme ahora y siempre. Os quiero

Jose

Simplemente eres tú el que me has escuchado día tras día, aconsejado, animado, ayudado, acompañado... y hoy sigues ese viaje conmigo...

Gracias

M.E.P.

mi compañera de viaje,
juntas conseguiremos todo lo que nos propongamos!
Gracias por estar siempre a mi lado!

Marta, Eva Cro, Evita , Nurieta

Pero cuantos años hace ya que nos conocemos?
Ha sido un largo camino, desde que comenzamos la carrera de biología hasta que todas conseguimos el doctorado, conmigo encabezando la cola (solo por unas horas) ja ja ja
Nos hemos visto crecer y avanzar, siempre apoyandonos las unas a las otras sin dudarlo. Hemos pasado juntas por momentos increibles, momentos divertidos, momentos dificiles,
y aquí seguimos, avanzando y superándonos.

Gracias chicas, estemos donde estemos siempre juntas!

Antonia

Como te quiero tía Toni. Gracias por esos cafés!

Ascension, Antonio, Toñi, Benito, Merce

Gracias por cuidarme tanto y el apoyo recibido. Sobretodo el Papo y la Moma que son lo mejor de lo mejor.

Raul, MariCarmen, Laura, Maria y Alicia

cuantas cosas os he explicado verdad? Pues aun quedan jaja
Laura te agradezco la energía que me has pasado.
Y Raulete... bueno, simplemente eres tú. Gracias

Thanks…

Summary

4F2ed: *Heavy subunit 4F2 ectodiminum*

4F2hc: *Heavy chain 4F2*

Ab: *Antibody*

AGT1: *Aspartate and Glutamate Transporter-1*

APC: *Amino acid Polyamine organocation transporter family*

ArpAT: *Aromatic Preferring Amino acid Transporter*

Asc1: *System asc amino acid transporter-1*

Asc2: *System asc amino acid transporter-2*

B^{0+}AT: *System b0,+ amino Acid Transporter*

BCCT: *Betaine-choline-carnitine transporter family*

BM: *3-(N-maleimidylpropionyl) biocytin*

BMGY: *Buffered Glycerol-complex medium*

BMMY: *Buffered Methanol-complex medium*

CD98: *4F2hc*

cDNA: *Complementary DNA (from a RNA sequence synthetized from a retro-transcription)*

COS cells: *Cercopithecus aethiops, origin-defective SV-40*

cpm: *Counts per minute*

cRNA: *Complementary RNA*

DMEM: *Dulbecco's Modified Eagle's Medium*

DMSO: *Dimetilsulfoxide*

DNA: *Desoxirribonucleic acid*

dNTP: any desoxinucleotid

ER: *endoplasmatic reticulum*

et al.: *lat. "and co-workers"*

CMC: *Critic micellar concentration*

DLS: *Dinamic light scattering*

DDM: *Dodecyl-ß,D-maltoside*

DTT: *Dithiothreitol; (2S,3S)-1,4-bis(sulfanyl)butane-2,3-diol)*

EK: *Enterokinase*

EM: *Electron microscopy*

EpCAM: *Epithelial Cell Adhesion Molecule*

ESRF: *European Synchrotron Radiation Facility*

FPLC: *Fast performance liquid chromatography*

GFP: *Green Fluorescent Protein*

HATs: *Heteromeric amino acid transporters*

HRP: *Horseradish Peroxidase*

ICAM: *Intercellular Adhesion Molecule*

Kb: *Kilobases*

KDa: *kilodaltons*

KM: *Constant of Michaelis-Menten*

KO: *knock-out*

KSHV: *Kaposi´s sarcoma associated herpesvirus*

LAT1: *L-type Amino acid Transporter-1*

LAT2: *L-type Amino acid Transporter-2*

LAT3: *L-type Amino acid Transporter-3*

LAT4: *L-type Amino acid Transporter-4*

LB: *Luria Broth* Medium

LPI: *Lisinuric Protein Intolerance*

LSB: *Laemmli Sample Buffer*

MCT: *Monocarboxylate transporter*

MD: *Molecular dinamics*

MDCK: *Madin Darby canine kidney Dog*

MLV: *Multilamellar large vesicles*

MW: *Molecular weigh*

NCS-1: *Nucleobase cation symport 1 family*

NEM: *N-ethyl maleimide*

NS-TEM: *Negative Stain- Transmission Electron Microscopy*

NSS: *Neurotransmitter solute symporter family*

OD: *Optical density*

OG: *n-Octylglucosdide*

OLV: *Oligolamellar large vesicles*

ON: *Over-night*

PA: *Phosphatidic acid*

PBL: *Pig brain lipids*

PBS: *Phosphate Buffered Saline*

PC: *Phosphatidylcholine*

PCR: *Polimerase chain reaction*

PDB*: Protein Data Bank*

PE: *Phosphatidylethanolamine*

PG: *Phosphatidylglycerol*

PI: *Phosphatidylinositol*

PIAs: *Primary inherited aminoacidurias*

PS: *Phosphatidylserine*

rBAT*: Related to bº,+-amino acid transporter*

RT: *Room temperature*

SAXS: *Small angle X-ray diffraction*

SCAM: *Substituted Cysteine Accessibility Method*

SDS-PAGE: *Sodium dodecyl sulfate polyacrylamide gel electrophoresis*

SEC: *Size exclusion chromatography*

SLC: *Solute Carrier Family*

SP-NS: *Single Particle-Negative staining*

SSS: *Sodium solute symporter family*

SUVs*: Small unilamellar vesicles*

TM: *Trans membrane*

Thr: *Thrombine*

ULV: *Unilamellar large vesicle*

Vmax: *Maximum velocity*

xCT: *x-c type Cystine / Glutamic Acid Transporter*

y+LAT1: *System y+L Amino acid Transporter-1*

y+LAT2: *System y+L Amino acid Transporter-2*

YPD: *Yeast Extract Peptone Dextrose Medium*

Introduction

1. Membrane proteins and amino acid transporters

According to the results of various genome projects, up to 30 % of proteins encoded by eukaryotic cell are membrane proteins. Some of those proteins are bounded to the membrane surface (peripheral membrane proteins), whereas others are buried within the membrane (integral membrane proteins) (Wallin and von Heijne, 1998) and perform a wide range of biological functions including respiration, signal transduction and molecular transport. Inside membrane proteins group, amino acid transporters are essential for the absorption of amino acids from nutrition, mediating the interorgan and intercellular transfer of amino acids and the transport of amino acids between cellular compartments. Those proteins help to the maintenance of ionic concentration or flowing nutrients, providing amino acids to all tissues of the body (Reviewed by Palacín and Broër. 2011). Amino acids are the base for the protein synthesis and also play an important role in the general metabolism regulation and cellular growing. Different types of transport systems are known in the cellular membranes of mammals, as a combination of common (i.e. systems A, ASC, L, y^+ and X^{-AG}) and tissue-specific transport systems (i.e. systems $B^{o,+}$, Nm, and $b^{o,+}$ as well as variants of common transport systems). Amino acid transporters are tightly connected to metabolism and related to metabolic disorders. Thus, primary inherited amino acidurias (PIAs), like Cystinuria (in human [Calonge *et al*. 1994; Feliubadaló *et al*. 1999] and mouse [Feliubadaló *et al*. 2003; Peters *et al*. 2003]), Hartnup disorder (Kleta *et al*. 2004), Iminoglycinuria (Bröer *et al*. 2008), Dicarboxylic Amino aciduria (Bailey *et al*. 2011) or Lisinuric Protein Intolerance (LPI) (Torrents *et al*. 1999; Borsani *et al*. 1999) (Tables 1 and 2) are caused by defective amino acid transport activities and are some examples of illnesses associated with transporters. Thus, a more fundamental understanding of the structure-function relationships of the amino acid transporters would make invaluable contributions in pharmacology and medicine to prevent or treat different diseases. By the moment around 78,000 protein structures are available (protein data bank, PDB, 2011/11/07), but only a really small part of

them are membrane proteins (1,507 membrane proteins, 1,298 alpha helical and 209 beta barrel; protein data bank, PDB, 2011/11/07). The reason of this low percentage of membrane protein structures is due to the peculiarities of these proteins (i.e. high hydrophobicity and/or high aggregation tendency) making the crystallization process highly complicated.

2. Heteromeric Amino acid Transporters (HATs)

Secondary transporters (i.e., ion-coupled transporters, exchangers and facilitated diffusers) are grouped into SLC (SoLute Carrier) families according to sequence similarity in mammalian genomes. To date, almost 50 different SLC families have been identified of which 11 are known to comprise amino acid transporters (Table 1; Table 2). Although the majority of amino acid transporters have been identified and characterized, a significant number of orphan transporters remain, for instance in the SLC16 and SLC38 families (Bröer and Palacín. 2011). HATs are composed of a heavy subunit (SLC3 family; Table 2) and a light subunit (SLC7 family; Table 2), which are linked by a conserved disulfide bridge (Palacín and Kanai. 2004; Verrey *et al*. 2004). The cysteine involved in the formation of the disulfide bridge is strongly conserved in metazoan (Figure 1).

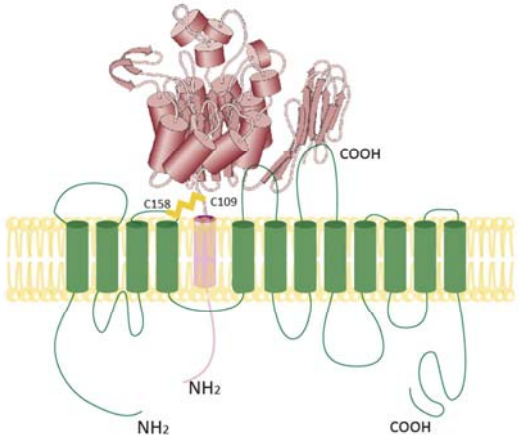

Figure 1. Scheme of a heteromeric amino acid transporter. The heavy subunit (pink) and the light subunit (green) are linked by a disulfide bridge (yellow) with conserved cysteine residues (cysteine 158 for the human light subunit xCT and cysteine 109 for human heavy subunit 4F2hc).

The SLC7 family proteins (i.e. LAT1, LAT2, y^+LAT1, y^+LAT2, asc1, xCT, b^{0+}AT, AGT1 and asc2) show a molecular weight around 50 kDa in SDS-PAGE and have a 12 transmembrane (TM) topology, none of them are glycosylated and the NH2 and the COOH termini are intracellular (Gasol *et al*. 2004) (Figure 1). The light chain is the catalytic subunit of the heterodimer complex (SLC3/SLC7) and confers the specific amino acid transport activity (Reig *et al*. 2002). The most closely family is the glycosylated CAT family (i.e. CAT1, CAT2, CAT3) which transport essentially cationic amino acids by facilitated diffusion as part of the system y^+ family (Table 1). These CAT transporters cross the membrane 14 times, two more than HATs family and are the first 12 helices similar with HATs, suggesting that there are two extra helices in COOH terminus (Broër *et al*. 2001).

SLC	Acronym	Substrate(s)	Function	Disease/phenotype
SLC1A1	EAAT3	D,E,Cn	System X– AG	Dicarboxylic aminoaciduria, OCD
SLC1A2	EAAT2	D,E	System X– AG	
SLC1A3	EAAT1	D,E	System X– AG	Episodic ataxia?
SLC1A4	ASCT1	A,S,C	System ASC	
SLC1A5	ASCT2	A,S,C,T,Q	System ASC	Tumor grown
SLC1A6	EAAT4	D,E	System X– AG	
SLC1A7	EAAT5	D,E	System X– AG	
SLC6A5	GlyT2	G	System Gly	Hyperekplexia
SLC6A7	PROT	P	Proline transporter	
SLC6A9	GlyT1	G	System Gly	
SLC6A14	ATB0,+	All neutral and cationic amino acids	System B0,+	Obesity?
SLC6A15	B0AT2	P,L,V,I,M	System B0	
SLC6A17	NTT4/B0AT3	L,M,P,C,A,Q,S,H,G	System B0	
SLC6A18	XT2/B0AT3	G, A	System Gly	Hyperglycinuria?Hypertension?
SLC6A19	B0AT1	All neutral amino acids	System B0	Harnup disorder, hypertension?
SLC6A20	IMINO	P	System IMINO	Iminoglycinuria
SLC7A1	CAT-1	K,R,O	System y+	
SLC7A2	CAT-2	K,R,O	System y+	
SLC7A3	CAT-3	K,R,O	System y+	
SLC16A10	TAT1	W,Y,F	System T	Blue diaper syndrome?
SLC17A6	VGLUT2	E	Vesicular Glu transporter	
SLC17A7	VGLUT1	E	Vesicular Glu transporter	
SLC17A8	VGLUT3	E	Vesicular Glu transporter	Non-syndromic deafness
SLC25A2	ORC2	K,R,H,O, Cit	Orn/Cit carrier	
SLC25A12	AGC1	D,E	Asp/Glu carrier	Global cerebral hypomyelination
SLC25A13	AGC2	D,E	Asp/Glu carrier	TipeII citrullinaemia, neonatal intrahepatic cholestasis
SLC25A15	ORC1	K,R,H,O,Cit	Orn/Cit carrier	HHH syndrome
SLC25A18	GC2	E	Glu carrier	
SLC25A22	GC1	E	Glu carrier	Neonatal myoclonic epilepsy
SLC32A1	VIAAT	G,GABA	Vesicular Gly/GABA transporter	
SLC36A1	PAT1	G,P,A	Proton AAT	Hair colour (horses)
SLC36A2	PAT2	G,P,A	Proton AAT	Iminoglycinuria
SLC36A4	PAT4	P,W	Amino acid sensor	
SLC38A1	SNAT1	G,A,N,C,Q, H,M	System A	
SLC38A2	SNAT2	G,P,A,S,C,Q,N,H,M	System A	
SLC38A3	SNAT3	Q,N,H	System N	
SLC38A4	SNAT4	G,A,S,C,Q,N,M	System A	
SLC38A5	SNAT5	Q,N,H,A	System N	
SLC43A1	LAT3	L,I,M,F,V	System L	
SLC43A2	LAT4	L,I,M,F,V	System L	
Not assigned	Cystinosin	Cn	Lysosomal Cys transporter	Cystinosis

Table 1. SLC family proteins and associated diseases. Substrates are given in one-letter code. Cit, citrulline; Cn, cystine; O, ornithine. The 'Function' column includes references to amino acid transport systems. These systems have acronyms indicating the substrate specificity of the transporter. Upper-case letters indicate Na^+-dependent transporters (with the exception of system L, system T and the proton amino acid transporters); lower case is used for Na^+-independent transporters (for example asc). X^- or x^- indicates transporters for anionic amino acids (as in X^- AG and x^- c). The subscript AG indicates that the transporter accepts aspartate and glutamate, and the subscript c indicates that the transporter also accepts cystine. B or b refers to amino acid transporters of broad specificity with superscript 0 indicating a transporter accepting neutral amino acids and superscript + indicating a transporter for cationic amino acids. T stands for a transporter for aromatic amino acids, and system N indicates selectivity for amino acids with nitrogen atoms in the side chain. In the remaining cases, the preferred substrate is indicated by the one-letter code for amino acids. For example, system L refers to a leucine-preferring transporter and system ASC to a transporter preferring alanine, serine and cysteine. Proline and hydroxyproline are referred to as imino acids. Owing to historic idiosyncrasies, the nomenclature for plasma-membrane amino acid transport systems is not completely consistent, but is widely used in the field. AAT, amino acid transporter (Adapted from Bröer and Palacín. 2011). The members corresponding with the HATs are included in the Table 2.

SLC3 members (i.e. rBAT [also called SLC3A1] and 4F2hc [also called CD98 or SLC3A2]; Table 2) are type II membrane N-glycoproteins, having six glycosylation sites in the case of rBAT, and only four in the case of 4F2hc, with a single TM (transmembrane domain) segment, an intracellular N-terminus and a large extracellular C-terminus (Figure 1). The human heavy subunits of HATs show a molecular weight of 90 kDa for rBAT, and 80 kDa for 4F2hc in SDS-PAGE and have an identity between them of 30% (Palacín et al. 1998). The first subunit identified was rBAT (related to $b^{0,+}$ system amino acid transporter), which was isolated and cloned independently by three groups (Bertran *et al*. 1992, Tate *et al*. 1992, Wells *et al*.1992). In short, 4F2hc was identified and characterized as part of y^+L system (Bertran *et al*. 1992, Wells *et al*. 1992). 4F2hc was also identified as CD98, a protein previously cloned as a surface antigen on activated lymphocytes (Haynes *et al*. 1981, Lumadue *et al*. 1987, Quackkenbush *et al*. 1987, Teixeira *et al*. 1987). Any transport function has been related to the heavy subunits, however, they have been identified as the responsible for trafficking the light subunit to the cellular membrane (Chillarón *et al*. 2001).

SLC	Acronym	Substrate(s)	Function	Disease/phenotype
SLC3A1	rBAT	Trafficking subunits	Heavy chains of heteromeric AAT	Cystinuria
SLC3A2	4F2hc	Trafficking subunits	Heavy chains of heteromeric AAT	Tumor grown
SLC7A5	LAT1/4F2hc	H,M,L,I,V,F,Y,W	System L	Tumor grown
SLC7A6	y+LAT2/4F2hc	K,R,Q,H,M,L	System y+L	
SLC7A7	y+LAT1/4F2hc	K,R,Q,H,M,L,A,C	System y+L	Lysinuric protein intolerance
SLC7A8	LAT2/4F2hc	All neutral amino acids except P	System L	
SLC7A9	b0,+AT/rBAT	R,K,O,Cn	System b0,+	Cystinuria
SLC7A10	Asc-1/4F2hc	G,A,S,C,T	System asc	
SLC7A11	xCT/4F2hc	D,E,Cn	Sytem x– c	
SLC7A12	Asc-2	G,A,S,C,T	System asc	
SLC7A13	AGT1	D,E	Asp, Glu transporter	

Table 2. Heteromeric amino acid transporters (HATs) and associated diseases. Substrates are given in one-letter code. Cn, cystine; O, ornithine. The 'Function' column includes references to amino acid transport systems. These systems have acronyms indicating the substrate specificity of the transporter. Upper-case letters indicate Na^+-dependent transporters (with the exception of system L); lower case is used for Na^+-independent transporters (for example asc, y^+ and x^- c). X^- or x^- indicates transporters for anionic amino acids (as in X^- AG and x^- c). Y^+ or y^+ refer to transporters for cationic amino acids (an Na^+- dependent cationic amino acid transporter has not been unambiguously defined and as a result Y^+ is not used), B or b refers to amino acid transporters of broad specificity with superscript 0 indicating a transporter accepting neutral amino acids and superscript + indicating a transporter for cationic amino acids. In the remaining cases, the preferred substrate is indicated by the one-letter code for amino acids. For example, system L refers to a leucine-preferring transporter and system ASC to a transporter preferring alanine, serine and cysteine. AAT, amino acid transporter.

3. Amino acid transport function of HATs

Functionally, HATs are amino acid antiporters (exchangers) with a 1:1 stoichiometry (Busch *et al*. 1994; Chillarón *et al*. 1996). Six members of the SLC7 family in humans (LAT1, LAT2, y^+LAT1, y^+LAT2, asc1 and xCT) heterodimerize with 4F2hc, but only one (b^{0+}AT) heterodimerize with rBAT (Table 2). The heavy subunits associating with AGT1 (aspartate/glutamate transporter 1, also called AGC1), asc2 and arpAT are presently unknown (Table 2). The transport systems corresponding to HAT members are system y^+L (light subunits y^+LAT1 and y^+LAT2 for system y^+L isoforms), x^{c-} (light subunit xCT), asc (light subunits asc1 and asc2 for system asc isoforms), $b^{0,+}$ (light subunit b^{0+}AT for system $b^{0,+}$), L (light subunits LAT1 and LAT2 for system L isoforms) and AGT1 for a system serving aspartate and glutamate transport. Next it follows a description of all these transport systems**.**

3.1 System y^+L

Amino acid transport system y^+L, mediates electro neutral exchange of cationic (y^+) and large neutral amino acids (L) plus Na^+ with a stoichiometry of 1:1:1 (Chillarón *et al*. 2001). Physiologically, the transporter mediates the efflux of a dibasic amino acid in exchange for an extracellular neutral amino acid plus Na^+, with an apparent K_M of 20 μM (Torrents *et al*. 1998; Pfeiffer *et al*. 1999; Bröer *et al*. 2000; Kanai *et al*. 2000). It is speculated that the Na^+ ion replaces the positive charge of the side chain of dibasic amino acids when neutral amino acids are transported. In support of this notion, the affinity of neutral, but not cationic, amino acids increases by approximately two orders of magnitude in the presence of Na^+. System y^+L is found in placenta (Eleno *et al*. 1994), erythrocytes (Deves *et al*. 1992), skin fibroblast (Smith *et al*. 1987), hepatocytes (Rajantie *et al*. 1981), small intestine (Desjeux *et al*. 1980), kidney (Rajantie *et al*. 1981), spleen and macrophages (Shoji *et al*. 2002; Rotoli *et al*. 2007). In polarized epithelial cells the transporter has a basolateral location. The light subunits

participating in system y^+L (i.e. y^+LAT1 and y^+LAT2) were initially identified and characterized in *Xenopus* oocytes by our group (Torrents *et al*. 1999).

y^+LAT1 is mainly expressed in the basolateral membrane of the epithelial cells of the proximal tubule and small intestine. Mutations in the *SLC7A7* gene encoding the HAT light chain y^+LAT1 cause LPI (see Lysinuric Protein Intolerance below) (Torrents *et al*. 1999; Borsani *et al*. 1999), an autosomal recessive disease.

y^+LAT2 is found in kidney and small intestine at much lower levels compared with 4F2hc/ y^+LAT1. As a result, 4F2hc/ y^+LAT2 cannot replace 4F2hc/ y^+LAT1 in the kidney and intestine, but it explains why 4F2hc/ y^+LAT2 lack of activity do not cause LPI.

3.1.1 Lysinuric Protein Intolerance (LPI)

LPI is a primary inherited aminoacinuria (PIA) with an autosomal recessive mode of inheritance. LPI is predominantly reported in Finland, with a prevalence of 1/60,000, Southern Italy and Japan (prevalence of 1/50,000 in the northern part of Iwate) (Reviewed by Palacín. 2005). In LPI there is massive excretion of dibasic amino acids, especially lysine, with a poor intestinal absorption of these amino acids (Reviewed by Palacín. 2005). As a result, plasma levels of dibasic amino acids are low. Arginine and ornithine are intermediates of the urea cycle that provide the carbon skeleton. Their reduced availability is thought to produce a functional deficiency of the urea cycle. Protein malnutrition and lysine deficiency contribute to the patient's failure to thrive.

Several organs are affected in LPI (Reviewed by Palacín. 2005). Patients with LPI are usually asymptomatic while being breast fed, and symptoms (e.g. vomiting, diarrhea, and hyperammonemic coma when force-fed high-protein food) appear only after weaning. Most patients show moderate retardation and/or acute or chronic respiratory insufficiency that can lead to fatal pulmonary alveolar proteinosis. Further symptoms, such as glomerulonephritis and erythroblastophagia, suggest that the immune system is affected in some patients. Low-protein diet and citrulline (i.e., a urea cycle intermediate that is not a substrate of system y^+L) are used to correct the functional deficiency of the urea cycle (Reviewed by Palacín. 2005). This treatment neither corrects

hepatosplenomegaly nor delay bone age or osteoporosis, probably due to lysine deficiency.

In *SLC7A7 (*gene encoding for the HAT light chain y^+LAT1*)*, 49 LPI-specific mutations in a total of 141 patients from 107 independent families have been described (Reviewed by Palacín and Broër. 2011). These known mutations explain >95% of the studied alleles. No LPI mutations have been identified in the heavy subunit *SLC3A2* (4F2hc). Probably, because 4F2hc serves to traffic other six amino acid transporter subunits (Palacín and Kanai. 2004) and is necessary for proper β1 integrin function (Feral *et al*. 2005; Cantor *et al*. 2009). Indeed *Slc7a7* knockout in mouse is lethal (Tsumura *et al*. 2003).

3.2 System xc^-

The light subunit xCT joined with 4F2hc were identified as the two subunits forming this transport system. This is the major system providing the cell with cystine (anionic form) and replenishing the intracellular glutathione store, which maintain cell viability in an environment of oxidative stress and contributes to maintaining the plasma redox balance in vivo (Satoh *et al*. 2005). It is a Na^+ independent transport system in macrophages, neuronal cells, fibroblast, pancreas, hepatocytes and kidney. Probably, one of the most important last reports about this transporter has been the xCT function as a potent fusion-entry receptor for the Kaposi' s sarcoma-associated herpesvirus (KSHV), increasing dramatically the efficiency of fusion in different overexpressing xCT cell lines (Kaleeba and Berger. 2006). Recently has been demonstrated the capability of KSHV up-regulating the expression of xCT (its own receptor) via miRNAs, these results offer an useful approach for the treatment or prevention of Kaposi' s sarcoma disease (Qin *et al.* 2010).

3.3 System asc

The mRNA was found in kidney, brain, placenta, heart, skeletal muscle, pancreas, liver and lung. It is important to remark that the light subunit asc1,

was the only light subunit joined to 4F2hc, which showed a significant uniport activity (Fukasawa *et al*. 2000). The first description was done in erythrocytes, identified as a Na^+ independent transport for short neutral amino acids (Ellory *et al*. 1981; Albi *et al*. 1994).

3.4 System $b^{0,+}$

rBAT was the first protein cloned as a possible candidate for this system (Bertran *et al*. 1992; Tate *et al*. 1992; Wells *et al*. 1992; Lee *et al*. 1993) inducing Na^+ independent transport of neutral, dibasic amino acids and cystine. Later it was determined that rBAT needs the presence of the light subunit b^{0+}AT to shown the same features than $b^{0,+}$ system in *Xenopus* oocytes and COS cells (Feliubadaló *et al*. 1999; Pfeiffer *et al*.1999; Chairroungdua *et al* 1999). This system was described first in mouse blastocyst (Van Winkle *et al*. 1988) and the interest in it has been growing with cystinuria disease, an inherited amino aciduria due to mutations in heavy subunit rBAT and light subunit b^{0+}AT. The rBAT/b^{0+}AT heterodimer mediates the exchange of cationic amino acids, cystine and other neutral amino acids, except imino acids (Chillarón *et al*. 1996; Bertran *et al*. 1992). The transporter has a high affinity for external cationic amino acids and cystine (K_M <100 μM) and a slightly lower affinity for neutral amino acids. The apparent affinity is much lower at the intracellular binding site (Reig *et al*. 2002). Two disulfide-linked rBAT/b^{0+}AT heterodimers form a non-covalent heterotetramer in native tissues (Fernandez *et al*. 2006).

3.4.1 Cystinuria

Cystinuria is the most common primary inherited amino aciduria, characterized by impaired transport of cystine and dibasic amino acids in the proximal renal tubule and the gastrointestinal tract (Reviewed by Chillarón *et al*. 2010). Patients present normal to low-normal levels of cystine and dibasic amino acids in blood, hyperexcretion in urine, and intestinal malabsorption of these amino acids. High cystine concentration in the urinary tract most often causes the formation of recurring cystine calculi (i.e. urolithiasis) due to the low solubility of this amino

acid. This is the only symptom associated with the disease. Therefore, treatment attempts to increase cystine solubility in urine (high hydratation, urine alkalinization, and formation of soluble cysteine adducts with thiol drugs). Cystinuria is not accompanied by malnutrition, suggesting that intestinal malabsorption is not severe. Cystinuria is usually considered to be an autosomal-recessive disorder, requiring two mutated alleles for the disease to occur, but two phenotypes of cystinuria have been described. In type I, individuals with one mutated allele have normal urinary excretion of amino acids, whereas in non type-I heterozygotes, urinary hyperexcretion of dibasic amino acids and cystine are observed (Chillarón *et al*. 2010).

Mutations in both *SLC3A1* (encoding rBAT) and *SLC7A9* (encoding $b^{0,+}$AT) cause cystinuria. Worldwide, 133 mutations have been reported in *SLC3A1* (in a total of 579 alleles) and 95 mutations have been reported in *SLC7A9* (in a total of 436 mutated alleles). Only ~13% of the studied cystinuria alleles have not been identified, leaving little room for other cystinuria-causing genes. The unexplained cystinuria alleles might correspond to mutations in unexplored regions of *SLC3A1* and *SLC7A9* gene (Reviewed by Chillarón *et al*. 2010). Type I cystinuria is usually caused by mutations in *SLC3A1* (Font-Llitjos *et al*. 2005), with <15% of the mutant alleles involving *SLC7A9*, in contrast non-type I cystinuria is usually caused by mutations in *SLC7A9*, with <4% having mutations in *SLC3A1* (Chillarón *et al*. 2010).

3.5 System L

The first evidence that system L is associated with expression of 4F2hc came from *Xenopus laevis* oocyte expression experiments (Broër *et al*. 1995) observing that induced system L activity was abolished by 4F2hc antisense cRNA or antisense oligonucleotides. The first subunit interacting with 4F2hc was identified by two groups independently (Kanai *et al*. 1998; Mastroberardino *et al*. 1998) and was eventually named LAT1. The second cDNA identified was called LAT2 on the base of its homology (Pineda *et al*. 1999).

LAT1 is expressed in non-epithelial cells such as brain, spleen, thymus, testis, skin, liver, placenta, skeletal muscle, and stomach (Kanai *et al*. 1998; Prasard *et al*. 1999). In the brain, LAT1 expression is found predominantly in the endothelial cells forming the blood-brain barrier (Boado *et al*. 1999). Human 4F2hc/LAT1 exchanges large neutral amino acids with high affinity (K_M ~50 μM) and glutamine and asparagine with lower affinity (K_M ~2 mM) (Yanagida *et al*. 2001).

The expression levels of the heterodimer 4F2hc/LAT1 (SLC3A2/SLC7A5) is elevated in a wide spectrum of primary human tumors, cancer cell lines (Fuchs and Bode. 2005; Wolf *et al*. 1996; Yanagida *et al*. 2001) and metastasis (Kaira *et al*. 2008) indicating that it may be involved in supporting the increased anabolic needs of tumors. In addition, Fuchs and Bode proposed that in tumor cells, LAT1 uses intracellular ASCT2 substrates (high affinity for small neutral amino acids, asparagine and glutamine [K_M ~20 μM]) to adjust the essential amino acid concentrations for metabolic demands and signaling to the Ser/Thr kinase mTOR (mammalian target of rapamycin) which regulates cell growth and autophagy (Fuchs *et al*. 2005). This has been demonstrated in cellular cultures in which L-glutamine flux is the main substrate regulating mTOR, translation and autophagy to coordinate cell growth and proliferation (Nicklin *et al*. 2009)**.**

LAT2 was identified and characterized in *Xenopus* oocytes in our group (Pineda *et al*. 1999) and, in association with 4F2hc induces the system L transport activity (Pineda *et al*. 1999; Rossier *et al*. 1999). The heterodimer 4F2hc/LAT2 is a sodium-independent obligatory exchanger that bears broad substrate specificity, including all neutral amino acids except proline. Kinetic analysis revealed an apparent K_M of 220 µM for the transport of L-leucine induced by 4F2hc/LAT2 expressed in the liver, showing also an increased substrate affinity at low pH´s (Pineda *et al*. 1999; Segawa *et al.* 1999; Rajan *et al.* 2000). Thus, the heterodimer 4F2hc/LAT2 is highly expressed along the basolateral membranes of absorptive epithelia in kidney and small intestine and also in the brain (Rossier *et al*. 1999; Pineda *et al*. 1999; Bauch *et al*. 2003; Dave *et al*. 2004). In fact, LAT2 had been related in mediate thyroid hormone uptake into *Xenopus*

oocytes (Friesema *et al*. 2001) and recently, into cultured astrocytes (Braun *et al*. 2011), although these results have not been demonstrated in the knockout Slc7a8 −/− mice. However, the knockout studies, revealed amino aciduria (Figure 2) and pointed LAT2 as a good candidate for glutamine uptake into neurons (Braun *et al*. 2011).

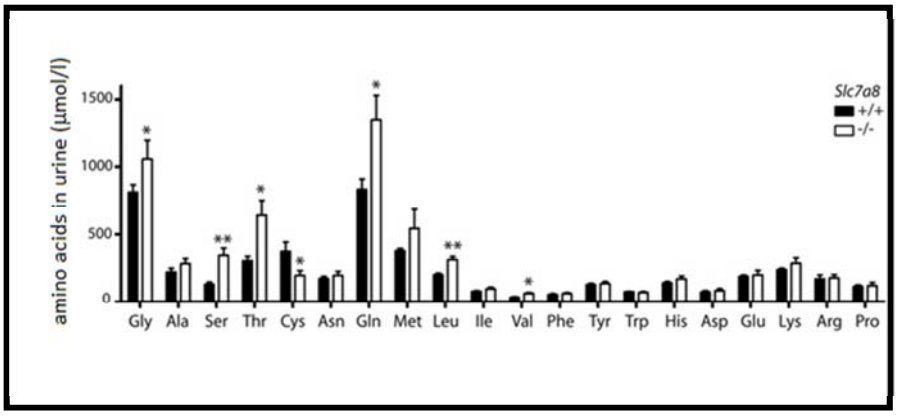

Figure 2. Amino acid analysis in urine revealed neutral amino aciduria in Slc7a8 −/− mice. Glycine, serine, threonine, glutamine, leucine and valine were increased in urine from mutant animals. Interestingly, some classical L-type amino acid transporter substrates such as isoleucine or aromatic amino acids were not affected. Braun and co-workers speculated that other amino acid transporters partially compensated for the loss of LAT2 transporters (Figure adapted from Braun *et al*. 2011).

4. Interaction between Heavy and Light subunits.

The most prominent element involved in the interaction between heavy and light subunits is the disulfide bridge. The disulfide bridge takes place in the reactive cysteine 114 in the case of human rBAT, and cysteine 109 in the case of human 4F2hc. In the heavy chains, this cysteine is localized in the extracellular neck, a few amino acids away from the transmembrane segment. Light subunits have a conserved cysteine (C158 for human xCT) between transhelices TM3 and TM4 (Wang *et al*. 1995; Pfeifer *et al*. 1998; Torrents *et al*. 1998; Mastrobernardino *et al*. 1998, Nakamura *et al*. 1999). The disulfide bridge and the consequently heterodimer formation is conserved in all the heteromeric amino acids transporters (HATs) (Reviewed by Palacín *et al*. 2005).

These heterodimers appear normally as a band around 100 - 130 kDa in SDS-PAGE, depending on the heterodimer and the expression system used. Apart from disulfide bridge, and although it is impossible to see them in a SDS-PAGE, there are also important evidences of non-covalent unions between both subunits. The role of the disulfide bridge and the non-covalent unions between both subunits in the transport function has been widely discussed.

The first studies reported the role of the heavy subunit (i.e. rBAT) in the trafficking of the light subunit to the membrane (i.e. b^{0+}AT) (Chillarón *et al*. 1997). These studies were strongly supported by the completely abolition of transport function when light subunit b^{0+}AT was overexpressed in absence of the heavy subunit (i.e. rBAT) in HeLa cells (Feliubadaló *et al*. 1999; for reviews see Verrey *et al*. 2000 and Chillarón *et al*. 2001). Surprisingly mutations in the reactive cysteine of rBAT (disrupting the disulfide bridge) did not avoid the transport but just decreased it (Pfeiffer *et al*. 1998; Nakamura *et al*. 1999) which evidenced the existence of non-covalent unions apart from the disulfide bridge. From that preliminary studies, non-covalent unions has been supported by deletions and mutations in the COOH termini of heavy subunit rBAT (rat or human), and although sometimes the data have been controversial (Deora *et al*. 1998; Miyamoto *et al*. 1996) all of them supported other interactions beside the disulfide bridge (for review see Broër *et al*. 2001). Truncations in the COOH terminus of heavy subunit 4F2hc were carried out trying to recreate the rBAT context (i.e. mutations and deletions in –COOH). Surprisingly, the 4F2hc –COOH termini truncations slowed down the traffic of the light subunit (i.e. LAT1) to the membrane but not abolished the transport, keeping the behaviour almost as efficient as the wild type (Bröer *et al* 2001). Meanwhile the same truncations produced a complete loss of function in LAT2 and y^{+}LAT2. In contrast, the studies by Fenczik and co-workers using chimeras between 4F2hc and CD69 (a type II transmembrane protein nor participating in transport), pointed to the relevancy of the extracellular domain (-COOH) of 4F2hc in combination with the light subunit LAT1, not the transmembrane or cytoplasmic, to keep the amino acid transport system L^{+} (Fenczik *et al*. 2001). In contrast, recent exhaustive studies

recreating the same Fenzick´s chimeras of 4F2hc/CD69, demonstrated that only a 10 % of chimeric heterodimer was found in the cellular surface, explaining the lack of system L^+ transport as a defect in trafficking and not as a transport absence (De la Ballina. 2011). The last result remarked the importance of the 4F2hc extracellular domain joined with the light subunit LAT1 in concordance with Bröer and co-workers, suggesting that the different light subunits (i.e. LAT1, LAT2 and y^+LAT2) recognition would require different domains from the heavy subunit (i.e. non-covalent unions). Franca and co-workers developed chimeric and truncated forms of rBAT/4F2*hc* co-expressed with light chains in *X. laevis* oocytes (Franca *et al*. 2005). The experiments showed that association with light subunit (i.e. $b^{0,+}$AT), required the presence of the intracellular domain of heavy chain (i.e. rBAT). In addition, only the presence of both, transmembrane domain and extracellular domain of rBAT permitted the trafficking to the membrane and the transport function of heterodimer rBAT/b^{0+}AT, while the chimeras lacking the rBAT transmembrane domain (i.e. carrying 4F2hc tans membrane domain), remained in the surface without any kind of transport.

To sum up, all that experiments point that the whole heavy subunit structure (i.e. extracellular domain, transmembrane domain and intracellular domain) plays an important role in interaction with, trafficking to the membrane and transport function of light subunits. Structurally, all these data indicate that the heavy subunit might contact closely with the light subunit to keep trafficking to the plasma membrane and functionality of the holotransporter.

5. Heavy and light subunits, the profits of a close association

Reconstitution in liposomes has been a powerful tool in the study of transporters since is a clean system where the transporter could be reconstituted independently of trafficking to the plasma membrane. Reig and co-workers reconstituted system $b^{0,+}$ activity from extracts of HeLa and MDCK cells transfected with the monomer $b^{0,+}$AT or the heterodimer rBAT/b^{0+}AT. The study showed that the light subunit (i.e. $b^{0,+}$AT) in the absence of its heavy

subunit (i.e. rBAT), folded into an active form, showing full transport activity (Figure 3).

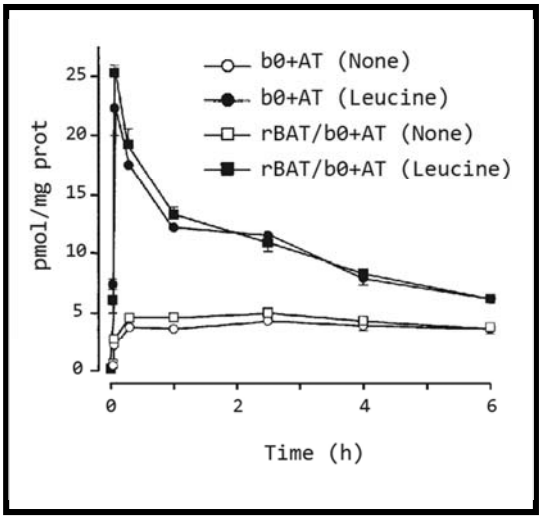

Figure 3. **A time course of the transport of 0.5 mM L-[3H] arginine into liposomes**. Transport was measured at 5 s, 1 and 15 min, and at 1, 2.5, 4 and 6 h. Liposomes uncharged (None) do not show any kind of overshoot in any case. Monomer b^{0+}AT and heterodimer rBAT/b^{0+}AT reconstituted in loaded liposomes (i.e. Leucine 2mM) show an overshoot in both cases. It suggests monomer b^{0+}AT is fully functional in absence of its heavy subunit rBAT (Adapted from Reig *et al* 2002).

In addition, trafficking of $b^{0,+}$AT and the expression of transport system $b^{o,+}$ in the plasma membrane required the presence of the heavy subunit (Feliubadaló *et al*. 1999; for review see Chillarón *et al*. 2001). Indeed, processing of rBAT from the ER to the Golgi (i.e. maturation of the N-glycosylation of rBAT) depended on the presence of the light subunit $b^{0,+}$AT (Reig *et al*. 2002). This study introduced a new concept in terms of function in light subunits. The light subunit b^{0+}AT might protect its heavy subunit rBAT against cellular degradation and might act as a specific chaperone for rBAT.

Supporting Reig and co-workers observations, the half live of the heavy subunit rBAT in absence of its light subunit was studied by pulse-chase experiments followed by immunoprecipitation with specific antibodies (Bartoccioni *et al*. 2008). In MDCK cells expressing only rBAT, this protein ran as an

endoglycosidase-H sensitive band, which, after a lag phase of 1 h, disappeared. In contrast, in MDCK cells expressing only b^{0+}AT, more than 60% and 30% of the pulse-labelled band of $b^{0,+}$AT was detected after 8 and 24 h of chase, respectively. The results were compared with different rBAT type I cystinuria mutations (Figure 4). rBAT transmembrane mutation L89P (Leu 89 is the putative second residue of the transmembrane segment) showed an important defect in assembling with the light subunit b^{0+}AT. The TIM-barrel mutants (i.e. M467T/K, T216M, R365W) showed a deficient maturation of their glycosylations and a consequent folding deficiency, leading to degradation after assembly with b^{0+}AT. Transmembrane mutation and TIM barrel mutations showed two different deficiencies to lead the same cystinuria Type I pathology and both showed that the absence of transport activity was primarily due to strong trafficking defects.

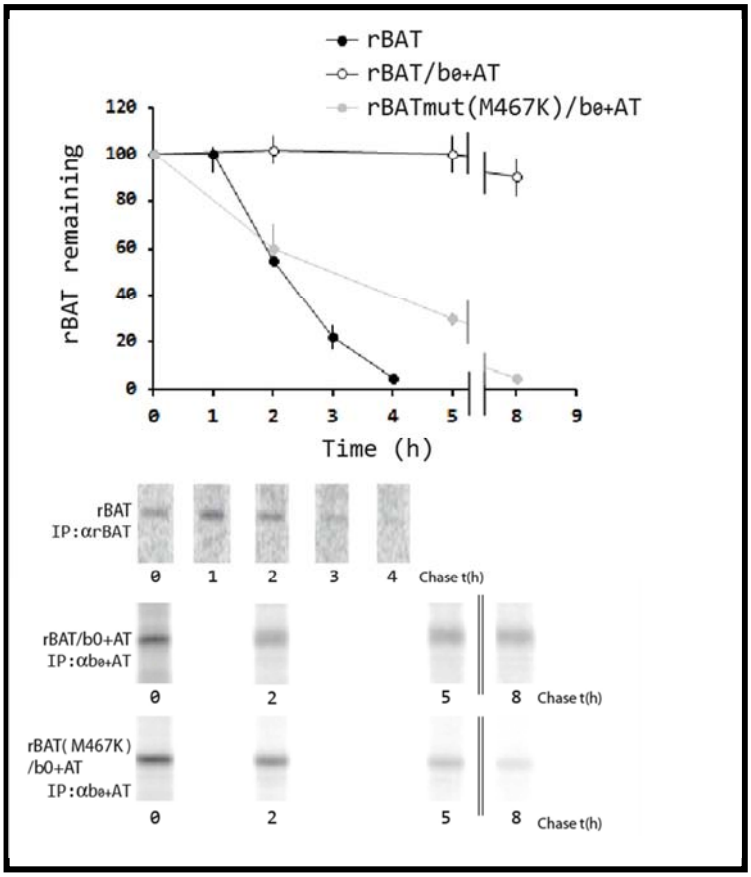

Figure 4. **rBAT half live in absence or presence of b^{0+}AT.** In the graphic is observed the quantifications (mean+SEM) of at least three independent experiments for each condition. The value at each point of the chase was divided by the value at point zero, which was set to 100. rBAT/b0+AT (WT) remains stable up to 8 hours while the signal of rBAT and rBAT mutant (M467K) falls down. The western blots (αrBAT or αb^{0+}AT antibodies as indicated) show the degradation of the extracellular domain rBAT (monomer rBAT, heterodimer rBAT/b^{0+}AT or rBAT mutant (M467K)/ b^{0+}AT) (Figure adapted from Bartoccioni *et al.* 2008).

In conclusion, light subunit b^{0+}AT acts as a chaperone for heavy subunit rBAT increasing its half live while the light subunit b^{0+}AT needs the heavy subunit rBAT to trafficking to the cell membrane. By the moment, the role of 4F2hc and/or its light subunits (Asc1, LAT1, LAT2, y^+LAT1, y^+LAT2 or xCT) in the heterodimer stabilization is still unknown, but it might be probably to find a similar chaperone-like behaviour in some of these proteins.

6. 4F2hc is a multifunctional protein

4F2hc (CD98hc, SLC3A2) is a multifunctional type II membrane glycoprotein, ubiquitous in the organism and probably overexpressed in all the tumor cell lines (Parmacek *et al.* 1989; Nakamura *et al.* 1999), because of that 4F2hc properties, ablation of 4F2hc in mouse lead to embryonic lethality (Tsumura *et al*. 2003). An important number of experiments involve that heavy subunit (i.e. 4F2hc and also rBAT) as an active part in heterodimer formation and transport function (Pfeifer *et al*. 1998; Pineda *et al*. 1999; Peter *et al*. 1999; Rajar *et al*. 2000; Broër *et al*. 2001; Fenczik *et al*. 2001; Franca *et al*. 2005; De la ballina. 2011). Moreover, 4F2hc has been described as a multimeric protein involved in such processes as cell fusion (Tsurudome *et al*. 2000), cell adhesion (Fenczik *et al*. 1997), integrin signaling (Feral *et al.* 2005), cellular fusion in placenta (Dalton *et al*. 2007) or macrophages activation through interaction with galectine3 (Mackinnon *et al*. 2008). All these functions should be at the basis of the overexpression of 4F2hc in primary tumors and metastasis (Boyd *et al*. 2008).

6.1. 4F2hc bounds integrin β1

Fenczik and co-workers determined that 4F2hc interacts with integrin β1 and that the covalent association of 4F2hc with a light chain (i.e. 4F2hc/LAT1) was not required for its interaction or for the functional regulation of integrins (Fenczik *et al*. 2001). Second, they replaced different domains in 4F2hc (i.e. cytoplasmic, transmembrane or NH2 domains) with the equivalent of CD69 (another type II transmembrane protein not implied in transport or integrins binding) (Figure 5), and found that, both, the cytoplasmic and the transmembrane domains of 4F2hc, were necessary for binding and keep function to the integrin β1. When either of these domains, cytoplasmic or transmembrane were removed from 4F2hc and replaced by CD69, integrin interactions and function were lost. These studies suggested that the interaction between 4F2hc and integrins or between 4F2hc/LAT1 was carried out by different domains. In contradiction with this results, Kolesnikova and co-

workers described that the loss of the covalent union (the mutation 4F2hc [C109S]; i.e. the cysteine responsible for the disulfide bridge) was responsible for β1 integrin dissociation with 4F2hc (Kolesnikova *et al*. 2001). Later it was found that the association between 4F2hc and integrin β1 could differ in order to the 4F2hc light subunit associated (i.e. 4F2hc/LAT2), concluding that more experiments are necessary to determine how the heavy subunit 4F2hc and integrins interact depending on the light subunit associated (Franca *et al*. 2005).

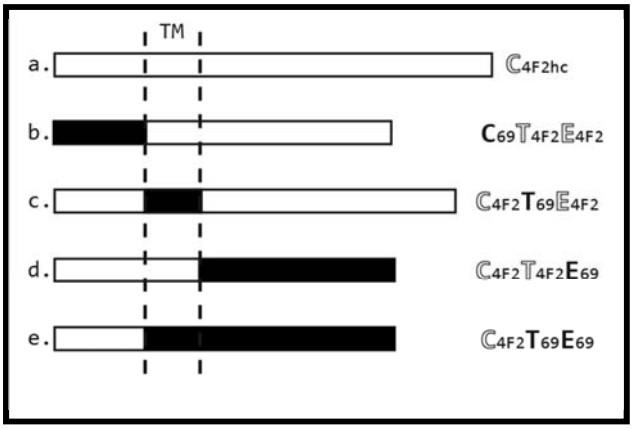

Figure 5. Chimeras between the heavy subunit 4F2hc and CD69. **(a.)** 4F2hc wild type; **(b.)** CD69 N-term/4F2hc TM/4F2hc extracellular domain; **(c.)** 4F2hc N-term/CD69 TM/4F2hc extracellular; **(d.)** 4F2hc N-term/4F2hc TM/CD69 extracellular; **(e.)** 4F2hc N-term/CD69 TM/CD69 extracellular. TM, transmembrane domain and C, cytoplasmatic. T, transmembrane. E, extracellular (Figure adapted from Fenczic *et al*. 2001)

4F2hc influences multiple integrin-dependent functions, including virus-induced cell fusion, T-cell co-stimulation and cell adhesion (Fenczik *et al*. 1997; Warren *et al*. 2000). The role of 4F2hc in integrin signalling is being characterized. Merlin and co-workers demonstrated that β1 integrins associate with 4F2hc/LAT2 basolaterally in intestinal polarized epithelial cells, influencing β1 integrins distribution and affecting the cells shape and the cytoskeletal order (Merlin *et al*. 2001). In addition, Feral and co-workers established than 4F2hc contributes in fibronectin matrix assembly via integrin union, providing with the necessary

force (cellular contractility) to deform integrin bound fibronectin (Feral *et al*. 2007). The deformation of fibronectin had been described as a necessary step to matrix assembly (Zhong *et al*. 1998). This fact may have implications in the relationship between cell proliferation and formation of the extracellular matrix. Proliferating cells, up regulate 4F2hc expression, which would promote fibronectin matrix assembly. It is directly related with tumours, in which the marked up-regulation of 4F2hc (Deves and Boyd. 2000) could promote the excess of fibronectin matrix proliferation (Feral *et al*. 2007). In addition, experiments in 4F2hc knockout mice determined the absence of 4F2hc lead to embryonic lethality (Tsumura *et al*. 2003) which could be explained again by regulation of matrix assembly controlled by the activity of cellular integrins, a 4F2hc-dependent process (Feral *et al*. 2005).

The Integrin-4F2hc complex is related with B-cells too in such a way that integrin signalling is involved in clonal proliferation during immune responses (Cantor *et al*. 2009). Has been established that 4F2hc is absolutely required for the rapid B cell clonal proliferation, necessary for their subsequent differentiation into antibody-secreting plasma cells (Cantor *et al*. 2009) providing with a profound selective advantage, the increased 4F2hc expression antigen-stimulated B cells. Again chimeric constructions with 4F2hc, emulating Fenczik and co-workers (Fenczik *et al*. 2001), showed that only transmembrane and cytoplasmic segments were sufficient to rescue proliferation of 4F2hc-null B cells.

6.2. 4F2hc bounds Galectin 3

Galectin 3 was originally found as a surface marker called Mac2, which is present on the cell surface of inflammatory macrophages (Ho and Springer. 1982). It up-regulated when monocytes differentiate into macrophages (Liu *et al*. 1995) and down-regulated when macrophages differentiate into dendritic cells (Dietz *et al*. 2000). Galectins belong to a β-galactoside-binding family of proteins and is expressed widely in epithelial and immune cells, and its expression is correlated with cancer aggressiveness and metastasis. It is reported to be involved in

various biological phenomena, including cell growth, adhesion, differentiation, angiogenesis and apoptosis. 4F2hc coimmnuprecipitated with galectin 3 in BeWo cells (trying to emulate cellular differentiation in placenta) (Dalton *et al*. 2007). It was suggested that 4F2hc could traffic to the plasma in both forms, glycosylated or not, using the classic secretory pathway or an alternative route, respectively. It was demonstrated that 4F2hc glycosylation was necessary for cell fusion and that this in turn required interaction between 4F2hc and galectin 3 (Dalton *et al*. 2007). 4F2hc bounded to galectin 3 in macrophages may have an important role in immunology. 4F2hc is related to the alternative macrophage activation, which plays in diverse pathologies. It was found that inhibiting galectin 3, the alternative macrophage via was blocked (Mackinnon *et al*. 2008). Up-regulation of galectin 3 expression is a feature of the alternative macrophage phenotype. In order to galectin 3 binds 4F2hc on macrophages, blocking this binding alternative macrophage activation was prevented. That process is related again with the union 4F2hc/β1 integrin, since 4F2hc stimulates PI3K activation via an association with β1 integrins, this study suggested that 4F2hc-mediated PI3K activation is a key mediator of alternative macrophage activation. The use of products such as cynaropicrin inhibiting 4F2hc, could be a new therapeutic target for manipulating macrophage phenotype in the treatment of cancer, chronic inflammation and fibrosis (Mackinnon *et al*. 2008).

6.3. 4F2hc bounds ICAM 1

ICAM1 is a protein that plays an important role in extracellular matrix interactions and cellular interactions such as the immune response. This protein is expressed in basolateral and apical membranes of endothelial cells in the small intestine, swollen epithelial cells and, it is the receptor of CD11a and CD18 of leukocytes.

In the intestine epithelial (cell line Caco2-BBE), ICAM1 may interact with 4F2hc/LAT2 as a 250 kDa multicomplex (Liu *et al*. 2003). Merlin and co-workers demonstrated that cross-linking, 4F2hc with anti-4F2, or cross-linking ICAM1

with anti-ICAM 1, decreased or increased respectively the Vmax of LAT2 mediated leucine uptake. Furthermore, crosslinking 4F2hc studies suggested that this transport activity change could be done of the result of a direct or indirect phosphorylation of LAT2 in threonine (Liu *et al*. 2003) in order to 4F2hc, LAT2 and ICAM 1 proteins have predicted threonine phosphorylation sites. Cross-linking 4F2hc or ICAM 1 may induce phosphorylation of LAT2 itself on threonine and change transport activity of LAT2, or phosphorylation of associated proteins such as ICAM 1 or 4F2hc may influence LAT2 transport activity. Thus, the changes in the transporter LAT2 may play a role in delivering intracellular signals on cell adhesion.

6.4. 4F2hc bounds CD147

CD147 is a protein ubiquitously expressed with highest levels on metabolically active cells, such as lymphoblast (Koch *et al*. 1998), inflammatory cells (Betsuyaku *et al*. 2003), brown adipocytes (Nehme *et al*. 1995), and malignant tumours (Toole *et al*. 2003). Thus, CD147 is involved in reproduction, neural function, inflammation, tumour invasion, and human immunodeficiency virus infection (Pushkarsky *et al*. 2001; Toole *et al*. 2003; Dumitrescu *et al*. 2004) sharing similar physical and functional characteristics with 4F2hc. Both proteins (i.e. 4F2hc; CD147) are cell surface glycoproteins with a single transmembrane domain highly expressed on activated or proliferating cells, in addition are associated directly with transporters containing several transmembrane domains, and are required to bring those transporters (Monocarboxylate transporters, MCTs [CD147] or LAT1 [4F2hc] and related molecules) to the cell surface (Mastroberardino *et al* 1998; Kirk *et al*. 2000; Halestrap *et al*. 2004; Verrey *et al*. 2004). Xu and co-workers proposed a protein macro-complex model with 4F2hc bounded to CD147 in the core (Xu *et al*. 2005) (Figure 6). The union between both complexes (i.e. 4F2hc/LAT1 and CD147/MCT) was functionally co-regulated, which make sense in order that both are associated with nutritional transport and the serine/threonine kinase mTOR activity.

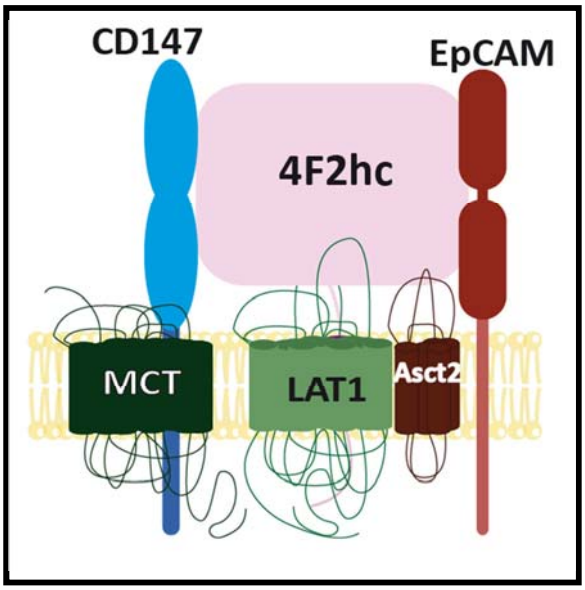

Figure 6. Scheme of the 4F2hc supercomplex. Xu and co-workers established a direct association between CD147 and 4F2hc. Also CD147 associates directly with MCT1 and MCT4, 4F2hc associates directly with LAT1, and EpCAM. Experiments suggested that ASCT2 could contact both CD147 and 4F2hc. Figure adapted from Xu *et al*. 2005.

7. HATs structure. General structural evidences

Very few structural evidences are found by the moment in bibliography for the heteromeric amino acid transporters. The most relevant structure, the extracellular domain of 4F2hc, was solved in 2007 by Fort and co-workers (Fort *et al*. 2007). The 4F2hc ectodomain sequence (Gabrisko *et al*. 2009) and also the ectodomain structure showed a great homology with bacterial α-amylases. Despite this homology, 4F2hc did not show glycosidase activity (Fort *et al*. 2007). Furthermore, none of the eukaryotic light subunits structures have been solved by the moment. The light subunits of HATs belong to the LAT (SLC7) family, within the large APC (Amino acid, Polyamide and Organocation) superfamily of transporters. The structure of LAT family is expected to be homologous with that of the sequence-related (<20% amino acid identity) AdiC (an arginine/agmatine antiporter from *Escherichia coli*) (Casagrande *et al*. 2008; Gao

et al. 2009; Fang *et al*. 2009; Gao *et al*. 2010; Kowalczyk *et al*. 2011 [PDB codes 3LRB, 3L1L and 3OB6]) and to the amino acid transporter ApcT (Shaffer *et al*. 2009 [PDB code 3GIA]) both belonging to APA family in APC superfamily. Surprisingly the folding of these proteins is shared by at least four other apparently non-sequenced-related families of transporters (Kowalczyk *et al*. 2011).

7.1. The crystal structure of the heavy subunit 4F2 ectodomain

The structure of the ectodomain of human 4F2hc was solved in our laboratory using monoclinic (Protein Data Bank code 2DH2) and orthorhombic (Protein Data Bank code 2DH3) crystal forms at 2.1 and 2.8A˚, respectively (Figure 7) (Fort *et al*. 2007). Fort and co-workers described the structure of 4F2hc-ED in terms of topology and multidomain organization of α-amylases (glycosyl hydrolase family 13 members), due to the high homology described with that enzymes (Janacek *et al*. 1997; Chillarón *et al*. 2001). The crystal structure suggested more similarities between 4F2hc and other α-amylases families, but despite the structural similarities found, the putative active site of 4F2hc presented major differences with respect to these enzymes. The crystal structure showed in 4F2hc-ED a deep and wide cleft, placing the highly conserved key catalytic residues of the A-domain present in many α-amylases. Therefore, the structure indicates that despite its general similarity to α-amylases, 4F2hc is not likely to have α-glycosidase activity. In fact, a detailed screening using D-glucose, D-galactose, or D-mannose derivatives of 4-methylumbelliferone as substrates failed to detect α-glycosidase activity. Accordingly, purified 4F2hc-ED showed no α-glycosidase activity for glucose-, galactose-, and mannose intervening substrates.

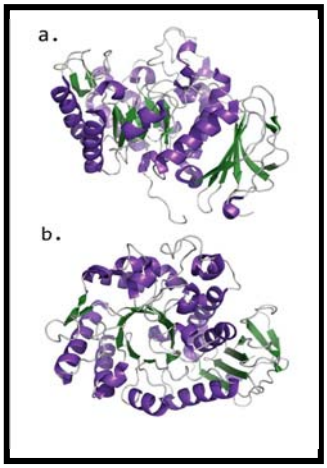

Figure 7. ***4F2hc-ED structure*** (i.e. monoclinic crystal). Lateral **(a.)** and upper **(b.)** view of 4F2 ectodomain. The structure related with α-glycosidases, including two domains: a TIM-barrel (α/β)8 and a C-terminal domain with eight antiparallel β-sheets.

7.2. 4F2hc tends to homodimerize (4F2hc/4F2hc)

Human 4F2hc overexpressed in several cell types (i.e. Hela cells, CHO-K1, *Xenopus* oocytes…) resulted in a disulfide bridge-linked homodimer showing a band around 190 KDa in SDS-PAGE. *In vivo* 4F2hc/4F2hc homodimers (i.e. overexpression in cells) are bound by a disulfide bridge via Cys109, the same residue responsible for heterodimerization of 4F2hc with its corresponding light subunits (Fort *et al*. 2007). In addition, Fort and co-workers crystallized homodimers of 4F2hc (Figure 8) (PDB 2DH3), in which a Zn^2 atom, presenting a tetrahedral coordination, was found at the interface of the two subunits.

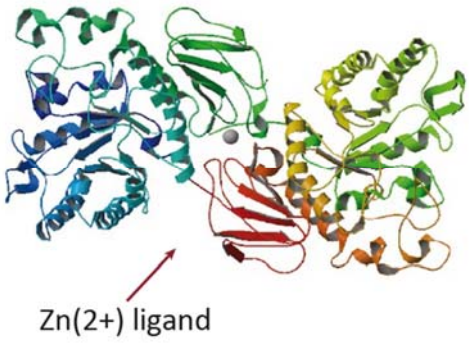

Figure 8. Homodimer of 4F2hc ectodomain. That was the s**econd crystallized structure** (i.e. orthorhombic) showed as a dimer with Zn(2+) (grey sphere) coordination at interface.

Supporting this structure, the tendency of 4F2hc to form homodimers was confirmed by cross–linking experiments *in vivo* (Fort *et al*. 2007) sharing the same architectural features with crystal homodimers (Fort *et al*. 2007). Nowadays if the homodimer of 4F2hc is an overexpression artefact or has a physiological role in nature (i.e. lymphocytes T activation [Haynes *et al*. 1981]) remains still unclear, in fact any homodimer has been found in normal tissues or tumours, suggesting that homodimerization is the result of 4F2hc overexpression. Fort and co-workers tried different strategies to abolish the presence of 4F2hc-ED/4F2hc-ED homodimers without success. In all, the crystal structure, optimal desolvation area analysis, and docking simulations revealed electrostatic interactions as the driving force for homodimerization. In contrast, 4F2hc-ED homodimerization in solution has not been demonstrated (Turnay *et al*. 2011). Apart from Cys109, human 4F2hc contains another cysteine residue, Cys330 which has a lateral side chain that in appearance is not accessible to the surface. Surprisingly, De la Ballina and co-workers demonstrated that Cys330 was a relevant hidden residue which intervening in a disulfide bridge with a hypothetic unknown protein in transfected Hela cells, forming a complex of around 200 KDa (De la Ballina. 2011). In all, these results suggest that homodimerization of 4F2hc only occurs when 4F2hc is expressed in the absence of associated light subunit and within cell membranes.

7.3. Proposed model of 4F2hc orientation in the membrane

The crystallized 4F2hc homodimer allowed proposing a model for the disposition of 4F2hc in the membrane based on charges and hydrophobicity interactions. The surface charges distribution displayed a marked positive surface in the N-terminus only four residues far from Cys109 disulfide bridge and the transmembrane domain. On base of this, the proposed model showed how the phospholipid polar heads of the plasma membrane interact directly with 4F2hc-ED by an electrostatic interaction (Figure 9), which is a characteristic of several peripheral and integral membrane proteins (McLaughlin and Aderem. 1995;

Bhatnagar and Gordon. 1997; Garnier *et al*. 1998; Conte and Matthews. 1998; Gelb *et al*. 1999; Resh. 1999; Mulgrew-Nesbitt *et al*. 2006). Thus, the provided information positioned the homodimerized heavy subunits (i.e. 4F2hc) in a similar angle with minimum variations suggesting a cellular membrane deformation to interact with the 4F2hc-ED positive charged surface (Figure 9).

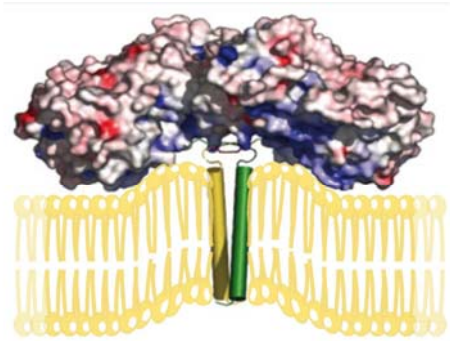

Figure 9. Model of 4F2hc homodimer interacting with membrane phospholipids. The positive face of the homodimer has a concave surface and 4F2hc-ED monomer is a rigid structure. The ectodomain homodimer deforms the phospholipid bilayer to adapt the structure.

In the case of monomeric 4F2hc, the lack of transmembrane domain in the crystal structure, lead to build a new model based on Glycophorine A, a transmembrane dimer found in red blood cells proposed as a general model for transmembrane proteins (Lemmon *et al*. 1994). Glycophorine A addition suggested a tilt of 90° probably found in nature as consequence of the transmembrane segment. In contrast, molecular dynamic studies (García R. and Orozco M. unpublished results) did not show any cavity of the plasma membrane. The proposed model (Figure 10) showed an ectodomain in contact with the plasma membrane phospholipids by the positive charged surface region. The hypothetic light subunit will be placed next to the heavy subunit, avoiding any close-interaction between both subunits (apart from the covalent union) and allowing the transport function of the light subunit.

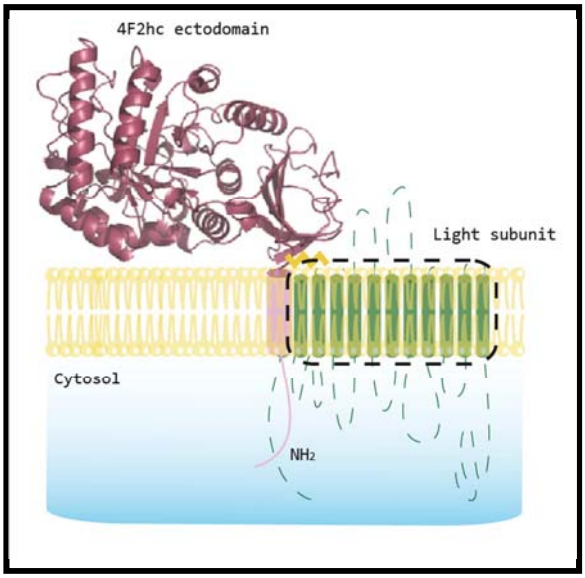

Figure 10. Proposed situation of 4F2hc respect the cellular membrane and the light subunit. The ectodomain is in contact with phospholipids by the positive charged surface region. The hypothetic light subunit is placed next to the heavy subunit (4F2hc) (Figure adapted from Fort. 2007).

8. AdiC, the prokaryotic structural paradigm of HATs

AdiC, an L-Arginine (extracellular)/ L-Agmatine (intracellular) antiporter in *Escherichia coli* and other enteric bacteria in extremely acid environments, is by now, the closest APC structural paradigm for LATs and the first 12 of the 14 transmembrane domains of CATs (~20% amino acid identity) (Kowalczyk *et al*. 2011). AdiC belongs to the APA family of transporters, which together the LAT family are two of the clever families within the APC transporters. The first structure of AdiC, at subnanometric resolution was reported in 2008 (Casagrande *et al*. 2008). In 2009, the first atomic structure of AdiC was determined (Gao *et al*. 2009 [PDB 3LRB] and Fang *et al*. 2009 [PDB 3NCY]) and represented the transporter in the open-to-out apo conformation, followed by the atomic structure of AdiC in the outward-facing L-Arginine bound conformation (Gao *et al*. 2010 [PDB 3L1L]). In short, our lab reported the crystal structure at 3.0 Å resolution of the L-Arginine-bound AdiC mutant N101A in the

open to out conformation, an intermediate state between the previous known AdiC conformations (Kowalczyk *et al*. 2011 [PDB 3OB6]). AdiC structure shared the "LeuT fold", initially described in a Na^{+}/Cl^{2}-dependent transporter from *Aquifex aeolicus* (i.e. LeuTAa) (Figure 11) (Yamashita *et al*. 2005).

8.1. The LeuT fold

The "LeuT fold" shares the same core domain of 10 transmembrane helices (i.e. TM1–10) with different symporters (i.e. LeuT [Yamashita *et al*. 2005], Mhp1 [Weyand *et al*. 2008], BetP [Ressl *et al*. 2009]and vSGLT [Watanabe *et al*. 2010]), despite to belong at different gene families. All of them have an inverted topology where TM1–TM5 is related to TM6–TM10 (TM1 - i.e. transmembrane segment 1) by an apparent two fold symmetry around an axis through the center of the membrane plane (Figure 11). In LeuT structure TM1, TM3, TM6 and TM8 built the affinity substrate core or pocket. TM1 and TM6 are oriented antiparallel to one another and are not continuous helices. In fact, TM1 and TM6 have breaks in helical structure at positions approximately halfway across the membrane bilayer. The same interruption, in greater dimensions, is found for the helical structure in TM6, adopting extended non-helical conformations. These two breaks expose main-chain carbonyl oxygen and nitrogen atoms for hydrogen bonding and ion coordination. The other two helices, TM3 and TM8, are long helices tilted by 50° from the membrane normal, are also related by the pseudo-two-fold axis and possess key conserved amino acid residues located near the unwound segments of TM1 and TM6. The remaining transmembrane segments surround TM1, TM3, TM6 and TM8, support the protein core and comprise most of the lipid-exposed LeuTAa surface.

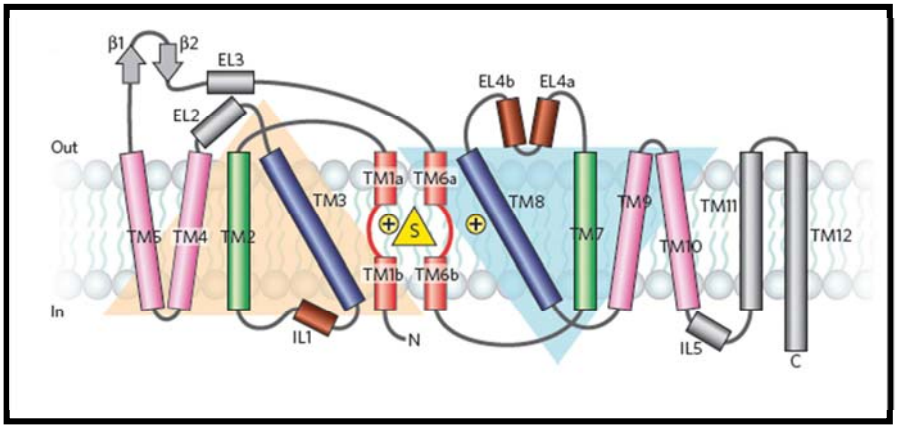

Figure 11. "Leu T fold" or "5+5 fold" scheme, where the inverted topology of TM1-TM5 and TM6-TM10 is represented. (TM, transmembrane) Figure adapted from Krishnamurthy et al. 2009

8.2. Amino acid substrate recognition and substrate occlusion in the periplasmic side of LeuT and AdiC.

Two transporters with solved LeuT-fold have been crystallized in the presence of their amino acid substrates, LeuT and AdiC, in the outward-facing conformations (i.e. interaction with the substrate from the periplasmic side) (Yamashita *et al*. 2005, Gao *et al*. 2010, Kowalczyk *et al*. 2011). In LeuT, the high resolution of the outward-facing L-leucine-bound occluded conformation structure (1.65 Å) allowed to show that L-leucine is completely dehydrated (Yamashita *et al*. 2005). Eric Gouaux lab (Yamashita *et al*. 2005) describes the substrate binding site as follows (Figure 12a): "L-leucine amino group is coordinated by main-chain carbonyl oxygens from Ala22 in TM1, Phe253 and Thr254 in TM6, and by a side-chain hydroxyl from Ser256 in TM6. The α-carboxy group interacts with a sodium ion, amide nitrogens from Leu25 and Gly26 in TM1, and a hydroxyl from Tyr108 in TM3. The aliphatic side chain of L-leucine is cradled within a hydrophobic pocket created by the side-chain atoms of Val 104 and Tyr108 in TM3, Phe253, Ser256 and Phe259 in TM6, and Ser355 and Ile359 in TM8". The resolution achieved (3.0 Å) in AdiC structure in the outward-facing L-arginine^{+}-bound occluded conformation of the double mutant N22A-L123W (PDB 3L1L) suggests that L-arginine is also dehydrated (Gao *et al*. 2010). The lab of Yigong Shi (Gao *et*

al. 2010) describes a similar recognition site for the amino acid substrate in AdiC (Figure 12b): "L-arginine is surrounded by five transmembrane helices: TM1, TM3, TM6, TM8 and TM10. At one end of the extended Arg molecule, the positively charged α-amino group donates three hydrogen bonds to the carbonyl oxygen atoms of Ile 23 in TM1, and Trp202 and Ile205 in TM6. The α-carboxylate group accepts two hydrogen bonds from the side chain of Ser26 and the amide nitrogen of Gly27, both residues located on the helix-breaking GSG motif of TM1. At the other end of L-arginine, the guanidinium group stacks against Trp293 in TM8, probably through cation–π interactions. In addition, the nitrogen atoms of the guanidinium group are located with approximate hydrogen-bond distance to four oxygen atoms in AdiC: the side chains of Ser357 in TM10 and Asn101 in TM3, and the carbonyl groups of Ala96 and Cys97 inTM3. In contrast to the charged head groups, the aliphatic portion of L-arginine interacts with the side chains of three hydrophobic amino acids, Met104 in TM3, and Trp202 and Ile205 in TM6".

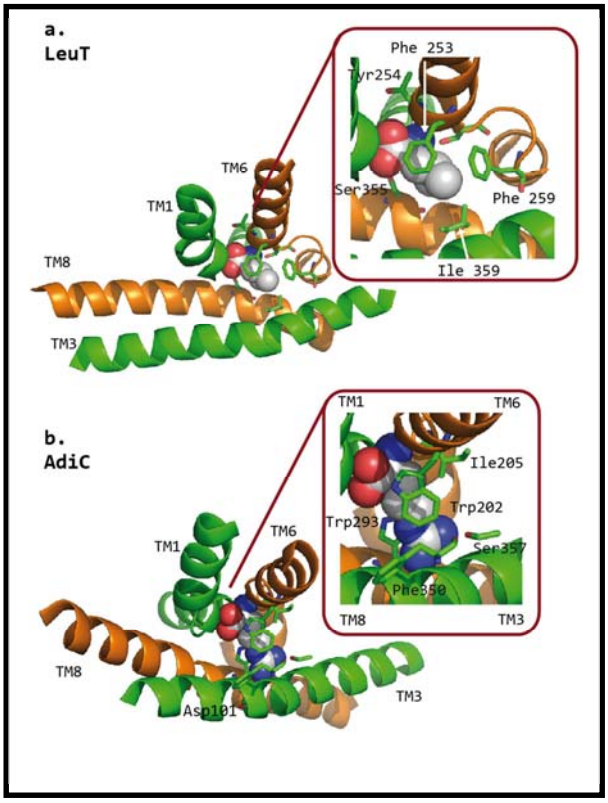

Figure 12. Susbtrate recognition in LeuT and AdiC in occluded conformation (LeuT PDB 2A65; AdiC PDB 3L1L). Is possible observe the relevant residues and the transmembrane segments (indicated in the image) recognizing the substrate (grey molecule) in LeuT (a.) and AdiC (b.). TM, transmembrane

Thus, both LeuT and AdiC recognize their amino acid substrates with, in general, a similar pattern: interaction of the α-amino carboxylate group with the unwound regions of TM1 and TM6 and of the lateral chain mainly with residues in TM8, TM3 and TM6. Indeed, the interaction of the lateral chain of the substrate is very alike between the two transporters: Tyr103 (TM3), Phe253 and Phe259 (TM6) and Ile359 (TM8) in LeuT, and Met104 (TM3), Trp202 and Ile205 (TM6), and Trp293 (TM8) in AdiC. It is worth mentioning that an aromatic residue in TM6 in both transporters occludes the lateral chain of the substrate, Phe253 in LeuT and Trp202 in AdiC. This is highly significant because LeuT and AdiC only share 10% amino acid sequence identity.

Our lab provided the first clues on the initial substrate recognition of LeuT-fold transporters from the extracellular medium with the open-to-out L-arginine-bound conformation of the AdiC mutant N101A at 3.0Å (PDB 3OB6) (Kowalczyk *et al*. 2011) (Figure 13). L-arginine^{+} docking to the open-to-out apo structure of AdiC (PDB 3LRB) Gao *et al*. 2009) showed only two residues with lateral chains interacting with the substrate, Trp293 (TM8) (π-cation interaction with the guanidinium group) and Asn101 (H bond with the guanidinium group) (TM3) (Kowalczyk *et al*. 2011). Then, mutations in Trp293 showed that only aromatic residues (i.e., Tyr and Phe) hold AdiC transport, even though reducing V_{MAX} to ~10% and increasing K_M to ~100μM (i.e. 3-fold increment). Mutations in Asn101 were more dramatic: N101A reduced V_{MAX} to around 1% and increased K_M to around 100μM (i.e., 3-fold increment). Interestingly, N101D variant recovered V_{MAX} to wild-type levels and kept the high K_M (around 100μM). This demonstrated functionally the π-cation interaction of Trp293 with L-arginine guanidinium group and highlighted the relevance of Asn101 for substrate translocation.

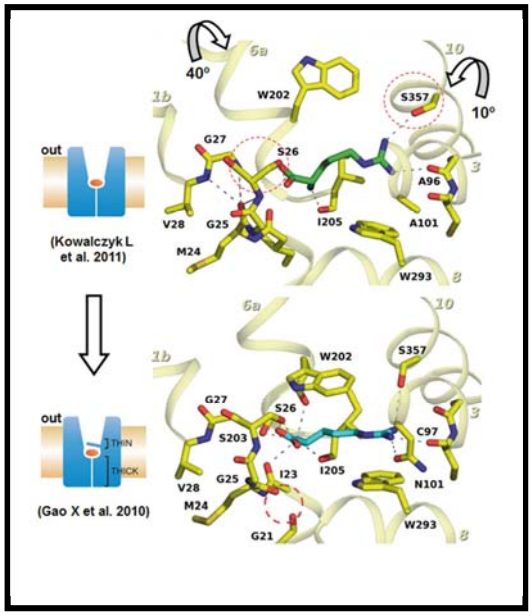

Figure 13. Proposed mechanism of Arg^+ recognition and induced fit by AdiC. Periplasmic Arg^+ is recognized by the apo conformation of AdiC (A; 3NCY) and binds with a similar orientation (B; 3OB6) as in the Arg+- occluded conformation (D; 3L1L). The proper Arg^+ binding samples the semioccluded state (C; docked Arg^+ in 3LRB) by stabilizing Trp202 (TM6a) and Phe350 (loop TMs 9–10) interaction. This semioccluded conformation evolves to the occluded state mainly by pivoting TM6a. Transition from the apo (A) to the semioccluded state (C) is defective in mutant N101A. TM segments are numbered in italics. (Kowalczyk *et al*. 2011)

The crystal structure of AdiC N101A revealed the open-to-out conformation with L-arginine bound with high mobility of the guanidinium group. Interestingly, the presence of L-arginine modified the orientation of the lateral chain of Ser26 (unwound region of TM1), as a first mechanism of induced-fitting in order to establish a H bond with the α-carboxylate of L-arginine in a similar pose like in the outward-facing L-arginine-bound occluded conformation (PDB 3L1L) (Figure 14). In contrast, L-arginine guanidinium group was displaced from Trp293 and closer to Ser357 (TM10) (Figure 14). These results suggested that Asn101 facilitates a proper interaction of L-arginine with Trp293 to trigger the transition from outward-facing to inward-facing. Thus, when residue 101 losses the capacity to H-bonding with L-arginine, the guanidinium group is misplaced and V_{MAX} is dramatically reduced. Interestingly, molecular dynamics (MD) also

showed the high mobility of L-arginine in the AdiC N101A structure between residues Trp293 and Trp202, whereas the position of L-arginine docked in the open-to-out apo structure of AdiC (PDB 3LRB) (Gao *et al*. 2009) is very stable (Kowalczyk *et al*. 2011). In the later structure, Trp202 (TM6) and Phe350 (loop TM9-TM10) have the orientation and distance of a π-π interaction, contributing to hold Trp202 in a rotamer closer to the substrate. Indeed, the presence of L-arginine freeze Trp202-Phe350 interaction (MD studies), which in turn might contribute to hold L-arginine (guanidinium group)-Trp293 (π-cation interaction) (i.e. semi-occlude state) (Figure 14) (Kowalczyk *et al*. 2011). This represents the second L-arginine-induced fitting mechanism (or conformational sampling) in the interaction of periplasmic L-arginine with AdiC. Transition from the semi-occluded state to the outward-facing L-arginine occluded state (PDB 3L1L) (Gao *et al*. 2010) occurs through 40° tilting of TM6a (i.e., the N-terminal part of TM6) and 10° tilting of TM10 towards the substrate. At present, MD analysis has not yet been able to reproduce this transition. In conclusion, Trp293 and Asn101, two residues that are totally conserved among APA family members, play a dual role in the transport cycle: first, by recognizing the substrate in the open-to-out state, and second by stabilizing the occluded conformation, which is a mandatory step in the transition to the inward-facing conformations.

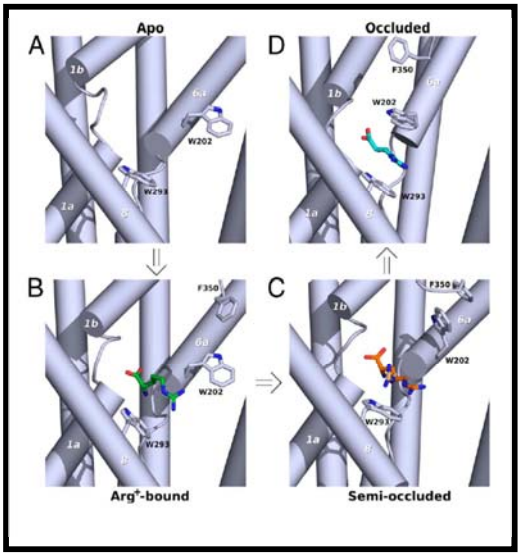

Figure 14. Transition from the semi-occluded state to the outward-facing L-arginine occluded state. The change occurs with a 40° tilt of TM6 and 10° tilt of TM10.

8.3. Transition of L-arginine-bound outward- to inward-facing conformations

When the substrate binds, the transporter undergoes changes not only at the level of internal residues, also, there is a general conformational change that makes the protein transit from outward to inward conformation (Figure 15). In the current transport cycle (Figure 15; Kowalczyk *et al.* 2011), initial recognition between the substrate and the binding site of the transporter in the ground state (open-to-in [PDB 2X79; PDB 2WSW] or open-to-out [PDB 2JLN;PDB 3LBR; PDB 3NCY] apo conformations) triggers the transition to a transient state (occluded [PDB 2A65; PDB 2JLO; PDB 3L1L; PDB 3DH4] or fully occluded state [PDB 2WIT; PDB 3GIA]), where the binding site is reorganized to attain an optimum fit with the substrate. AdiC represents by the moment, the initial substrate recognition state (open-to-out; PDB 3LRB), the substrate-bounded open outward-facing conformation (PDB 3OB6) and the substrate-bounded closed outward-facing conformation. Indeed, among this class of transporters, CaiT has also been crystallized in the initial substrate recognition state (open-to-in; PDB 2WSW) and the transient substrate-bounded open inward-facing conformation (PDB 3HFX), but not in the inward-facing occluded state.

Thus, in the current transport cycle of LeuT fold-transporters (Figure 15), an inward-facing state corresponds to each outward-facing state and both are symmetrical (it was found for the crystal structures of Mhp1 apo states; PDB 2JLN and PDB 2X79) which make easy to hypothesize that the symmetry is leading the transport cycle. In particular, fully occluded states represent the most symmetrical arrangement as they correspond to the edge of the transition between outward- and inward-facing conformations.

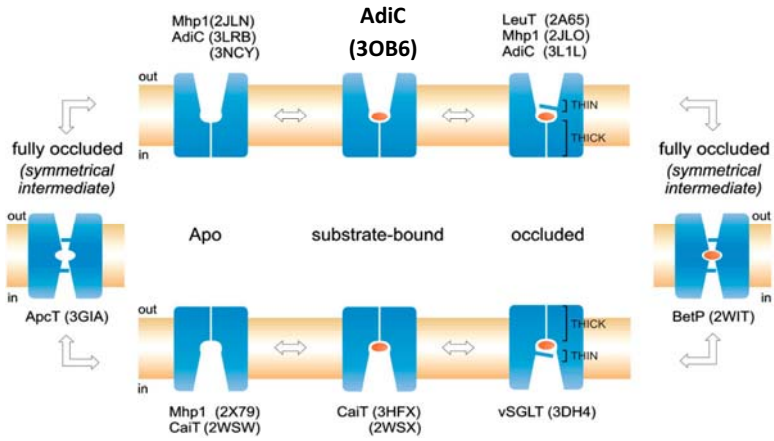

Figure 15. Symmetrical states along the alternative access mechanism of transporters with the "LeuT fold". Transporters from 5 families with 10% amino acid sequence identity between them, share this protein fold: the Neurotransmitter: Sodium symporter (LeuT), Nucleobase: Cation Symporter-1 (Mhp1), Solute: Sodium Symporter (VSGLT), Betaine/Carnitine/Choline Transporters (BetP, CaiT) and Amino acid, Polyamide and organocation transporters (AdiC, ApcT). Upon substrate (red ellipsoid) binding to the open-to-out apo state, the substrate-bound state (3OB6 AdiC structure) evolves to an occluded state, where two gates (thick and thin) prevent the diffusion of the substrate to either side of the membrane. Occlusion of the substrate by a thin gate is a common mechanism in the transport cycle of these transporters, in spite of involving different molecular events, as described for LeuT, vSGLT, Mhp1, BetP, and AdiC. The inward-facing states are symmetrically related to the outward-facing ones. Transition to the inward-facing states requires a transient fully occluded symmetrical intermediate. In antiporters (AdiC and CaiT), the return to the outward-facing states requires the binding and translocation of a new intracellular substrate that will move the transporter back through all the states but in the opposite direction (Figure provided by Kowalczyk *et al*. 2011)

The transmembrane segments location in the LeuT fold is fairly well defined, among the outer ring of helices, symmetry-related TM4 and TM5, and TM9 and TM10, form inverted V-shaped pincers that cradle the interior pair of TM3 and TM8, whereas TM2 and TM7, also related by the two-fold axis of symmetry, link TM1 and TM6 with the intracellular and extracellular helix–loop–helix structures, IL1 and EL4 (Figure 16). It is suggested that the outer ring of helices, which nestles around the interior pairs, provides a framework to stabilize the transporter within the lipid membrane, and that it couples conformational changes on one side of the membrane to movements on the other side (Yamashita *et al*. 2005).

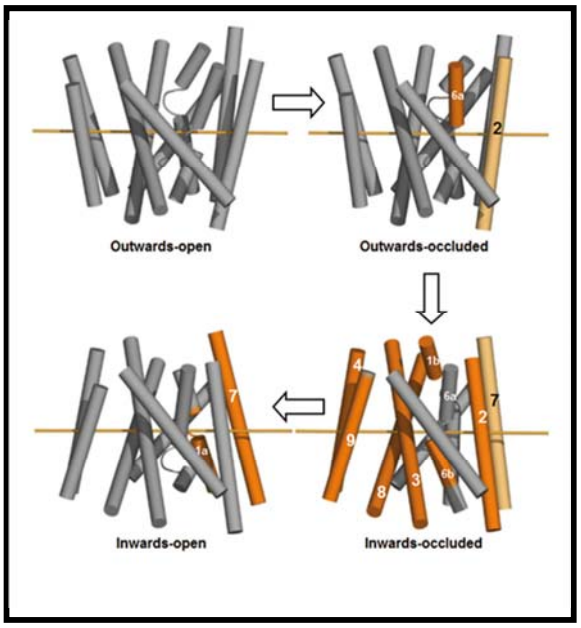

Figure 16. Proposed conformational changes in AdiC transmembrane domains. According to the two axis symmetry from outwards conformation to inwards conformation (Image provided by Prof. Palacín).

Thus, in contrast to the inner changes associated with residue and substrate binding, the isomerization between the outward-facing and inward facing states involves larger-scale conformational changes spread throughout the transporter carried out by transmembrane helices packed close together (i.e. TM1, TM3, TM5, TM6, TM8, and TM10) in combination with extracellular and intracellular loops such as N termini, IL1 or EL4. Gasol and co-workers had already observed that, surprisingly in the topology of xCT, the internal loop 1 (IL1) had residues in contact with the extracellular side (Figure 20 [Gasol *et al*. 2004]). According with the known open-outward structures, the IL1, is the responsible to occlude the intracellular face (i.e. LeuT PDB 2A65 or AdiC PDB 3OB6/3L1L), acting as "floor" of the binding pocket, and based on the two-fold axis symmetry we would expect that EL4 will act exactly the same when the intracellular gate is closed and the extracellular gate is open (Figure 17 [Krishnamurthy *et al*. 2009]).

Actually, in the topology of LeuT is possibly to observe that EL4 is partially embedded in the cellular membrane as IL1, pointing to a similar function in the inward conformation (Figure 17).

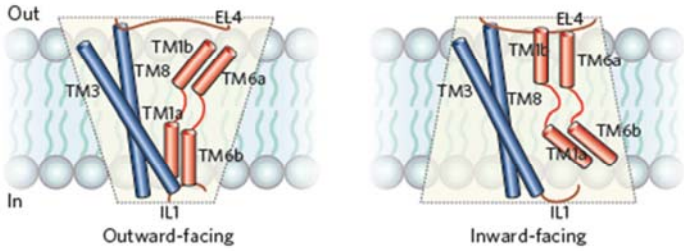

Figure 17. Position of the external loop 4 (EL4) and the internal loop 1 (IL1) from outward to inward conformation. In the figure is possible to observe the role of EL4 and IL1 acting as lids that seal the extracellular and intracellular gates in their closed states, as indicated. The outward-facing corresponds to the arrangement of central helices in substrate-bound LeuT and the inward-facing to the arrangement of central helices in substrate-bound vSGLT. TM1 and TM6 rotate approximately 37° relative to TM3 and TM8 in transitioning from the outward-facing state adopted by LeuT (outward facing) to the inward-facing state adopted by vSGLT (Image property of Kirshnamurthy *et al*. 2009).

The tilt of TM6 is the most important conformational change suffered from the open-outward (PDB 3OB6) to the close-outward conformation (PDB 3L1L). The EL3 (i.e. external loop between TM5 and TM6) is the longest external loop (around 20 residues) in AdiC structure, which is necessary in order than TM5 is located in the ring of helices cradling the interior loops, meanwhile TM6 is located in the core centre (i.e. TM1 and TM6). The dramatic change in the angle of TM6 (around 40°) should stretch the EL3 caused by the conferred stress which may modify the location of the loop apex (Figure 18). Actually, if the amino acid alanine 180 (A180) is analysed in the occluded-outward conformation (PDB 3L1L) it is found a shift of 8.42Å respect the open-outward conformation (PDB 3OB6) (Figure 18). The same behaviour is expected in HATs (Gasol *et al*. 2004), due to they may share the LeuT fold with their prokaryotic homologues. It is not clear if these conformational changes will affect HATs in a different way, in order heteromeric transporters are linked with a heavy subunit. If the conformational change in the loop EL3 could induce any kind of effect will be discussed later.

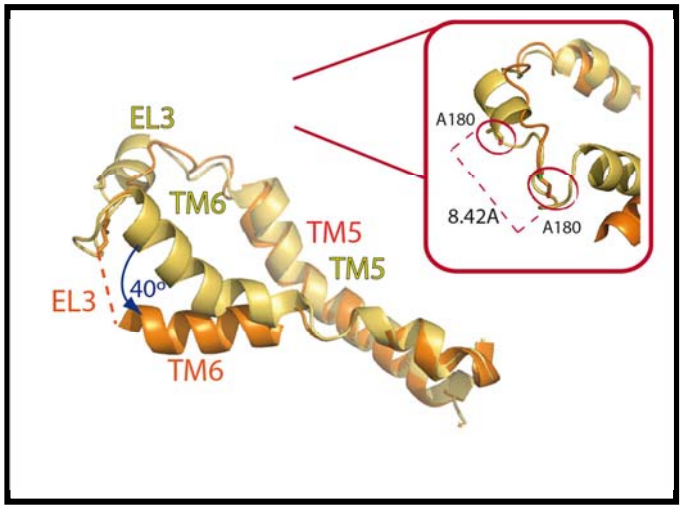

Figure 18. **AdiC representation of transmembrane 6 tilt in open to close outward conformation.** It is possible to observe how the external loop 3 must to change it location due to the extra-stress caused by the TM6 movement from **open (in orange) to close (in yellow).** The Alanine 180 (A180) is placed 8.42Å from open to close conformation as indicated.

Other external loops as EL1 where analysed, in order to TM2 has a small movement (around 10° tilt) during the process (i.e. open-occluded outward conformation) but any of their residues changed or was shifted (Figure 19 (a)). The same occurred with EL5, which is quite long (around 11 amino acids) or EL4 (around 22 amino acids), but again, any residues shift was found (Figure 19 (b)).

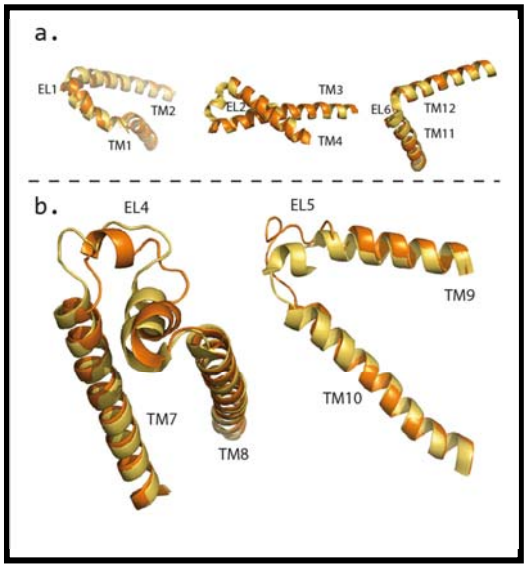

Figure 19. Representation of external loops in AdiC structure in open and occluded –outward conformation. (a) EL1, EL2 and EL6 did not show any difference. **(b)** EL4 and EL5 were longer than the other external loop but did not show any difference when some amino acid residues where analyse (EL; external loop); Open (in orange), Occluded (in yellow).

9. Similitudes with eukaryotic HATs

The structure of those prokaryotic transport proteins is providing with new and surprising information around the LATs, and is expected to find a similar "LeuT" fold in eukaryotic structures. The topology of xCT was the first model in provide real information about eukaryotic light subunits by performing a cysteine scanning accessibility study (Gasol *et al*. 2004). Now is possible to gather all the known information about the catalytic subunits of amino acid transporter and check the similitudes between topology and solved structures. The Substituted Cysteine Accessibility Method (SCAM) assay carried out by Gasol and co-workers in our laboratory was based in punctual mutations of specific residues to Cysteine in an xCT cys-less protein, these residues were biotinylized one by one. With that method, was described a re-entrant loop in IL1 (Figure 20), coinciding with the fact that IL1 in prokaryotic homologues is the bottom lid of the

transporter located just in the translocation pathway. Later, De la Ballina and co-workers continued the study of topology in xCT and found another re-entrant loop in the IL4 which is located between TM8 and TM9 (De la Ballina. 2011). However the explanation for the re-entrant IL4, in which the residues in the apex where labelled from outside, was unclear due to the discordance with the structural models, in which all these residues were embedded in the membrane. The only explanation will remain in the rotation of TM8 making the IL4 closer to the translocation pathway. This fact only could be possible in case of a change of conformation triggered by the 3-(N-maleimidylpropionyl) biocytin (BM) agent used in SCAM or the possibility to capture the protein in different conformation promoted by a method on life cells.

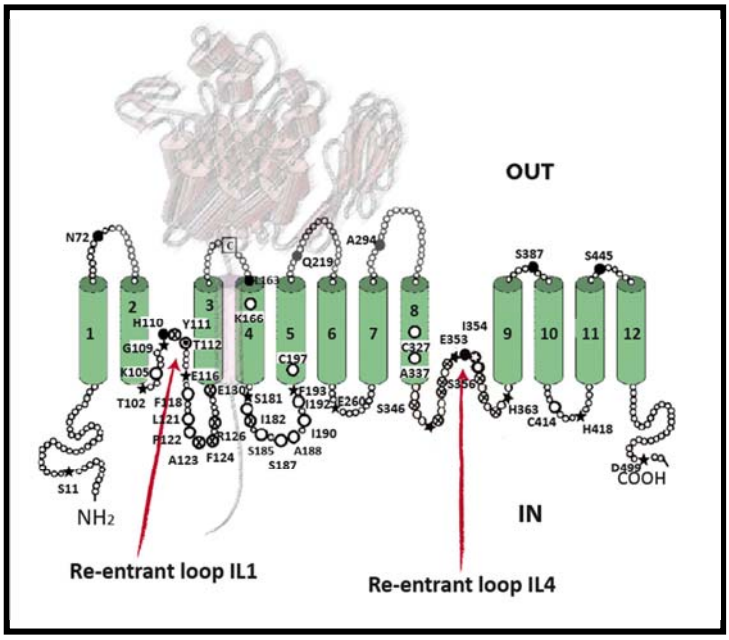

Figure 20. Topological model of human xCT. The 12 transmembrane domains are numbered, and the re-entrant loop is marked with a red arrow. The *dark circles* indicate biotinylation from outside, and the *stars* indicate biotinylation from inside. The *large white circles* indicate no biotinylation even after permeabilization, and the *crossed circles* indicate very low activity when substituted by cysteine (~25% of His-Cys-less xCT). Cys158 involved in the disulfide bridge with 4F2hc is indicated with a *C* in a *square*. The hypothetical heavy subunit is drawn in light pink. Figure adapted from Gasol *et al*. 2004 and De la Ballina. 2011.

10. Importance of eukaryotic heteromeric amino acid transporters.

The aim of this study was to find structural evidences of eukaryotic HATs, isolating pure protein and performing crystallographic methodologies, which is highly complicated due to the poor stability behaviour of eukaryotic membrane proteins. Thus, the expression of one of these heterodimers could help us to understand the real relationship between light and heavy subunits, in order that by now, only the structure of 4F2hc ectodomain is available and the most similar light subunit homologous structure is AdiC, with only a 15% of sequence homology. The study of the HATs substrate binding mechanism, the full transport cycle, the real effect of the known mutations involved in diseases (cystinuria or LPI), the relative position between the heavy and the light subunit in the heterodimer and the consequent role of the heavy chain in transport, are some of the questions remaining unknown by the moment. Apart from that, the structural information may let docking studies with integrins and other proteins that may interact with 4F2hc. In order to express these proteins with final structural purposes, we chose the yeast *P.pastoris* as expression system.

11. Why *Pichia pastoris* as expression system?

Currently, the search for eukaryotic membrane protein structures with a higher identity with human proteins has been a target with infructuous results. The difficulty to keep the protein folding integrity in an adequate expression system has been one of the most important reasons due to many proteins end up as inactive inclusion bodies in bacterial systems. Thus, the number is increased dramatically when we are talking about membrane proteins. In fact there are only few examples of mammal membrane proteins and none of them are transporters. *Pichia pastoris* is a single-celled microorganism easy to manipulate and easy to grown in culture with some advantages and disadvantages over bacteria. It is also an eukaryote organism with all the privileges associated, is capable of many of the post-translational modifications performed by higher

eukaryotic cells such as proteolytic processing, folding, disulfide bond formation and glycosylation. One of the major advantages is that can be grown to very high densities, which makes them especially useful for the production of membrane proteins for crystallization. The yeast system is generally faster, easier, and less expensive than expression systems derived from higher eukaryotes such as insect and mammalian tissue culture cell systems and usually gives higher expression levels (Reviewed by Cregg *et al*. 2009). Based on the work of Mackinnon with a potassium rat channel (Long *et al*. 2005), Dr. Rosell set up in our laboratory the expression of the eukaryotic HATs in *Pichia pastoris*. Among eukaryotic microbial systems, *P. pastoris* stands out as a successful expression host to obtain recombinant transmembrane α-helical proteins for which high-resolution structures have been successfully solved (Table 3).

There are numerous reviews describing the system, the Pichia Expression Kit Instruction Manual (Invitrogen Corporation, Carlsbad, California) is a very complete and effective instructor. On the other hand, web sites provide additional strains and vectors that can be obtained (http://www.invitrogen.com; and http://faculty.kgi.edu/cregg/index.htm).

Protein	PDB code	Resolution	Reference
Kv1.2 voltage-gated potassium channel: *Rattus norvegicus*	2A79	2.9 Å	Long et al. 2005
Kir2.2 inward-rectifier potassium channel: *Gallus gallus*	3JYC	3.1 Å	Tao et al. 2009
Voltage-gated potassium channel subunit beta-2 : *Rattus norvergicus*	3LNM	2.9 Å	Tao et al. 2010
AQP4 aquaporin water channel: human	3GD8	1.8 Å	Ho et al. 2009
AQP5 aquaporin water channel (HsAQP5): human	3D9	2.0 Å	Long et al. 2007
SoPIP2;1 plant aquaporin: *Spinacia oleracea*	1Z98	2.1 Å	Long et al. 2005
Aqy1 yeast aquaporin: *Pichia pastoris*	2W2E	1.15 Å	Fischer et al. 2009
Leukotriene LTC4 synthase in complex with glutathione: human	2UUH	2.15 Å	Martinez et al. 2007
P-Glycoprotein: *Mus musculus*	3G5U	3.8 Å	Aller et al. 2009
Glioma pathogenesis-related protein 1: Homo Sapiens	3Q2R	2.2 A	Asojo et al. 2011

Table 3. **3D- Crystallyzed eukaryotic membrane proteins produced in Pichia pastoris**. Solved structures (Updated from Ramón and Marín. 2011; source http://pdbtm.enzim.hu/)

Objectives

Background

This study was started at 2005 by Dr. Rosell, which attempted the heterologous expression of the human rBAT ectodomain in *E. coli* with the aim to solve its atomic structure. Dr. Rosell used different E..*coli* strains and various expression vectors, however, rBAT was expressed as inclusion bodies in all cases. For this reason, Dr.Rosell changed the expression system, choosing the methylotrophic yeast *Pichia pastoris* due to the success obtained for different groups in the expression of eukaryotic membrane proteins using this organism (Long *et al.* 2005). Thus, the human heavy subunits rBAT and 4F2, the human light subunits asc1, LAT1, LAT2, y^+LAT1, y^+LAT2, xCT and $b^{0,+}$AT, and four human heterodimers (4F2hc/asc1, 4F2hc/LAT1, 4F2hc/LAT2, 4F2hc/xCT) were cloned into the pPICZ vector. At 2007, Dr. Rosell had managed to set up the expression of the aforementioned proteins in *Pichia*, at the time the author of this thesis joined to the project.

The objectives corresponding to the present work were:

(I) To overexpress in the methylotrophic yeast *Pichia pastoris* the human HATs: the heavy subunits (rBAT and 4F2hc), the light subunits (asc1, LAT1, LAT2, y^+LAT1, y^+LAT2, xCT and b^{0+}AT) and different heterodimers (4F2hc/asc1, 4F2hc/LAT1, 4F2hc/LAT2, 4F2hc/xCT).

(II) To check the functionality of LAT2 and 4F2hc/LAT2 by transport assays in whole cells and after protein reconstitution in liposomes.

(III) To get the 3D structural model of the 4F2hc/LAT2 heterodimer by single-particle negative-staining analysis.

Results

Working in membrane proteins crystallography is considered nowadays as a long and hard journey, and even more if we think in eukaryotic proteins. During the first stages of the experimental study, the main goal is find a stable protein which accomplishes different characteristics, (i) a protein expressed in high levels in the hosted system, (ii) a protein stable and functional in an extremely purity state, and finally (iii) a pure protein which conserves at the end of the process enough amount to carry out all the possible crystallization trials. When all these parameters are accomplished, a crystal will grow, with the hope to get a clear and ordered diffraction pattern. Currently, laboratories working with eukaryotic membrane proteins around the world have been adapted to start the process with a large number of possible candidates.

1. Human HATs expression trials

Thirteen human HATs were expressed in the methylotrophic yeast *Pichia pastoris* (considering heavy/light subunits and heterodimers separately) based on the results of the potassium channel crystallization in Mackinnon´s lab (Long *et al*. 2005). Always working in small volume cultures (with a final volume of rich medium BMMY, 3 ml), heavy subunits (i.e. 4F2hc, rBAT), light subunits (i.e. LAT1, LAT2, y^+LAT1, y^+LAT2, xCT, asc1, b^{0+}AT) and the heteromeric forms (i.e. 4F2hc/asc1, 4F2hc/LAT1, 4F2hc/LAT2 and 4F2hc/xCT) were expressed in optimal conditions (EasySelect™ *Pichia* Expression Kit, Invitrogen). The expression level of each one was checked by Western Blot using antibodies against StrepTag II (i.e. light subunits), 4F2 ectodomain (anti-CD98 (H-300); SantaCruz biotechnology) and rBAT (Furriols *et al*. 1993), rejecting the proteins in which the band was hardly visible.

1.1 Light Subunits of HATS

The expression levels of 6-8 clones were tested by western blot for each of these seven candidates (i.e. asc1, xCT, b0+AT, y^+LAT1, LAT1, LAT2 and y^+LAT2). After

these experiments, asc1, xCT, b0+AT and y^+LAT1 were discarded while LAT1, LAT2 and y^+LAT2 passed to the following step as promising candidates (Figure 21).

A.

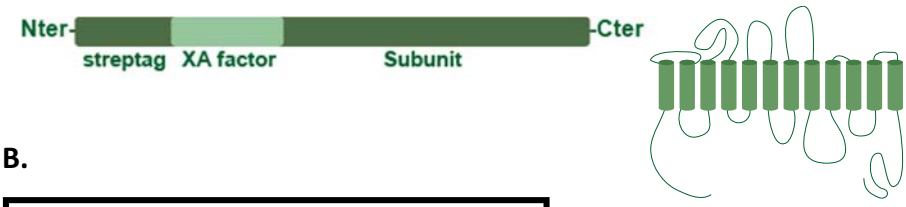

B.

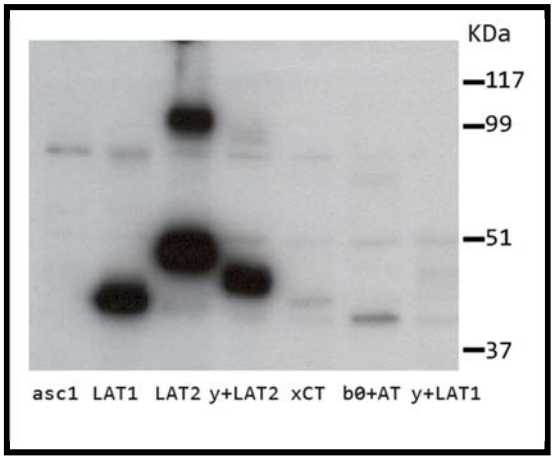

Figure 21. (a) Recombinant light subunits Scheme (b) Western Blot (anti-streptag) of the light subunits expression levels. *1.* asc1, *2.* LAT1, *3.* LAT2, *4.* y+LAT2, *5.* xCT, *6.* b^{0+}AT, *7.* y+LAT1. In all cases 5µg of total protein per well was charged. In the case of LAT2 (3rd well) some homodimer LAT2/LAT2 was revealed (~100 KDa).

1.2. Heavy subunits of HATS

Both human heavy subunits (rBAT and 4F2hc) were tested and in both cases the protein was expressed although the expression levels for 4F2hc were clearly higher. These heavy subunits are glycosylated proteins and in the case of human 4F2hc, it contains four putative N-linked glycosylation sites (i.e. Asn264, Asn280, Asn323 and Asn405). Carbohydrate chains are troublesome principally due to the heterogeneity that confers to the sample and the interferences that they could cause in the crystal formation process, due to the possibility to obstruct any inter-molecule contact zone. Thus, human 4F2hc glycosylation sites were

removed changing the Asparagine (Asn) to Glutamine (Gln; very similar but with an extra methylene group), in all the cases. 4F2hc was revised in both forms, glycosylated and unglycosilated (Figure 22).

A.

B.

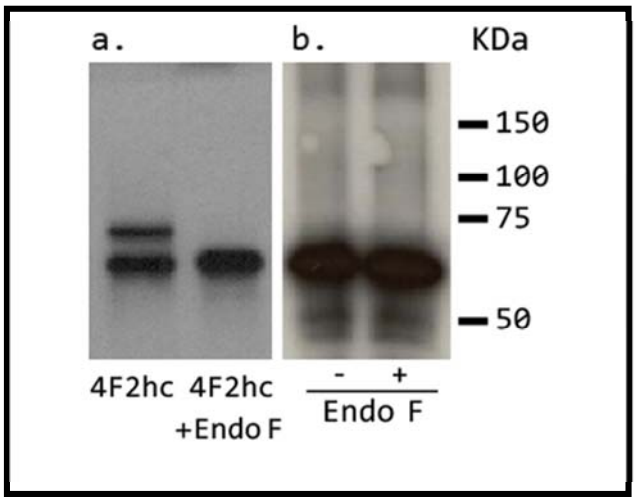

Figure 22. (A) Recombinant heavy subunits design. (B) Western Blot using anti-CD98 (H-300) to test the expression of 4F2hc. **(a.)** Glycosilated 4F2hc , two bands are appreciated. Adding EndoF to the same 4F2hc sample (1h; 37°C) only one band remains. The upper band (~80 KDa) corresponds with the glycosilated form of 4F2hc and the lower band (~70 KDa) with the unglycosylated form, accordingly this upper bands disappeared upon EndoF treatment. **(b.)** Western Blot to check the expression of mutated 4F2hc in the four glycosylation sites. In this case, only unglycosilated 4F2hc was expressed. Adding EndoF or not, the bands appeared at the same molecular weight indicating that the unglycosilated form was successfully cloned. 5µg of total protein was charged in each well.

1.3. Heterodimers

Four different heterodimers, all based in 4F2hc heavy chain, were cloned successfully (i.e. 4F2hc/asc1, 4F2hc/LAT1, 4F2hc/LAT2 and 4F2hc/xCT), choosing the best expression clone from 6 - 8 for each heteromeric protein. Both, anti-

4F2ed and anti-streptag antibodies detected the heterodimers. In the analysis of the heterodimers, DTT (Dithiothreitol) is usually added as a control, so when DTT is added the disulfide bridge connecting the heavy and the light subunit is broken and two bands of a lower molecular weight must appear (Figure 23). The heterodimer 4F2hc/LAT2 was considered a good candidate to pass to the following step, the solubilization. 4F2hc/LAT1 and 4F2hc/asc1 were expressed in *P.pastoris* (Figure 23 [a] and [b]) but the small amount precluded further studies with this expression system. 4F2hc/xCT was not expressed in *P.pastoris*.

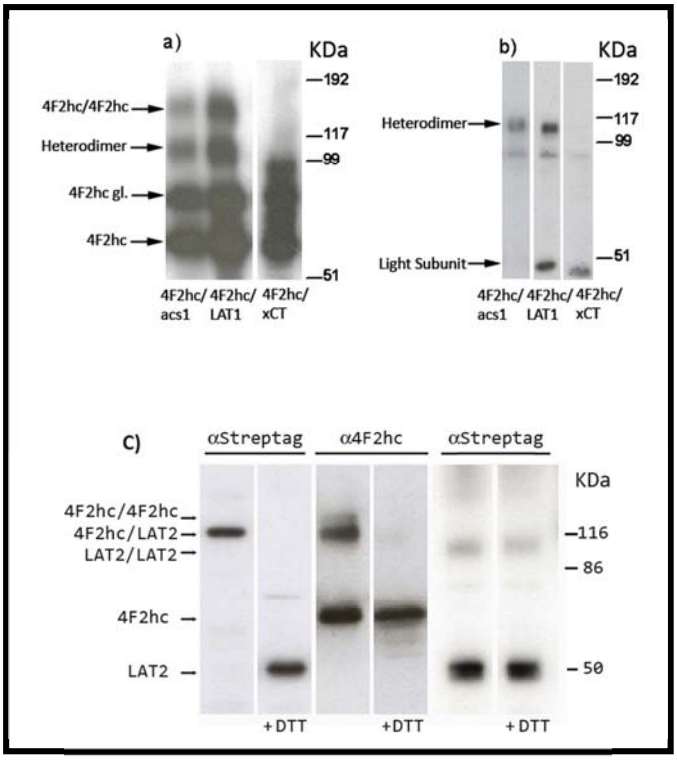

Figure 23. Western Blot analysing human 4F2hc/asc1; 4F2hc/LAT1, 4F2hc/xCT and 4F2hc/LAT2. The expression of the protein was analysed using anti-4F2 **(a)(c)** and anti-streptag **(b)(c). a)** 4F2hc/asc1 and 4F2hc/LAT1 bands appeared at ~100 KDa meanwhile 4F2hc/xCT is not present. The other low bands correspond with the heavy subunit 4F2hc in different glycosilation states. The upper band corresponds with the homodimer 4F2hc/4F2hc. **b**) The band of the heterodimer is seen detecting the light subunit. We can observe that 4F2hc/asc1 and 4F2hc/LAT1 are present but 4F2hc/xCT is absent again. **c)** The expression of the protein was analysed using anti-streptag and anti-4F2ed antibodies as indicated. In absence of DTT when using anti-streptag antibody, only one band corresponding to the heterodimer (~120 KDa) is visible. This band felt down to ~50 KDa when DTT was added. When using anti-4F2ed antibody 4F2hc/4F2hc dimer (~140 KDa), 4F2hc/LAT2 heterodimer (~120 KDa) and 4F2hc monomer (~70 KDa) were visible. The addition of DTT reverted in monomers as the only species of 4F2hc were visible in the gel. These results are in agreement with previous reports showing that overexpression of human 4F2hc in HeLa cells resulted in homodimers linked by a disulfide bridge (Fort *et al.* 2007). In the western blot also is possible to observe the light subunit LAT2 (antibody anti-streptag) as indicated, only the light subunit band is present, in absence or presence of DTT. 5μg of protein was added in each well.

2. Detergent screening solubilization

With the aim to extract the proteins from the membranes and check the stability, solubilization conditions were tested for the best expressing human light subunits, LAT2, LAT1 and y^+LAT2. Representative detergents based on literature were selected, mild detergents as DDM (one of the most popular detergents), DM (shorter than DDM), crystal-friendly Cymal 7 and the most aggressive detergent in the group, Foscholine 10. The experiment was set up in small volumes of 300 µl, 1h at 4°C always with a concentration of 1mg/ml of total protein and adding different concentrations of detergents. The solubilization ratio was checked by Western Blot comparing the soluble fraction (solubilized protein) *versus* pellet (aggregated protein and inclusion bodies) after an ultracentrifugation of 250,000 g for 1 hour at 4°C.

2.1. Light subunits of HATS

LAT1, LAT2 and y^+LAT2 were all well-expressed as separated light subunits, showing LAT2 the best amount of total protein, as already described in Figure 21. A Western Blot was carried out to compare the soluble fraction with the pellet (non-solubilized protein) (Figure 24) after solubilization at different detergent concentrations (DDM from 0.1% to 1%, DM from 0.5% to 4%, Foscholine10 from 0.5% to 4%). DDM and Foscholine10, had the better solubilization rate in the case of LAT2 (Figure 24 [a]). DDM was chosen as the referent detergent since Foscholine10 is able to solubilize non-functional membrane proteins. LAT1 was solubilized successfully again with DDM and Foscholine10 (Figure 24 [b]). Using DM and Cymal 7 the solubilized protein showed tendency to aggregate. In any case the recovered amount of protein was too low to continue with the assay. y^+LAT2 was impossible to solubilize with none of the detergents used (Figure 24 [c]).

In summary only human LAT2 showed a good combination of significant expression levels in *P.pastoris* and solubilization by detergents for further studies.

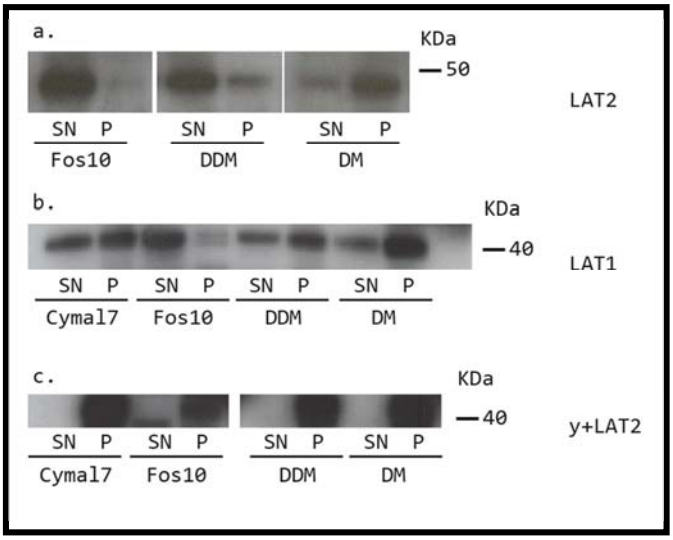

Figure 24. **Detergent screening for the solubilization of human LAT2, LAT1 and y$^+$LAT2.** Three different detergents were tested, having DDM and FosCholine10 the best results in most of the cases, while DM and Cymal 7 were less effective. Y$^+$LAT2 was not solubilized in any of the cases. All the detergents were used at 1% concentration. SN, supernatant. P, pellet.

Following these results, different total protein concentrations were tried in order to see the interference with the solubilization ratio. Thus, different protein concentrations, 1, 3 and 5mg/ml where solubilized in DDM 2% (standard buffer based in Tris 20mM) during 1 hour (see Material and Methods "8. Solubilization trials"). The measurement was done comparing the supernatant and the pellet after one ultracentrifugation of 1h at 4°C, 250.000 g, and analysed by Western blot (Figure 25). Finally the solubilization efficiency was the same in all the cases, allowing increased concentrations of total protein during the solubilisation process.

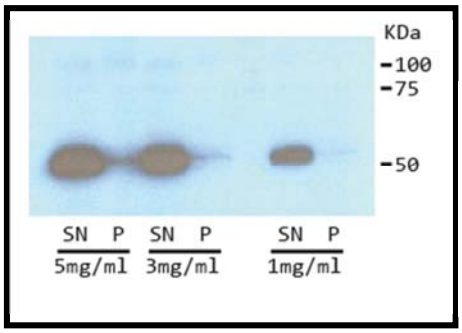

Figure 25. LAT2 solubilization efficiency increasing protein concentration. (1 mg/ml, 3 mg/ml and 5 mg/ml), the solubilization efficiency of LAT2 by 2% DDM was good in all cases.

2.2. Heavy Subunits of HATs

Good results were obtained for 4F2hc with all the detergents showing this protein a stable behaviour. Again DDM was chosen to continue with the assays, always thinking in a future solubilization improvement (Figure 26 [a]). In contrast to 4F2hc, none of the *Pichia pastoris* clones expressing human rBAT yielded protein able to be solubilized with DDM, DM, Foscholine10 or Cymal7 (Figure 26 [b]). rBAT results are endorsed by the results of Bartoccioni and co-workers, in which, the instability of expressed rBAT in MDCK cells only was improved in the presence of the corresponding light subunit partner, b^{0+}AT (Bartoccioni *et al*. 2008).

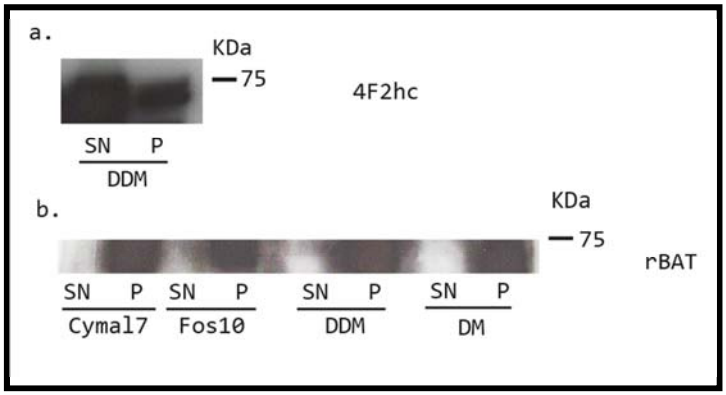

Figure 26. Detergent screening for the solubilization of human 4F2hc and rBAT. Western Blot anti-histidines to check 4F2hc **(a)** and rBAT **(b)** solubilization was performed. 4F2hc solubilization with DDM 1% was successful solubilizing approximately 50% of the expressed protein, which represents enough material for further purification steps. None of the tested detergents solubilized rBAT at 1% concentration. SN, supernatant. P, Pellet.

In addition, the solubilization of human 4F2hc with 2% DDM (i.e. around 50%) of total protein concentration tested (i.e. 1,3,5 mg/ml) (Figure 27) indicated the possibility to use high protein concentrations during the solubilisation process.

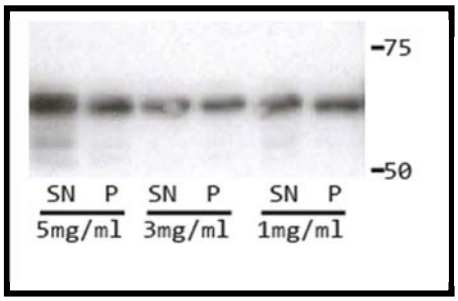

Figure 27. 4F2hc solubilization efficiency increasing protein concentration. Solubilization adding 2% of DDM at the indicated total protein concentration.

SN, supernatant. P, pellet.

2.3. Heterodimers

The only heterodimer analysed for solubilization conditions was 4F2hc/LAT2 due to the good expression levels obtained.

2.3.1. 4F2hc/LAT2

Surprisingly, the heterodimer 4F2hc/LAT2 was full solubilized (100%) in 1% DDM, the amount of protein was enough to further functional structural studies (Figure 28).

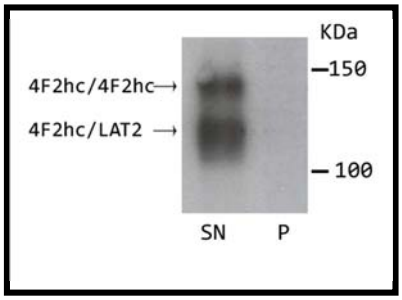

Figure 28. Western Blot of the heterodimer 4F2hc/LAT2 solubilized with DDM 1% (anti- 4F2hc antibody). The upper band corresponds to the homodimer 4F2hc/4F2hc and the lower band corresponds to the heterodimer 4f2hc/LAT2 (~120 KDa). The amount of protein per well was 5µg. SN, supernatant. P, pellet.

The solubilization yield for the light subunit LAT2 was 50% meanwhile the solubilization rate for the heterodimer 4F2hc/LAT2 was 100%. This difference

could be explained by the presence of the heavy subunit 4F2hc which may confer a folding advantage to the heterodimer.

3. Summary of the expression and solubilization of human HATs expressed in *Pichia pastoris*.

Clearly, the light subunit LAT2, the heavy subunit 4F2hc and the heterodimer 4F2hc/LAT2 are the best candidates to further functional and structural studies (Table 4). Thus, LAT2 is the most expressed protein among the light subunits tested (Figure 21). About heavy subunits 4F2hc was solubilized successfully in contrast with rBAT (Figure 26). Finally, 4F2hc/LAT2 heterodimer was the best expressed among the heterodimers tested (4F2hc associated with asc1, LAT1, LAT2 or xCT). The rBAT/b^{0+}AT heterodimer was not tested in this study, due to rBAT was impossible to solubilized and b^{0+}AT was practically unexpressed (Figure 21; Figure 26 [b]). Since the atomic structure of 4F2hc ectodomain has been solved (Fort *et al*. 2007), LAT2 and 4F2hc/LAT2 heterodimer were selected for further studies. It is worth mentioning that our studies also indicate a chaperone-like activity for human 4F2hc. Thus, coexpression in *P. pastoris* of 4F2hc increased the expression levels of asc1, LAT1 and LAT2 (data not shown). Indeed, only xCT expression was not increased upon expression of the heavy subunit. Moreover, coexpression of 4F2hc improved detergent-solubilization of LAT1 and LAT2 (data not shown). To our knowledge this is the first data indicating the chaperone-like activity of 4F2hc for their associated light subunits. This ability of 4F2hc is reminiscent of the role of the human light subunit b^{0+}AT in helping the folding, maturation and cell surface expression of the heavy subunit rBAT (Bartoccioni *et al*. 2008).

Proteins	Expression	Solubilization
Light Chains		
asc1	-	-
LAT1	+	+
LAT2	+++	++
y^+LAT1	+	+
y^+LAT2	++	-
xCT	+	+
b^{0+}AT	+	+
Heavy Chains		
4F2hc	+++	++
rBAT	++	-
Heterodimers		
4F2hc/asc1	+	++
4F2hc/LAT1	+	++
4F2hc/LAT2	++++	+++
4F2hc/xCT	-	-

Table 4. Relative solubilization levels regarding the protein expression. The table shows schematically the expression and the solubilization rates of all the analyzed proteins. Solubilization rate is expressed respect the solubilization rate. The grey shadow remarks the best protein candidates to continue with the study. (- Very Poor; + Poor; ++ Regular; +++ Good; ++++ Very Good)

4. Purification of 4F2hc and LAT2

In order to get a very pure sample adequate to crystallization assays the protein has to be purified from all the other proteins in the membrane. In the present study, two different tags were used, a histidine tag placed C-terminal of 4F2hc, and a streptag II located in N-terminal of LAT2 (Figure 59, Material and Methods).

Pooled fractions of the corresponding elutions (LAT2 from StrepTag affinity purification and 4F2hc or 4F2hc/LAT2 from His-affinity purification) were concentrated to 2-3 mg/ml using centricon with a cut-off of 100 KDa (Millipore).

Size exclusion chromatography (SEC) was performed to separate small particles (i.e. detergent micelles) and small protein aggregates after affinity chromatography. SEC was run at 4°C with an ÄKTA purifier™ and using alternatively Superdex 200 5/150 GL (3 ml of bed volume, low resolution) or Superdex 200 10/300 GL (24 ml of bed volume, middle resolution) columns. Data was processed with UNICORN™ 5.1 software (GE Healthcare, life science).

4.1. Heavy subunit 4F2hc

The unglycosylated heavy subunit was attached at 10 Histidines tag (see Material and Methods) in order to purify using cobalt^{2+} or niquel $^{2+}$. To purify 4F2hc, the resin chosen was cobalt^{2+} (Clontech TALON® Cobalt) due to, this protein showed or this protein showed highest purity with this system, although the amount of protein in the elution was lower.

The experiment followed the standard protocol specified in Materials and Methods (“9. Protein purification”). The elution was done with Imidazole (200 mM) and the detergent DDM concentration was decreased slowly during the process (i.e. solubilization step at 2%, first and second purification washing steps at 0.25% and elution step at 0.15% of DDM) to avoid future problems in crystallization trials in order to a high concentration of detergent could allow the formation of soft and heterogenic detergent crystals (see Material and Methods

for detailed protocol "9. Protein purification). The result was a pure peack of protein (Figure 29).

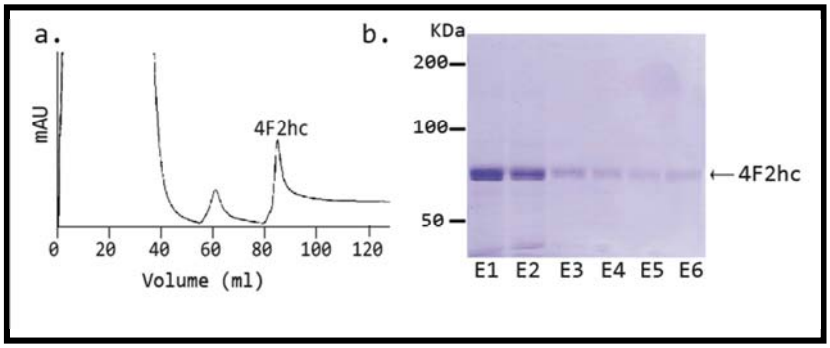

Figure 29. Affinity purification and pooled fractions analysis of 4F2hc. **(a)** 4F2hc affinity purification chromatogram (cobalt^{2+}), the 4F2hc peak is indicated. **(b)** Coomassie staining corresponding with the 4F2hc peak. In all fractions (500 µl) almost totally pure 4F2hc (~70 KDa) is visible.

Then, ultracentrifugation at 250,000 g for 1h at 4° was carry out to precipitate the aggregated protein. The gel filtration was done with a Superdex 200 10/300 GL and the sample was previously concentrated to 2 mg/ml (200 µl of volume). 4F2hc appeared as a main peak at 10.88 ml. A small peak in the void volume of the column (~8 ml) was observed, indicating only partial aggregation (Figure 30). Another peak at 14.29 ml appeared corresponding with smaller molecules (~40 KDa) as DDM detergent micelles. The main peak was wide, as expected for the presence of 4F2hc monomers and dimers. The result was a yield of ~500 µg of protein from 1l of culture, enough to continue with further studies.

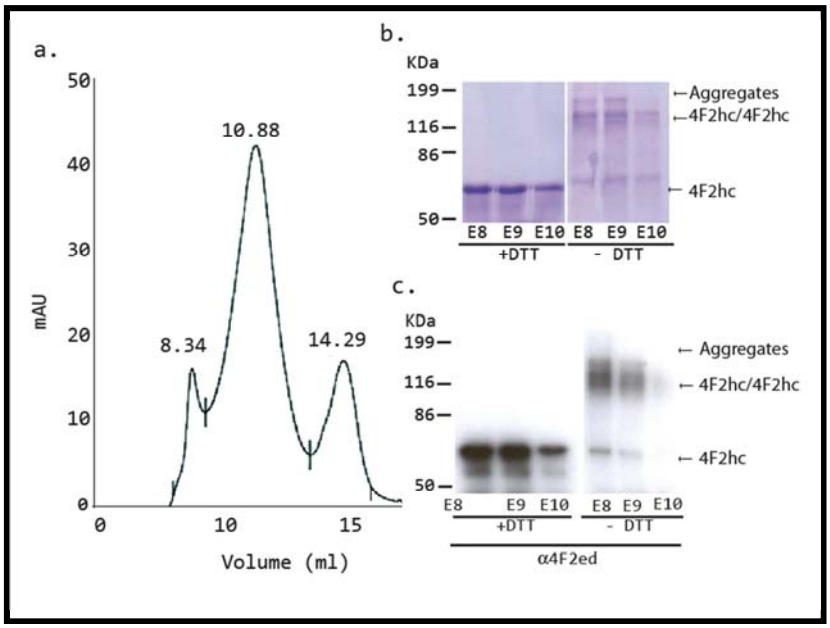

Figure 30. **Size Exclusion Chromatography and protein staining analysis (a)** 4F2hc Size Exclusion Chromatography (Superdex200), 4F2hc peak appeared at 10.88 ml, and partial aggregation appeared at 8ml (void column volume), a third peak at 14.29 ml appeared corresponding with smaller molecules (i.e. DDM detergent micelles). **(b)** Coomassie staining of the gel filtration fractions E8, E9 and E10 correspond with the fractions of 4F2hc peak. 4F2hc monomer, homodimer 4F2hc/4F2hc and aggregates (< 250 KDa) are visible. **(c)** Western blot anti-4F2ed adding DTT. E8, E9 and E10 correspond with 4F2hc peak fractions. Both, 4F2hc homodimer and 4F2hc monomer are visible. Adding DTT, 4F2hc homodimer disappears and only 4F2hc

The fractions corresponding with the main peak were kept overnight at 4°C, ultracentrifuged to remove aggregates and injected again two days later in order to study the stability of the protein. The void and the excess of detergent peak were reduced. The apex of the peak was moved from 10.88 ml to 10.59 ml meaning a low aggregation kinetic or an increased 4F2hc homodimerization (Figure 31).

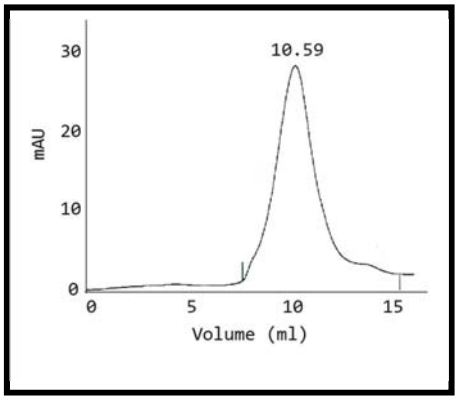

Figure 31. 4F2hc Size Exclusion Chromatography two days after purification. 4F2hc peak appeared at 10.59 ml, and partial aggregation and the third peak disappeared.

4.2. Light subunit LAT2

Starting from a total protein concentration of 5mg/ml, the solubilization was done with 2% of DDM, during 1 hour at 4°C. The protocol was the standard described in Materials and Methods ("8. Solubilization trials"). LAT2, was built with the commercial short-tag call StreptagII (Strep-tag II, IBA Strep-tag® Technology), composed by 8 amino acids. The purification in that case, is based in the well-known binding of biotin to streptavidin (http://www.ibago.com /prottools/prot_i_story.html) and was done with the superflow prepacket columns from IBA (streptactin superflow, IBA), a friendly one step purification (see Material and Methods for detailed protocol). The most important remark in this protocol is the elution step, using D-Desthiobiotin (2.5 mM) (IBA). The starting DDM concentration and the progressive reduction to 0.15% was exactly the same as in the case of 4F2hc purification (See Results 4.1. Heavy subunit 4F2hc). LAT2 protein was purified as monomers, dimers and aggregates (Figure 32).

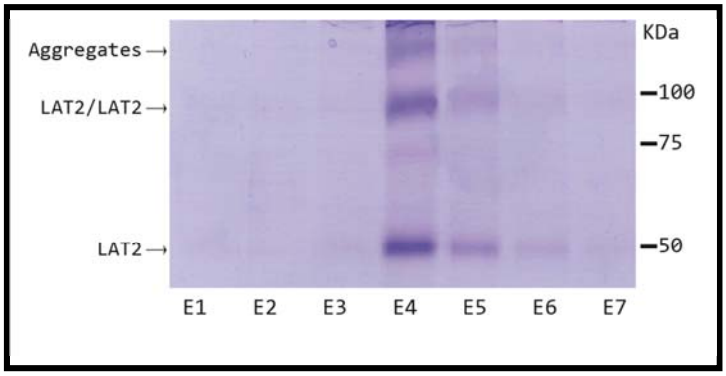

Figure 32. Coomassie staining of LAT2 purification. The complete elution volume was sampled in seven fractions (E1 to E7) of about 500 µl each. Three speers of LAT2 are visible: monomer (~50KDa), homodimer (~100KDa) and aggregates (< 250 KDa, not enough resolution in the acrylamide gel).

The SEC was done with a Superdex 200 10/300 GL and the sample was previously concentrated to 2 mg/ml (200 µl of volume). All LAT2 appeared in the void volume of the column (around 8ml previously calibrated) indicating complete-aggregation (Figure 33).

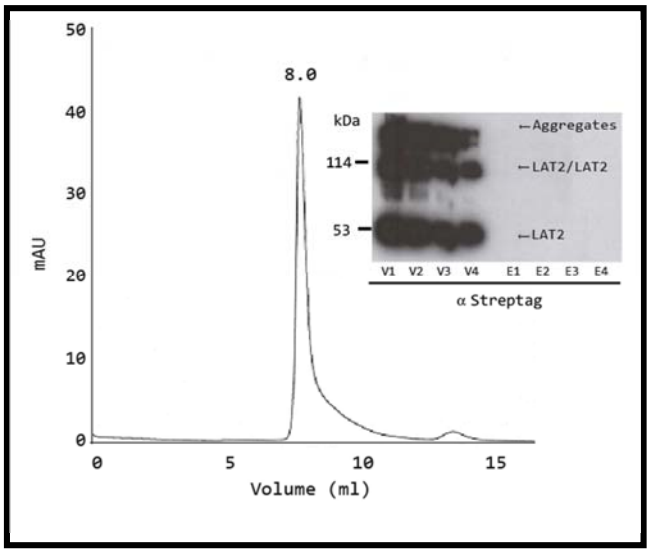

Figure 33. **Size Exclusion Chromatography of LAT2 and western Blot**. In the upper corner, Western Blot anti-streptag. Protein is only visible in the peak corresponding to the column void volume (V1 to V4), whereas no protein appeared in the fractions expected to contain LAT2 monomers and dimers (E1 to E4). The small peak at ~13 ml of elution corresponds to DDM micelles

The amount of protein purified (0.15 mg) from 1l of culture was much less than that for 4F2hc (0.5 mg from 1l). Thus, the light subunit LAT2 had a very low final protein yield and showed a clear aggregation tendency, which concluded further studies.

5. Purification of 4F2hc/LAT2

To set up the glycosylated 4F2hc/LAT2 heterodimer affinity purification, the cobalt^{2+} resin was chosen because of its highest capacity of purification of 4F2hc/LAT2 heterodimer. The protocol was the standard explained in Material and Methods (See Material and Methods "9. Protein purification"), using Imidazole 200 mM in the elution step. Starting from ~150 mg of total protein (from 500 ml of culture) around 1.6 mg (Figure 34) of partially pure protein (4F2hc/4F2hc, 4F2hc/LAT2 and 4F2hc) was recovered at the end of this process

as demonstrated by western blot analysis with anti-4F2ED and antistreptag (LAT2) (Figure 34).

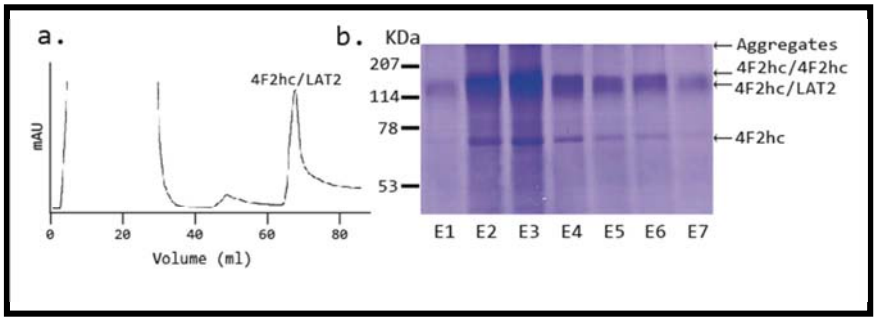

Figure 34. . One round purification of 4F2hc/LAT2 heterodimer (a) Chromatogram of the cobalt^{2+} affinity purification **(b)** Coomassie staining of the eluted fractions from the his-affinity purification. Aggregates, 4F2hc homodimers, 4F2hc/LAT2 heterodimers and 4F2hc monomers are visible as indicated.

The heterodimer was purified in a Co^{2+} column (i.e. one round affinity purification). The eluted protein was concentrated just after the His-tag affinity purification step, to 2mg/ml in 250 µl volume. The sample was run in SEC (Superdex 200 10/300 GL) at the moment after an ultracentrifugation round (1h at 4°; 250,000g). The chromatogram showed one main peak at 9.8 ml that may correspond to 4F2hc/LAT2 heterodimer. The second peak was probably an excess of detergent, and a very small pick of void was observed at 7.6 ml. Indeed Western Blot analysis of the main SEC peak showed 4F2hc/LAT2 heterodimer as the most prominent protein species, whereas LAT2 and 4F2hc monomers and their aggregates represented a very small part of the sample (Figure 35). To sum up, His-affinity purification followed by SEC, lead to an enriched preparation of 4F2hc/LAT2 heterodimer.

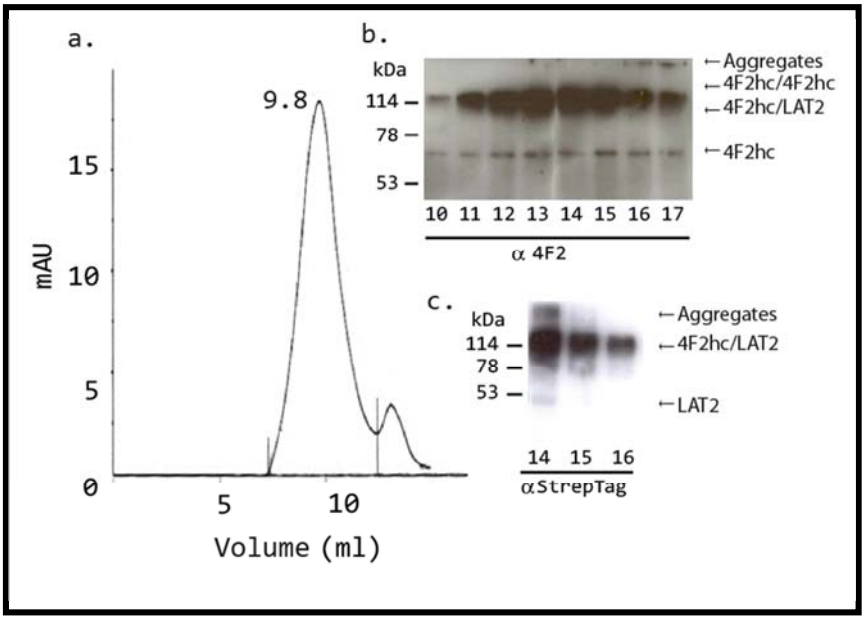

Figure 35. Size Exclusion Chromatography of 4F2hc/LAT2 after metal affinity chromatography. Western blot of fractions of the main peak of 4F2hc/LAT2 SEC (Superdex 200) **(a)**, decorated with anti4F2ed **(b)** or anti-streptag (i.e. LAT2) as indicated **(c).** The size exclusion chromatography **(a)** showed a broad main peak, as expected after only one round affinity purification, corresponding with 4F2hc/LAT2, 4F2hc/4F2hc and 4F2hc but did not show an aggregation void peak. Some LAT2 was observed in the anti-streptag western blot (c) due to the heterodimer split.

The aggregation state was studied injecting the sample one day after the His-affinity purification step and after an ultracentrifugation round (1h at 4°; 250,000g). The protein showed a clear aggregation pattern with most of the sample eluted in the void volume of the column (Figure 36). Due to this fast aggregation kinetics, the whole purification protocol was reduced to one simple day for future experiments.

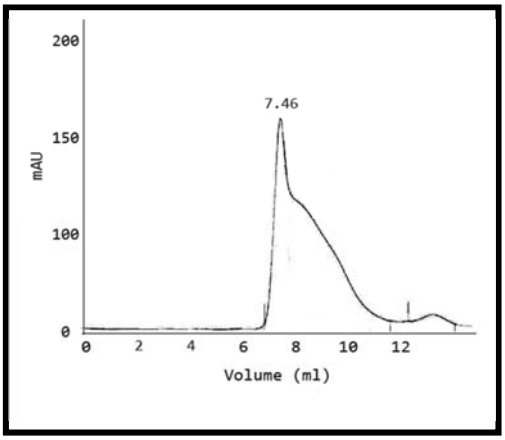

Figure 36. Size Exclusion Chromatography profile of 4F2hc/LAT2 purified in presence of L-glutathione. The protein was run one day after the affinity purification but showed an aggregated profile.

The fact that, 4F2hc in monomeric state was kept in soluble state during at least 48h, the heterodimer 4F2hc/LAT2 was kept in soluble state around 24h and the monomer LAT2 was aggregated rapidly, pointed clearly the tendency of 4F2hc to maintain the heterodimer in an stable state.

Next, in order to improve the purity of the sample, a two rounds affinity purification (i.e. $cobalt^{2+}$ and streptag) was set up using the tag in the heavy subunit 4F2hc (His-tag) and the tag in the light subunit LAT2 (StrepTag) (See Material and Methods Figure 59). The protocol was again the same for the solubilization step (2% DDM) and the detergent was decreased during the affinity chromatography to 0.25%. Starting with 150 mg of total protein (around 500 ml of final culture) and after the first purification step ($Cobalt^{2+}$), the yield in these experiments was always about 1.5 - 2 mg of almost purified protein (4F2hc/4F2hc, 4F2hc/LAT2 and 4F2hc), measured by the nanodrop device, Nano Drop 2000 (Thermo scientific). After the second purification step (i.e. StrepTactin chromatography) to remove the homodimer and the monomer of 4F2hc, the amount of heterodimer was reduced to 0.026 – 0.035 mg. Changing the first step purification to streptactin instead cobalt was even worse. Different strategies were tried to improve the yield of final protein during the binding, gravity (recommended by IBA) and batch (from 1 hour to overnight) but the protein was lost in the flowtrought and sometimes during the washes (depending on the experiment the lost during washes was more or less

dramatic). These results were indicating a low accessibility by the tag (i.e. StrepTag II) to the resin. Another important problem was the cleavage of the heterodimer. Streptag purification is long in time, the column flow oscillated between 0.13 and 0.18 ml/min meanwhile the cobalt flow was 0.4 ml/min. During this period of time splitting kinetics were observed. The result was a non-pure sample with monomers of 4F2hc and LAT2 (which should not be possible if both purifications had worked properly), meaning, that after the first purification ($cobalt^{2+}$) LAT2 monomer was not removed completely from the preparation. In the same way, 4F2hc and 4F2hc/4F2hc were present after streptag purification. This indicated splitting of the heterodimer into its two subunits 4F2hc and LAT2. Thus, some strategies to avoid the broken heterodimer and improve the final yield were tried.

5.1 Use of Glutathione to prevent reduction of 4F2hc/LAT2 heterodimer.

The splitting of 4F2hc/LAT2 in its two subunits required the reduction of the interconnecting disulfide bridge. The purification buffer is mainly composed of Tris 20 mM and NaCl 300 mM and any reducing agent is present. Then, a disulfide isomerase could be responsible for the reduction of the disulfide bridge. L-Glutathione salt was added as a competitor for the disulfide isomerase activity at a concentration of 2mM during the whole process. Adding glutathione avoid the presence of the homodimer 4F2hc/4F2hc (Figure 37). The homodimerization of 4F2hc was observed in presence of high amounts of 4F2hc in monomeric state. The abolition of this homodimer could be indicating a reduction in the heterodimer splitting, despite of that, was not possible to avoid completely the splitting of the heterodimer.

Due to this problem, added to the poor binding after streptag chromatography column, was impossible to get a good size exclusion chromatography after a double round purification. Interestingly, it was possible to get a homodimer 4F2hc/4F2hc free sample (Figure 37), in which case a single particle analysis was

possible to set up (It is explained in detail in “Results 8. Analysis by Single Particle-Negative staining of 4F2hc/LAT2”).

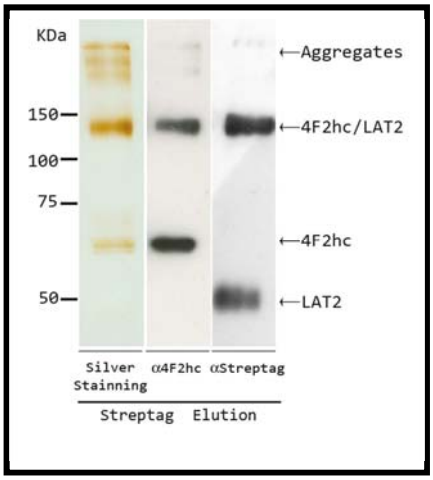

Figure 37. Silver staining and Western blot of the 4F2hc/LAT2 preparation after cobalt and streptag purification in the presence of oxidized L-glutathione. After the final purification step (i.e. streptag) the sample contains 4F2hc and LAT2 aggregates, 4F2hc/LAT2 heterodimer and 4F2hc monomers indicating the splitting tendency of the heterodimer. LAT2 monomers are rarely detected by silver staining’s in low concentration due to the high hydrophobicity which is possible to detect by western blot.

6. Improving 4F2hc/LAT2 production for structural studies

Due to different problems observed during 4F2hc/LAT2 purification process (i.e. a low stability behaviour and an extremely low yield after the StrepTag affinity chromatography) was decided to try different detergents in presence of cholesteryl hemisuccinate tris salt (CHS), with the aim to solve these aspects due to trying 2D or 3D crysatllization assays required this kind of study. Moreover, only the glycosylated form of 4F2hc/LAT2 was studied until the moment. Thus, in order to avoid the problems associated with glycosilations, the unglycosilated form of 4F2hc/LAT2 was generated by directed mutagenesis in the glycosylation targets (N264Q, N280Q, N323Q and N405Q)(Figure 38).

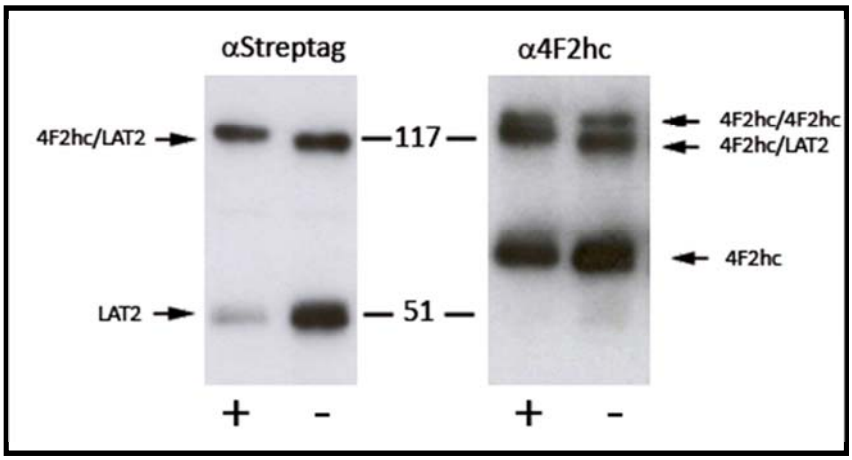

Figure 38. Western Blot of 4F2hc/LAT2 glycosylated (+) and unglycosilated (-). The expression of the protein was analysed using anti-4F2hc and anti-streptag as indicated. It is possible to see the weigh difference between the glycosylated and the unglycosilated bands. Also the expression level was similar between both.

Thus, once was found that the expression levels were similar (growing in Erlenmeyer) the stability studies were performed.

6.1. Detergent screening solubilization in presence or absence of N-ethylmaleimide (NEM) and cholesteryl hemisuccinate tris salt (CHS)

NEM (N-ethylmaleimide) was added with the aim to avoid the heterodimer disruption. Thus, different detergents from different families (adding cholesteryl hemisuccinate tris salt in all the cases) were tried in a solubilization test, with unglycosilated 4F2hc/LAT2 solubilized only with DDM as a control (Figure 39).

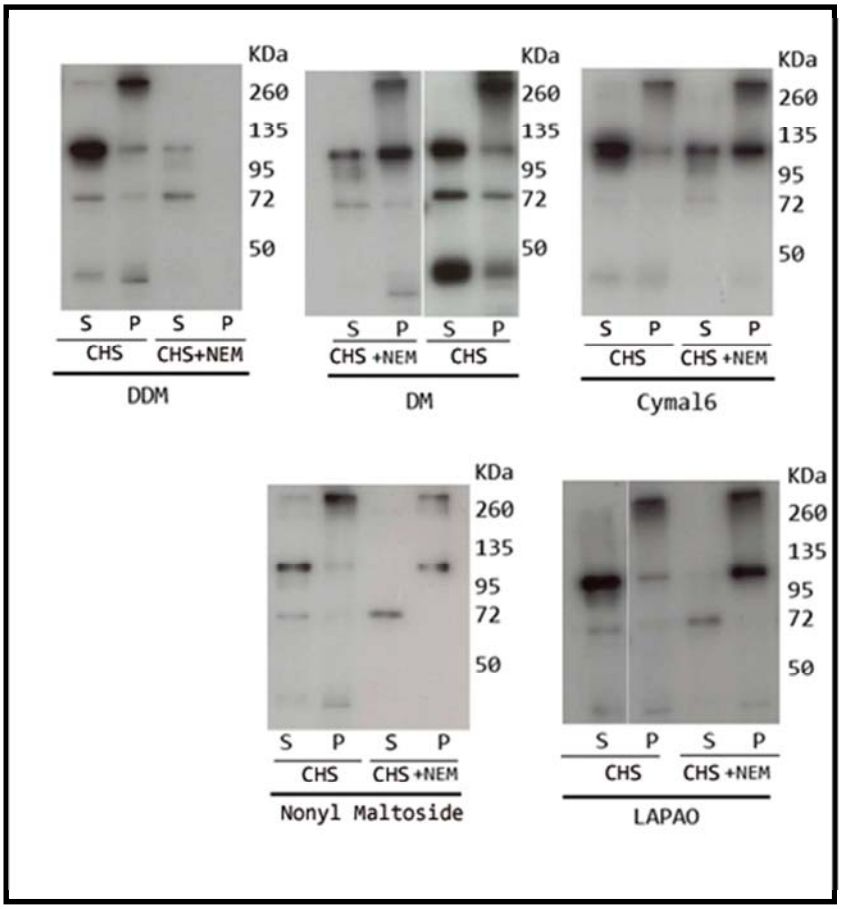

Figure 39. Solubilization screening of 4F2hc/LAT2 using CHS/NEM. It is possible to see the pellet fraction (P; aggregated protein) and the soluble fraction (S; soluble protein). (CHS) is referred to the detergent adding cholesteryl hemisuccinate tris salt and (CHS+NEM) is referred to the detergent adding both, cholesteryl hemisuccinate tris salt salt and NEM. In general the NEM treatment aggregated the protein (all the protein was found in the pellet fraction). In the case of DM a lot of light subunit appeared (LAT2 ~50 KDa) meaning the disruption of the heterodimer (apparently more than using DDM). LAPAO , Nonyl maltoside and Cymal6 (all of them +CHS) were interesting candidates in order to a high amount of protein appeared in the soluble fraction.

Thus, DM was discarded due to a poor solubilization rate. Cymal6, LAPAO and Nonyl Maltoside were all interesting candidates, but only LAPAO was studied in the present work remaining the other two for further studies in the future.

6.2. 4F2hc/LAT2 + LAPAO/CHS

Again the usual protocol was adapted. The starting total protein was 150 mg which was solubilized during 1:30h at 4^0C with 2% of LAPAO and 0.4% (w/w) of cholesteryl hemisuccinate Tris salt. The detergent was reduced during the purification step to 3XCMC to keep a detergent/CHS ratio of 5:1 (w/w). In this case, both purifications (i.e. His affinity chromatography and StrepTag affinity chromatography) were carried out separately to check the different behaviour of the protein in each case.

6.2.1. Streptactin resin, one purification round.

The protocol was carried out exactly in the same conditions. Again there was an excess of aggregated protein and an asymmetric peak of 4F2hc/LAT2 (Figure 40). Some LAT2 monomer remained non-aggregated to the end of the process, appearing in the last fraction of the second peak. Interestingly the problem of splitting heterodimer seems to be avoiding, in order to any 4F2hc monomer (~ 70 KDa) appeared in the silver staining gel (Figure 40 [b]).

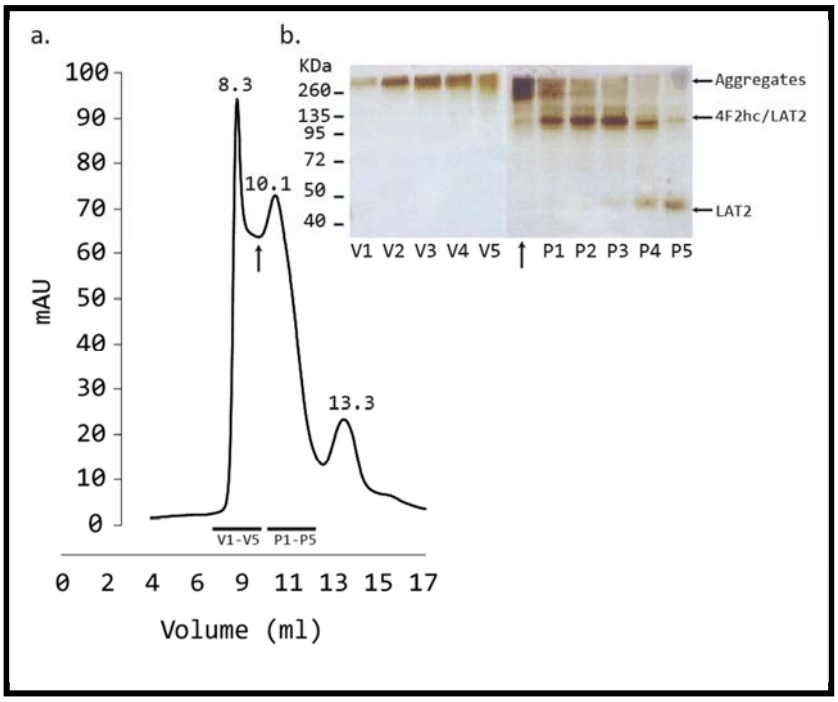

Figure 40. Size Exclusion Chromatography of 4F2hc/LAT2 purified by Streptactin affinity chromatography. Silver staining (b) of peak fractions, corresponding V1-V5 to the void (peak at 8.3 ml) and P1-P5 to 4F2hc/LAT2 (peak at 10.1 ml) (a). It is possible to observe some aggregates from fractions V1 to V5 (b). In the well-marked by an arrow (b) there are different populations with a high molecular weight (between void and peak). In the fractions from P1 to P3 is possible to see the heterodimer and in the two last fractions P4 and P5, some LAT2 appeared (b).

6.2.2. Co $^{2+}$ resin, one purification round.

The cobalt purification was tried to reduce the void peak (the light subunit LAT2 had a high aggregation tendency, thus the early separation of these monomers may improve the chromatogram shape) and study the ratio of the heterodimer 4F2hc/LAT2 regarding the homodimer 4F2hc/4F2hc and 4F2hc monomer. The elution step was done at 200 mM of Imidazole. As pre-supposed the column Superdex 200 couldn´t separate all this populations and the resulting peak was broad. The void peak was reduced indicating the aggregation corresponded principally to LAT2. Any LAT2 monomer (around 50 KDa) appeared in the silver staining gel that suggested any splitting of heterodimer (Figure 41).

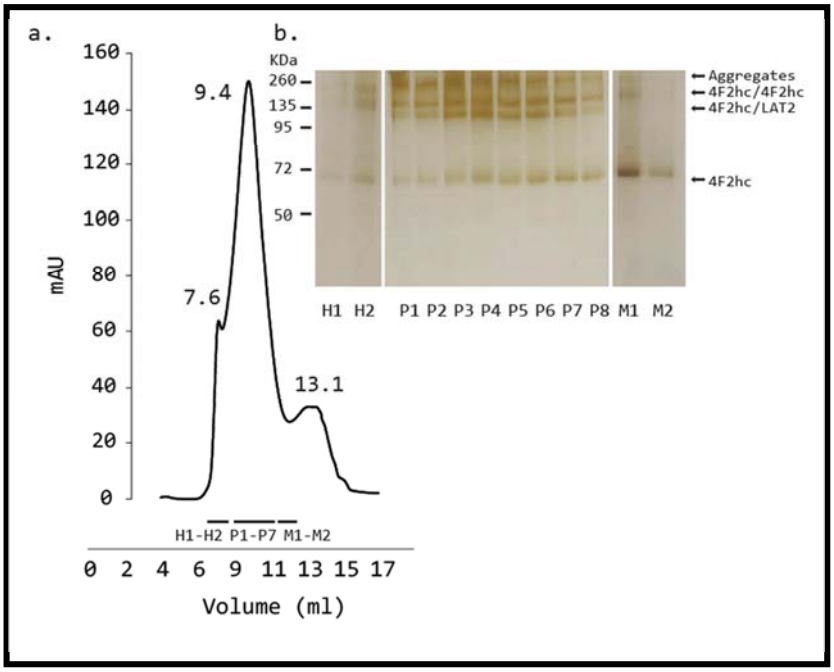

Figure 41. Size exclusion chromatography of 4F2hc/LAT2 purified by cobalt resin. The void peak appeared at 7.64 ml and was not properly separated from the protein peak at 9.40 ml (a). In this second peak was found 4F2hc/4F2hc and 4F2hc monomer apart from 4F2hc/LAT2. Silver staining (b) from size exclusion chromatography fractions (a) showed 4F2hc (~70 KDa) present in all the peak fractions (from H2 to M2) together with the heterodimer. In the end of the peak (M1, M2) the amount of 4F2hc was increased to. Apart from the heterodimer, 4F2hc/4F2hc is always present in a high amount.

The cobalt affinity chromatography reduced considerably the void volume respect to the protein peak (Figure 41 [a]) and inverted the behavior of StrepTag affinity purification (Figure 40 [a]). This concludes again with the high LAT2 monomer aggregation tendency and the chaperone effect of 4F2hc. On contrast, the cobalt affinity chromatography generated a highly heterogeneous population, due to the tendency of 4F2hc to homodimerizate. The exclusion chromatography (Superdex 200) is not able to separate those populations (i.e. 4F2hc homodimer [140 KDa]; 4F2hc/LAT2 heterodimer [120 KDa] and 4F2hc monomer [70KDa]). Testing another exclusion column (i.e. Superose 6), could help to separate the three populations. Anyway, using two different tags in each

of the proteins forming the heterodimer and the use of double affinity chromatography purification seems the correct strategy to get a pure 4F2hc/LAT2 heterodimer peak.

6.2.3. 4F2hc/LAT2 + LAPAO/CHS. Two rounds purification.

The two rounds purification was required to see if was possible to get a pure heterodimer sample using *Pichia pastoris* as expression system. The amount of starting total protein was increased to 350 mg due to the high loss of protein during streptag resin affinity purification. The solubilisation was done with 2% of LAPAO detergent and 0.4% (w/w) of Cholesteryl Tris Salt during 1:30 hours at 4^{o}C. After the ultracentrifugation step (250,000 g during 1:15h at 4^{o}C) the first round affinity purification (i.e. Co^{2+}) was carried out. The yield remaining after this affinity purification (Co^{2+}) was around 4 mg (measured by nanodrop system) of protein (4F2hc/4F2hc + 4F2hc/LAT2 + 4F2hc). The washes were reduced drastically (only 3 ml of washing buffer) to prevent the protein lose. The elution was done with 200 mM of Imidazole, and to the final volume, Tris buffer + detergent and cholesteryl hemisuccinate tris salt, was added to reduce the Imidazole concentration (i.e. 100 mM) and try to enrich the second binding affinity purification (i.e. streptag resin column). During that second affinity purification step (i.e. streptag) washes were reduced to 1 ml (5 ml as usually) but the yield was again really low and a high amount of protein was lost. The final yield was 0.46 mg of pure protein per 1l of culture (~88% of lost protein). Luckily, the final amount of protein was enough to concentrate to 100 µl the sample and carry out the size exclusion chromatography (Superdex 200 10/300 GL). After the chromatography, it was possible to observe by first time a non-glycosylated heterodimer 4F2hc/LAT2, after two rounds purification. The most critical point was some homodimer 4F2hc/4F2hc and monomer 4F2hc, were still resting in the gel, probably because of the drastic washes reduction (Figure 42).

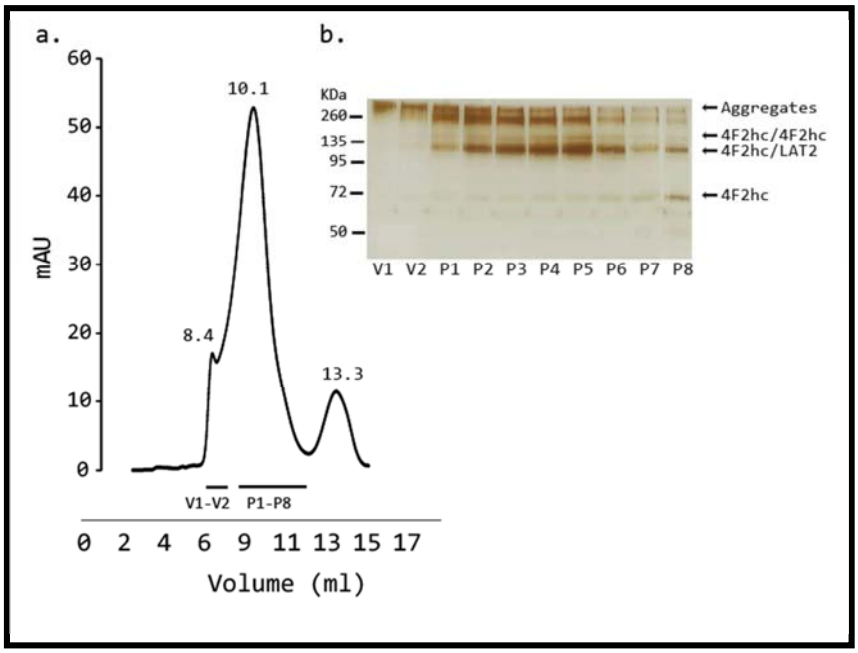

Figure 42. Size exclusion chromatography of 4F2hc/LAT2 purified by Co^{2+} and streptactin affinity chromatographies. **a)** The void peak appeared at 8.4 ml and was lower than the protein peak which was thinner than in the other experiments. **b)** Silver staining from the size exclusion chromatography fractions, V1-V2 are two fractions from the void peak, P1-P8 are the fractions corresponding to the 10.1 ml peack. 4F2hc/LAT2 is the most rich band in the gel (i.e. P2-P5), some 4F2hc/4F2hc is already resting in the gel. In the latest fractions (i.e. P7 and P8) the sample is enriched in monomer 4F2hc since is smaller in size. Some aggregated protein is observed in the top of the gel.

In Figure 43 is possible to observe the protein behaviour depending on the purification rounds and the used resin. The peak was narrower with the double purification (red line) and there was very few void. Anyway the peack was asymmetric meaning that more populations rested in the sample. In the silver staining of 4F2hc/LAT2 two rounds purification (i.e. cobalt and streptag) (Figure 42[b]) is possible to observe some homodimer 4F2hc/4F2hc and monomer 4F2hc.

This double purification round peak is promising, the heterodimer is apparently unbroken, the peak is narrow and the void is less abundant. In comparison with DDM, in which was impossible to arrive at this point, a single particle from the size exclusion chromatography could be done. The second purification round

(i.e. streptactin) should be set up in the future, increasing the washes to remove completely 4F2hc monomer and the homodimer 4F2hc/4F2hc.

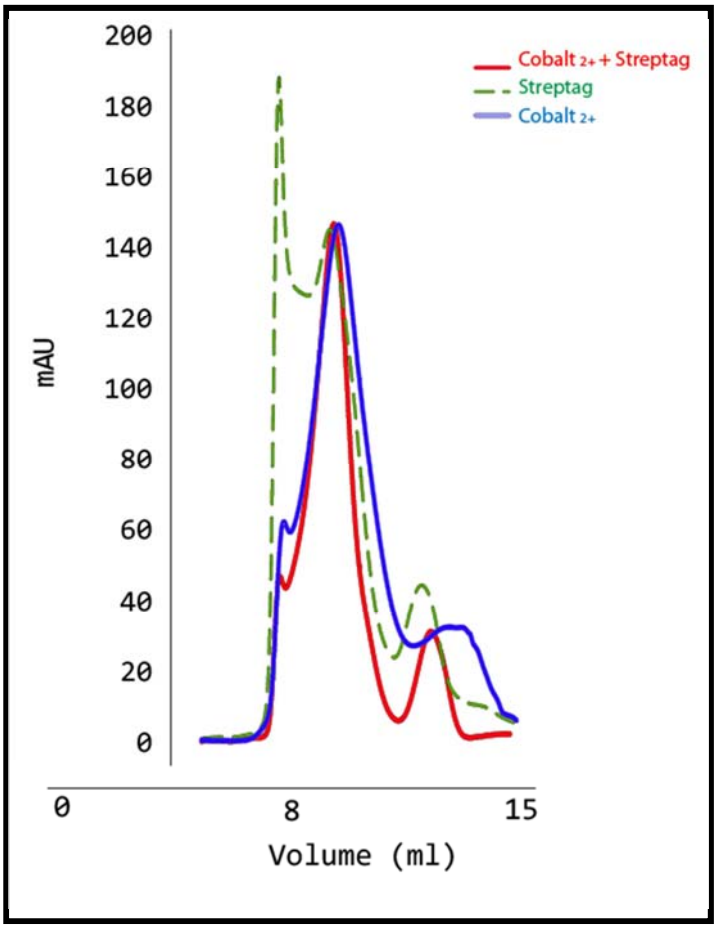

Figure 43. Normalized 4F2hc/LAT2 size exclusion chromatographs, purifying by Co^{2+}, Streptactin or Co^{2+}+streptactin using LAPAO/CHS. 4F2hc/LAT2 double round purification (red line), one single purification with cobalt (blue line) and one single purification with streptag (pointed green line) to compare all of them.

In order to these results, 4F2hc/LAT2 in presence of LAPAO/CHS may be a good candidate after improving the two rounds affinity purification.

7. Functional characterizations

In 1999, Pineda and co-workers cloned the cDNA of human LAT2 as one of the 4F2hc-associated light subunits (Pineda *et al*. 1999). The transporter was characterized in *Xenopus Laevis* oocytes; and as a result was found that oocytes expressing LAT2 showed almost no transport of [H^3] L-Leucine over background (water-injected oocytes) whereas oocytes expressing LAT2 and 4F2hc stored 30 fold increased transport rate of the labelled amino acid over background conditions (Pineda *et al*. 1999). The apparent K_M for L-Leucine in *Xenopus Laevis* oocytes was 220 μM. 4F2hc/LAT2 in this study was expressed in a different expression host (i.e. *Pichia pastoris*), and once the protein was purified, the functional characterization of the heterodimer was required. The functionality of 4F2hc/LAT2, before and after the extraction from the yeast membrane was analysed (i.e. *in vivo* transport and solubilized protein transport). In order that LAT2 alone was also overexpressed in *P. pastoris,* the transport properties of this protein and 4F2hc/LAT2 were studied together by "in vivo" transport system, to determine a possible role of 4F2hc in the transport function.

7.1. "In vivo" transport analysis

The functionality of glycosylated 4F2hc/LAT2 and LAT2 alone in *Pichia pastoris* membrane was checked. With this aim, the transport protocol was adapted from Doring *et al*. 1998 (see Material and methods "12.2. Transport Assay in *Pichia pastoris* cells"), measuring [H3] L-Leucine uptake at 5 minutes. Untransformed *Pichia pastoris* strain and overexpressing the heavy subunit 4F2hc alone were analysed as controls (Figure 44). *Pichia pastoris* overexpressing 4F2hc/LAT2 or LAT2, showed an increased uptake of L-Leucine over the background and the overexpressed 4F2hc (i.e. controls).

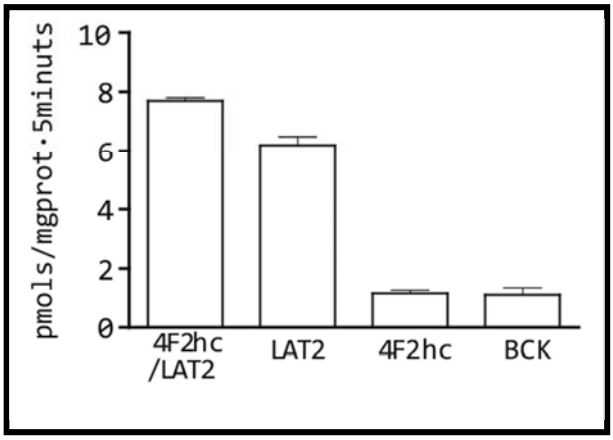

Figure 44. "In vivo" [H3] L-Leucine uptake in Pichia *pastoris* cells. The L-Leucine uptake was determined at 5 minutes for 4F2hc/LAT2, LAT2, the control 4F2hc and untransformed *Pichia pastoris* strain (BCK).

Once the functionality of both proteins was demonstrated, the kinetic characterization was carried out with the aim to detect any possible role of 4F2hc in transport. The uptake of [H^3] L-Leucine at different concentrations (10, 30, 50, 100, 300, 500 and 1000 mM) in the external medium was measured. That time course was carried out at 3 minutes considering was enough to see differences with the control. LAT2 and 4F2hc/LAT2 showed a K_M (Michaelis-Menten constant) of 120 μM and 178 μM respectively, based on the Eadie-Hofftee adjust, which was lineal until an amino acid concentration of 1000 mM (Figure 45).

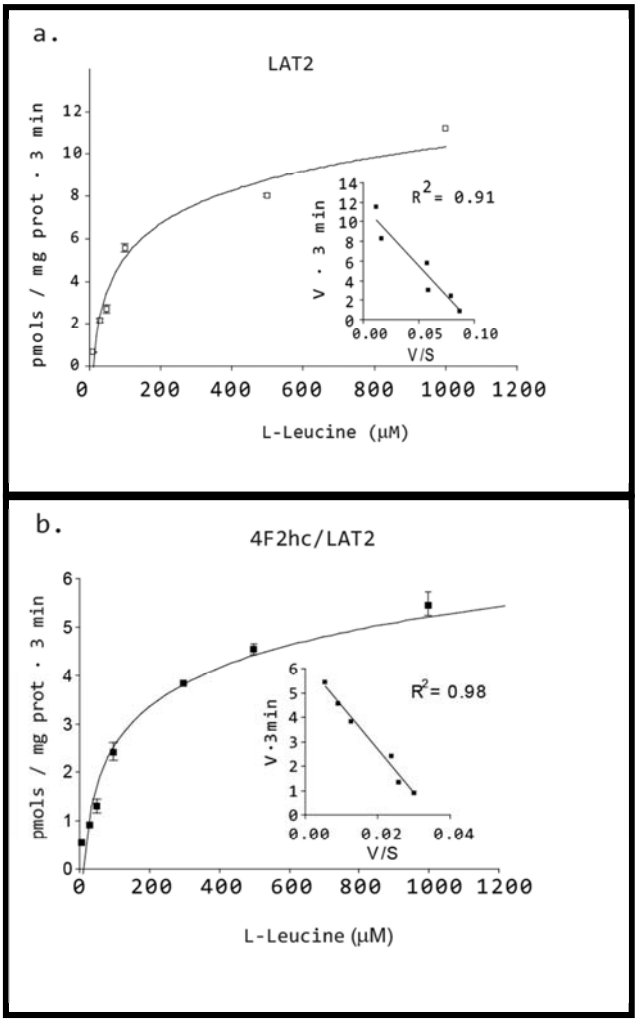

Figure 45. Transport activity kinetic analysis of transport induced by 4F2hc/LAT2 and LAT2. The uptake of different L-Leucine substrate concentrations was measured during 3minuts. The basal activity (control) is actually subtracted from the overexpressing LAT2 **(a)** and 4F2hc/LAT2 **(b)**. The concentrations were 10, 30, 50, 100, 300, 500, 1000 mM. The Eadie-Hofftee adjust, where is possible to see the velocity (V) and the velocity divided by the substrate concentration (V/S) shows any kind of significant difference between both samples.

The present study concluded that the heavy chain 4F2hc is not affecting the affinity for substrate of the light subunit, LAT2 due to not significant differences between both K_Ms were observed. Considering this data, LAT2 was fully functional in the absence of 4F2hc in the yeast membrane, which points to a

good folding in the host organism. This data is in concordance with the results for the light subunit b^{0+}AT reconstituted in liposomes (Reig *et al.* 2002).

7.2. Functional characterization of 4F2hc/LAT2 after solubilization

Different strategies were tried to reconstitute purified glycosylated 4F2hc/LAT2 after His-affinity purification but all of them failed (Data not shown). The previous fails in reconstitution (purified protein) fasted us to try the protocol previously used in our lab to reconstitute human b^{0+}AT expressed in HeLa cells (Reig *et al*. 2002). In this protocol the protein was not purified, the cells were lysated, mixed with liposomes and destabilized adding detergent (Sodium cholate) at the same time. In this case, the phospholipid mixture was a home-made mix of purified pig brain lipids (PBL) mixed with asolectin (Sigma-Aldrich) in a proportion of 40 mg/ml asolectin : 3 volumes of PBL (Reig. 2002).

7.2.1. Liposomes generation to reconstitute non-purified 4F2hc/LAT2

Oligolamellar large vesicles (OLV) were formed sonicating in a bath sonicator. To set up this protocol different parameters were needed to be tested. Different Asolectin- pig brain lipid ratios were tested to find the most uniform liposomes population. The analysis was done using Dynamic Light Scattering (DLS). DLS determines the size distribution profile of small particles in solution using a monochromatic (single wavelength) light source (laser). The calculation parameters are based on the particle Brownian motion and the particle diameter. As a result, all the different populations present in the sample are shown (based on particle diameter). DLS analysis showed that, the addition of asolectin: pig brain lipids in a ratio of 40 mg/ml : 1 volum of PBL, resulted in a uniform size liposomes population (Figure 46 [d]).

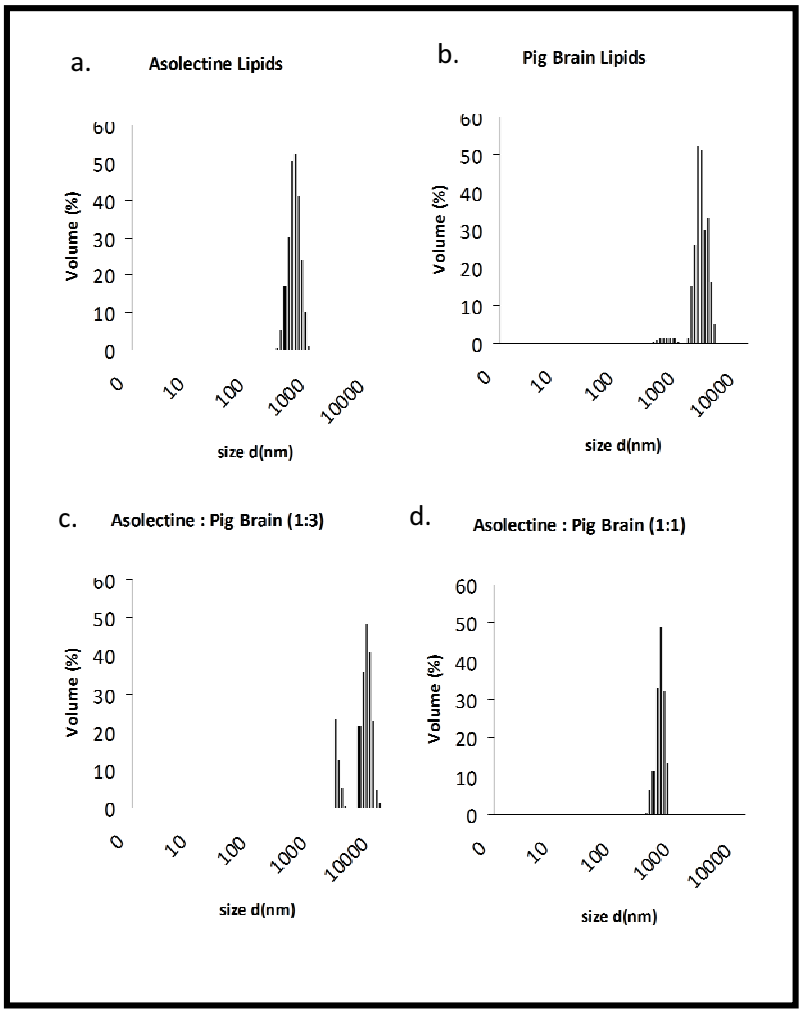

Figure 46. Dynamic Light Scattering of asolectin/pig brain lipids liposomes at different concentration ratios. The monodispersity and the size of the liposomes were analysed to find the most uniform population. **(a)** Liposomes generated with only pure asolectine showed a single and homogeneus population with a size of 1000 nm. **(b)** Liposomes generated using purified PBL resulted in two different populations with sizes of 1000 nm and 1 micra. **(c)** Mixing asolectine and PBL at 1:3 ratio resulted in two different populations of liposomes with a size of more than 5000 nm. **(d)** Mixing asolectine and PBL at 1:1 ratio resulted in a homogeneus liposomes population of 1000 nm. 1:3 means 40 mg/ml Asolectin: 3 volumes of PBL; 1:1 means 40 mg/ml asolectine: 1 volume of PBL.

7.2.2. Incorporation of the human 4F2hc/LAT2 heterodimer in liposomes

The ratio liposomes were mixed with 4F2hc/LAT2 and LAT2 to check by western blot the incorporation of protein in the liposomes membrane. Finally the parameters were set up and the experiment carried out as follows, the protein was solubilized at 3mg/ml concentration. The DDM detergent was reduced from 2% to 0.5% to avoid the excess during the solubilization. Solubilization run during 1 hour at 4°C, and then was ultracentrifuged at 250,000 g during 1 hour at 4°C. Asolectin at 40 mg/ml and Pig Brain Lipids (1:1 ratio) formed OLV. Moreover the same ratio asolectin: pig brain lipids (1:1) was used using a commercial polar brain lipid mixture (Avanti lipids) in parallel. The same mixture was used by Adam and co-workers for the reconstitution of a rat monoamine transporter (Adam *et al*. 2007) (Figure 47 [a]). Polystyrene beads (SM-Biobeads from Bio Rad) were used to remove the DDM detergent from the proteoliposomes sample. Two different incubation periods were tried (3 hours, changing biobeads periodically, and overnight) in order to optimize the proteoliposomes formation (Figure 47 [b]). Finally the protein was incorporated and the proteoliposomes were formed successfully. PBL homemade mix was more effective than the commercial one (Figure 47 [a]). The elimination of detergent was more effective during at three hours incubation than an overnight incubation, using the polystyrene beads (Figure 47 [b]). The same experiment was tried with the light subunit LAT2 alone, but the protein was not incorporated in any case (Data no shown) whereas the heavy subunit 4F2hc was incorporated successfully (Figure 47 [c]).

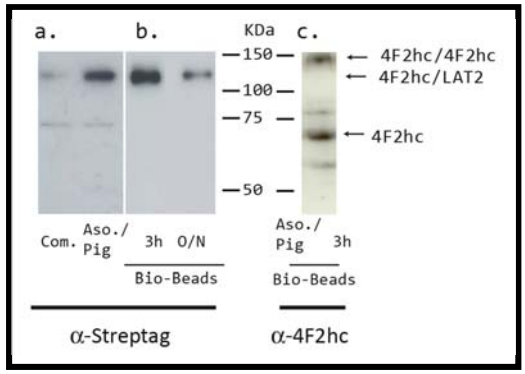

Figure 47. 4F2hc/LAT2 and 4F2hc reconstitution into liposomes. (a) 4F2hc/LAT2 was successfully incorporated in liposomes using the homemade lipids mix. **(b)** The detergent removal with Bio-beads was more effective during 3h of incubation. **(c)** The heavy subunit 4F2hc was incorporated under the same conditions into liposomes. COM means commercial pig brains mixture; Aso/Pig means homemade mix of asolectine and purified pig brain lipids ; 3h means three hours of biobeads incubation; O/N means overnight biobeads incubation.

7.2.3. Transport assay of reconstituted 4F2hc/LAT2

The transport assay was carried out using L-Leucine amino acid (medium) *versus* L-Isoleucine (proteoliposome lumen) based on the successful result in the case of LAT2 expressed in *Xenopus Laevis* oocytes (Reig *et al*. 2007). The proteoliposomes were loaded with L-Isoleucine (4 mM concentration) meanwhile control proteoliposome sample remained unloaded. Free [H^3] L-Leucine in a concentration of 10 µM (0.5 µCi) was added to the transport buffer (Figure 48).

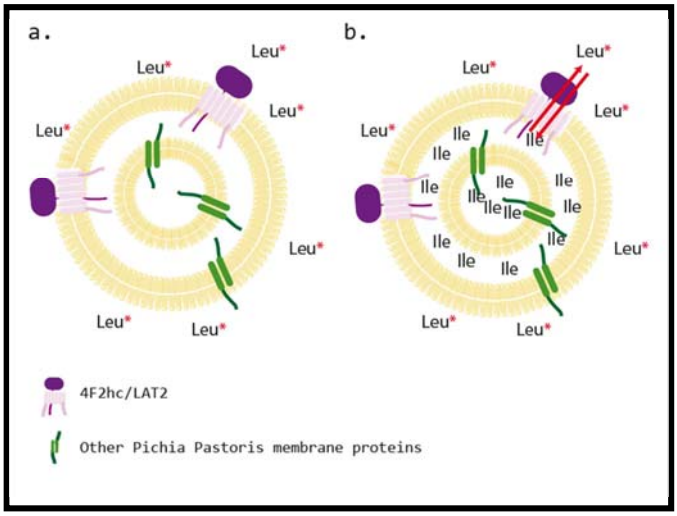

Figure 48. **Transport experiment scheme of sonicated proteoliposomes with non-pure solubilized 4F2hc/LAT2. (a)** Control group. The proteoliposome is empty with no amino acid loaded. **(b)** The proteoliposomes is loaded with cold L-Isoleucine (Ile) to study the exchange activity of 4F2hc/LAT2. In (a) and (b), L-[H3]Leucine (0.5 µCi) at 10 µM is added to the external medium to measure transport.

Different incubation periods (10, 30, 60, 90, 120, 150, 180, 210 minutes and 20 hours) were analysed to form a time course curve. At 20 hours the equilibrium between L-Leucine free in the medium and the L-Leucine transported into the liposome lumen was found. The overshoot energetic peak, typical in the transport proteins, was found at 1.5 hours using a protein: lipid ratio (LPR) of 1:50. The LPR resulted to be a critical parameter in order to, 1:100 LPR resulted in a low overshoot respect the background and 1:25 LPR resulted in aggregated proteoliposomes (Data not shown). 4F2hc monomer was incorporated in OLV liposomes and was used as a secondary control (Figure 47[c] and 49).

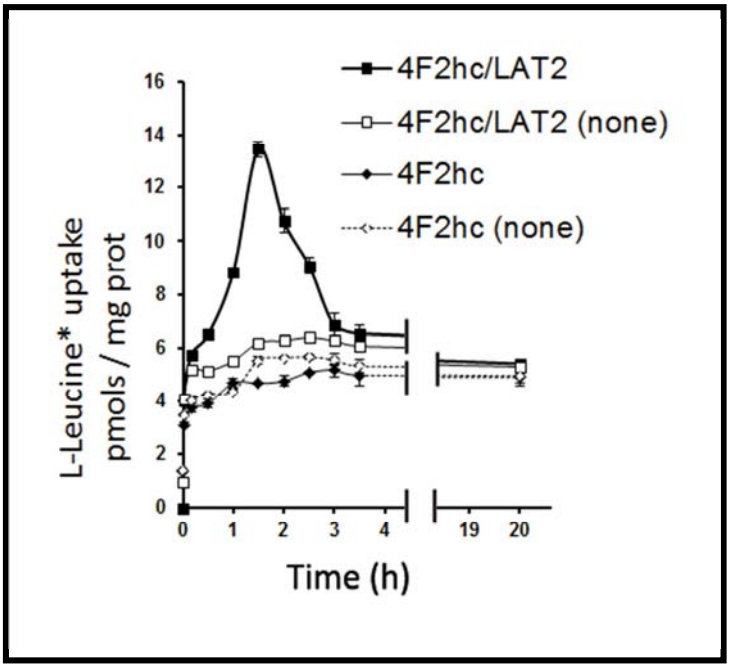

Figure 49. L-Leucine uptake in 4F2hc/LAT2 proteoliposomes. Labeled L-Leucine (10µM L-Leucine, 0.5 µCu) was measured against cold L-Isoleucine (4 mM) loaded in proteoliposomes. Incubation times of 10, 30, 60, 90, 120, 150, 180, 210 minutes and 20 hours. The heavy subunit 4F2hc was used as a control.

This result demonstrates that the human heterodimer 4F2hc/LAT2 expressed in yeast, remains functional, soluble in a detergent buffer after a lysis and a solubilization step.

8. Analysis by Single Particle-Negative staining of 4F2hc/LAT2

Two glycosylated 4F2hc/LAT2 preparations yielded best quality protein: (i) two-round purification (His and StrepTag affinity chromatography) in the presence of oxidized glutathione (Figure 37) and (ii) fast one-round purification (His affinity chromatography) (Figure 35). These two protocols rendered preparations enriched in the glycosylated 4F2hc/LAT2 heterodimer. In both cases the

enrichment of the heterodimer was the consequence of a limited disassembly of the heterodimer during purification. The first protocol was established with time enough during this thesis to analyse the preparation by Single Particle-Negative staining (SP-NS). The second protocol is a promising one to screen for 2D crystallization in the future. Single Particle-Negative staining requires a homogenous preparation. In contrast our preparation contains 4F2hc monomer and LAT2 aggregates in addition to 4F2hc/LAT2 heterodimers. The fact that the preparation was 4F2hc homodimer-free helps in the analysis of the images since the only dimer in the preparation was 4F2hc/LAT2 heterodimer. SP-NS requires an optimal concentration of the purified protein in order to avoid artefacts and make easy the tracking and digitalization of the protein images. For this reason, different protein concentrations were tried (from 2 to 8 μg/ml) and the best result was obtained with 2 μg/ml protein concentration (Figure 50 [b]). Interestingly, SP-NS showed clearly particles with a heterodimer nature corresponding to 4F2hc/LAT2 heterodimer (Figure 50 [b]) which could be easily differentiated from 4F2hc monomers and protein aggregates.

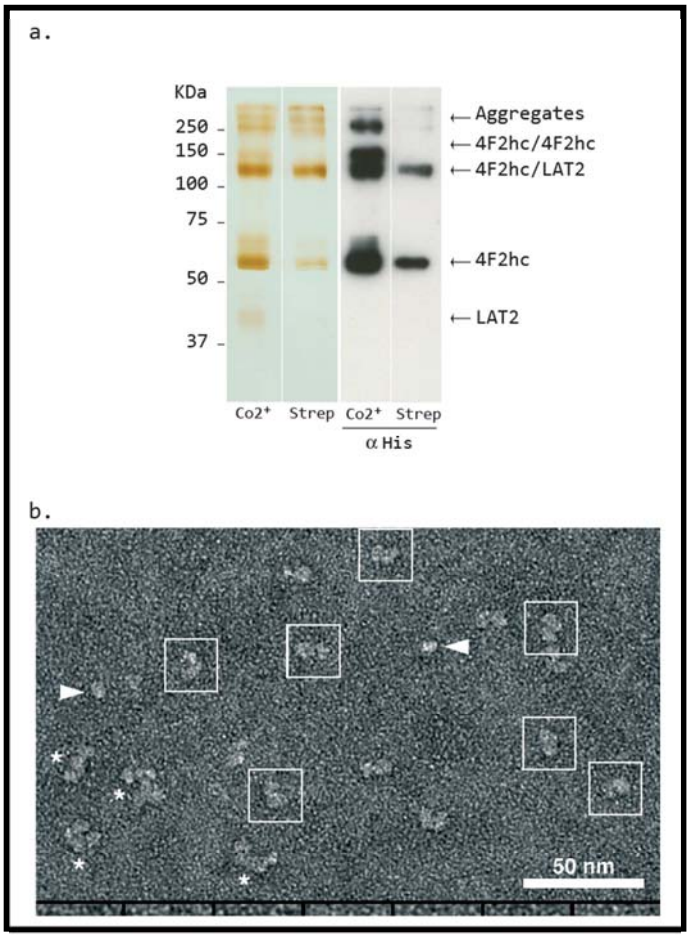

Figure 50. Single Particle-Negative staining of 4F2hc/LAT2 heterodimer. **(a)** Silver staining and western blot analysis of the protein preparation after the first (His-affinity chromatography) and the second (Streptag-affinity chromatography) purification step. 4F2hc homodimer (4F2hc/4F2hc) disappeared after the streptag-affinity purification. Confirming that, 4F2hc/LAT2 heterodimers and 4F2hc monomers plus aggregates were present in the preparation. **(b)** Single Particle-Negative staining (lower panel) shows particles compatible with 4F2hc/LAT2 heterodimers (framed), 4F2hc monomers (arrows) and aggregates (asterisk). A gallery of 4F2hc/LAT2 particles is shown below. SP-SN was performed by Mr. Marcel Meury at the lab of Prof. Dimitrios Fotiadis at the University of Bern, Switzerland.

Then, different protein captures were obtained and image particles were aligned and averaged in order to increase the signal to noise ratio. Later the averaged images were filtered and contrasted (Figure 51 [a]). Considering that, the

electron microscopy images are projections of the protein showing the distribution of density through it (2D projections), combining several images (from 6000 to 10,000) is possible to generate a three dimensional reconstruction of the protein, taken from a range of viewing angles (Figure 51 [b]).

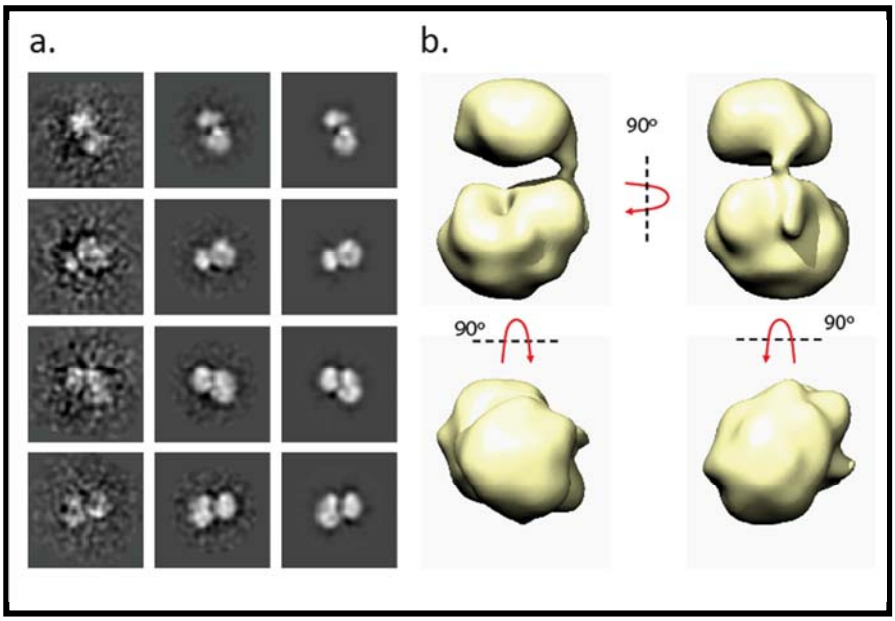

Figure 51. Library and refinement of some averaged images of the 4F2hc/LAT2 heterodimer. **(a)** An example of the set of 109 reference free class averages created with an average of 100 particles per class. Thus, up to 10,000 heterodimer particles were picked, averaged, filtered and contrasted to generate the image library**. (b)** The 3D reconstruction of the 4F2hc/LAT2 single particles gave rise to a bipartite model density (Image owned by Mr. Marcel Meury)

In the present study 11,000 particle images were captured to generate the 3D model of 4F2hc/LAT2 heterodimer (Figure 47) , but similar results were obtained with less than 6000 particle assays (Figure 46). Thus, SP-NS allowed us observe for first time a 3D model of a heteromeric amino acid transporter at 19Å, this resolution is pretty good for this microscopic method (normal range between 16-25 Å). Interestingly the atomic structure of the ectodomain of human 4F2hc solved at 2.1 Å resolution could be easily fit in the smaller particle with the N-terminal and the Cys residue involved in the disulfide bridge connecting with the

light subunit (i.e. LAT2), facing the larger particle (Figure 52). The larger particle has a toroid (donut-like) shape with a central depression facing the smaller particle (Figure 52). This shape is reminiscent of the prokaryotic homologues of LAT2, Stet (Ser/Thr exchanger from *B.subtilis*) (Reig *et al*. 2007) and the protomer of AdiC (Arginine/Agmatine exchanger for *E.coli*) (Casagrande *et al.* 2008). Unfortunately, SP-NS of membrane proteins includes the surrounding detergent (DDM in this case) precluding the fitting of the atomic structure of AdiC (Fang *et al*. 2009; Gao *et al*. 2010; Kowalczyk *et al*. 2011).

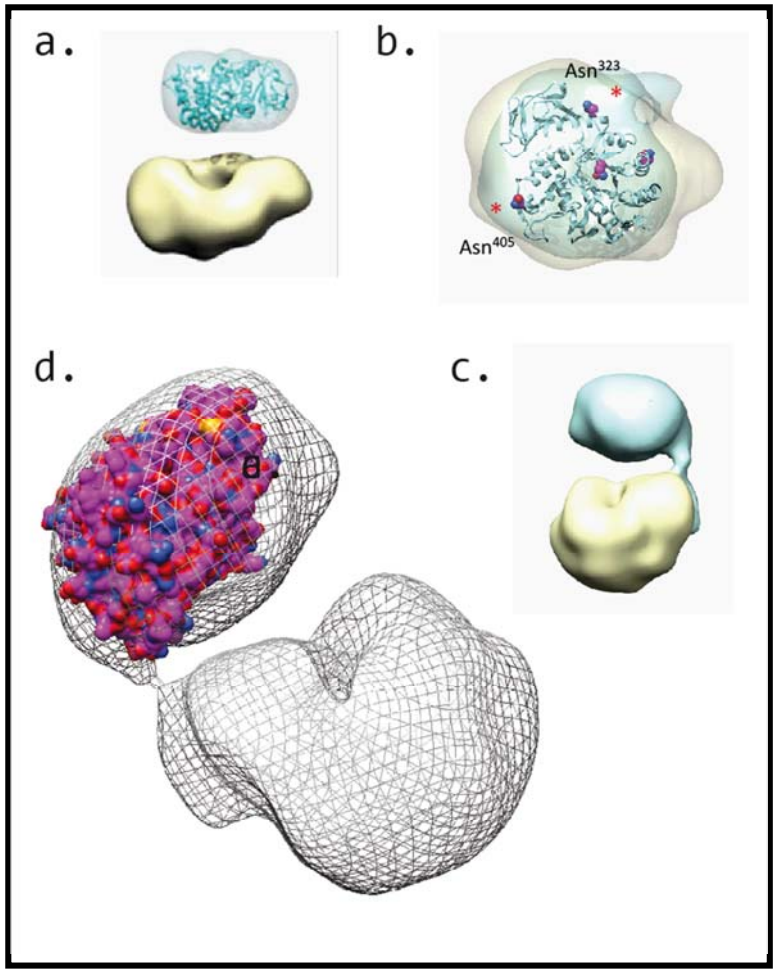

Figure 52. Refined 3D model of 4F2hc/LAT2. (a) In the first model of 4F2hc/LAT2 (6000 picks) the heavy subunit 4F2hc is on top of LAT2 like a true "Hat", meanwhile LAT2 could be in "opened" oriented conformation. The crystallized 4F2hc ectodomain (Fort et al. 2007) fitted well. **(b)** Human 4F2hc contains four putative N-linked glycosylation sites (Asn264, Asn280, Asn323 and Asn405). Especially for the glycosylation sites of Asn323and Asn405 additional density was observed in the model of human 4F2hc/LAT2. **(c)** Shows another side view of the heterodimer. **(d)** The refined model of 4F2hc/LAT2 (13,000 picks) shows the position of the 4F2hc transmembrane segment and the relative inclination angle between the heavy subunit (4F2hc) and the light subunit (LAT2).

Discussion

1. To sum up...

Two proteins were analysed widely from HATs family. The human heavy subunit 4F2hc, which hydrophilic ectodomain structure was previously published by our group (Fort *et al*. 2007), and the human light subunit LAT2, identified and characterized also in our group (Pineda *et al*. 1999). The association of both proteins induces system L activity (see introduction; table 2).

The co-expression of human 4F2hc and LAT2 in the yeast *Pichia pastoris*, which has been widely used in membrane protein studies (see introduction; table 3), resulted in the formation of disulfide-linked 4F2hc/LAT2 heterodimers, disulfide-linked 4F2hc homodimers and finally 4F2hc and LAT2 monomers. The stability pattern of each protein was different. Thus, 4F2hc showed a monodisperse peak in size exclusion chromatography (SEC) without aggregation 48h after purification. In contrast 4F2hc/LAT2 was only partially aggregated 24h after purification and LAT2 was fully aggregated already 24h after purification. In function of these results our structural studies were focused on 4F2hc/LAT2 heterodimer.

2. Concerning transport function.

Functional studies showed that the light subunit b^{0+}AT is functional in the absence of its heavy subunit rBAT. Thus, b^{0+}AT expressed in HeLa cells located in the ER and upon reconstitution in proteoliposomes showed full transport activity (Reig *et al*. 2002). This data demonstrated that b^{0+}AT folded properly in the absence of the heavy subunit rBAT. In order to check whether the light subunits of 4F2hc also fold in the absence of the heavy subunit, the functional expression of LAT2 and 4F2hc/LAT2 was analysed in *Pichia* cells.

2.1. LAT2 is properly folded and shows full transport activity in *Pichia pastoris*

The protein aggregation of purified LAT2 leads to the question whether the protein was misfolded in *Pichia* or whether was highly unstable in our purification conditions. *Pichia* might cause deficient folding of LAT2 due to the intrinsic cellular folding mechanisms or to the lipidic composition of its plasma membrane. One of the most well-known differences is the presence of ergosterol instead of cholesterol in yeast, fungi and protozoans plasma membrane (Alexander *et al*. 2001). As already mentioned 4F2hc and rBAT are needed to the proper trafficking of the holotransporter to the corresponding plasma membrane and at present no other role has been atttributed to the heavy subunits. For the rBAT/b^{0+}AT transporter the light subunit b^{0+}AT has a chaperone-like function. Like many non-associated subunits of plasma membrane oligomeric complexes, free rBAT is retained in E.R. and degraded in a mannosidase-dependent manner (Endoplasmatic reticulum associated degradation pathway [ERAD pathway]). Assembly of b^{0+}AT with the E.R. retained (core-glycosylated) rBAT to form a disulfide-link heterodimer abolishes degradation of rBAT (Bartoccioni *et al*. 2008). Recent experimental evidence indicates that at least part of the folding of the extracellular domain of rBAT occurs after its assembly with b^{0+}AT (Rius *et al*. 2012). These results indicate that b^{0+}AT acts as a chaperone of rBAT. In contrast the heavy subunit 4F2hc increases the stability of the light subunit LAT2. Thus, purified 4F2hc/LAT2 presented a more stable behavior than purified LAT2 (Figures 33 and 35). Supporting these data, C-terminal truncations of 4F2hc results in a complete loss-of-function of LAT2 expressed at the plasma membrane (Bröer *et al*. 2001). In any case, whether 4F2hc acts as a chaperone-like molecule in the biogenesis of LAT2 and whether 4F2hc also increases the stability of other of their light subunits, remains to be studied.

In order to check proper folding and trafficking, system L activity was analysed in *Pichia pastoris* overexpressing the light subunit LAT2 alone, the heterodimer

4F2hc/LAT2 or the heavy subunit 4F2hc as a control (i.e. basal transport activity). LAT2 and 4F2hc/LAT2 showed a clear transport activity of L-Leucine (Figure 44). This result indicated both, (i) LAT2 was present in *Pichia pastoris* membrane and (ii) it was properly folded in the absence of the heavy subunit 4F2hc. Moreover, these results indicated that functionally LAT2 expressed in *Pichia* is highly unstable upon solubilization.

The fact that LAT2 expressed alone in *Pichia*, wich genome does not code for 4F2hc or rBAT ortologues, locates at the plasma membrane suggest an artefactual trafficking. Indeed, expression of 4F2hc- and rBAT- associated light subunits in foreign expression systems like mammalian cells and *Xenopus* oocytes needs the co-expression of the corresponding heavy subunit for trafficking to the plasma mambrane. In contrast, when the ligh subunits of HATs are expressed alone in these systems these proteins are stacked at the E.R. (for review see Verrey *et al*. 2004; Palacín and Kanai. 2004). The expression of LAT2 alone at the *Pichia* plasma membrane might be the result of a permissive trafficking control machinerie due to the overexpession levels.

2.2. Is the heavy subunit 4F2hc affecting the light subunit LAT2 transport activity?

The functional expression of 4F2hc/LAT2 and LAT2 in *Pichia* cells allowed to compare their kinetic properties. The apparent constant affinity (K_M) for L-Leucine was 120 μM and 178 μM for LAT2 and 4F2hc/LAT2 respectively (See Figure 45). Interestingly, these K_M values are very similar to those obtained upon expression of 4F2hc/LAT2 in oocytes (220 μM) (Pineda *et al*. 1999). This indicates that the heterodimer with 4F2hc do not affect the apparent affinity of LAT2 for L-Leucine. We cannot compare the Vmax of L-Leucine transport in LAT2 and 4F2hc/LAT2 because the activity of the expressed transporter was very variable among different experiments and the amount of 4F2hc/LAT2 and LAT2 located at the cell surface has not been determined.

In contrast to this view that 4F2hc is not affecting the apparent substrate affinity of LAT2, Merlin and co-workers (Liu *et al*. 2003) showed in CACO cells that crosslinking of 4F2hc by monoclonal antibodies affects the kinetic properties of 4F2hc associated system L-transport activity (i.e. 4F2hc/LAT2 and/or 4F2hc/LAT1). Thus, 4F2hc crosslinking inhibited ~2-fold the Vmax of L-Leucine transport with a ~ 2 –fold decrease of the $K_{M.}$ Eventhough the molecular mechanism involved is unknown, these results suggest that under certain circumstances, 4F2hc might influence the transport properties of LAT2 and/or LAT1.

2.3. 4F2hc/LAT2 reconstitution in proteoliposomes

Both proteins (i.e. 4F2hc/LAT2 and LAT2, also 4F2hc as a control) were tried to be incorporated in proteoliposomes upon solubilization based on the reconstitution method used for the human light subunit b^{0+}AT and the human heterodimer rBAT/b^{0+}AT (see introduction Figure 3; [Reig *et al*. 2002]). 4F2hc/LAT2 was successfully reconstituted and showed an overshoot in the transport of L-Leucine. In contrast, the light subunit LAT2 alone was not incorporated in proteoliposomes due to their aggregation tendency upon solubilization. The overshoot of L-Leucine transport depended on (i) the incorporation of a functional LAT2 protein in the liposomes (in presence of 4F2hc) and (ii) the presence of system L-amino acid substrate on the trans-side. The overshoot of 4F2hc/LAT2 (~2-fold over equilibrium at 90 minutes) was shorter and slower than that of rBAT/b^{0+}AT (~7-fold over equilibrium at 5 seconds) (Figures 3 and 49). These differences might be due to several reasons. On the one hand, the protein manipulation to form the proteoliposomes had important differences. rBAT/b^{0+}AT and the light subunit b^{0+}AT were reconstituted directly from lysated HeLa cells with a mix of detergent (sodium cholate) and phospholipids (PC and Pig brain lipids). Indeed, Reig and co-workers described how the transport activity decreased dramatically (~50%) when the light subunit b^{0+}AT was reconstituted in proteoliposomes after solubilization with DDM 0.1% during 1h at 4ºC (data included in Dr. Reig thesis. 2002). The

reconstitution of 4F2hc/LAT2 took place after the solubilization step, which required a previous lysis step of the cell wall. This precluded the use of a fast-reconstitution protocol in yeast. On the other hand, the mix of lipids to generate the liposomes was not exactly the same than in the b^{0+}AT protocol in order to increase the homogeneity of the proteoliposome population. These differences could lead to a different number of inner lamella which is relevant to the incorporation of the hydrophobic protein; more inner lamellas, more protein that is not in direct contact with the external labelled amino acid.

The success to incorporate LAT2 in the presence of 4F2hc (and its lack for LAT2 alone) remarked the stability provided by the heavy subunit 4F2hc to the light subunit LAT2.

3. Concerning HATs structure

The stability and the final amount of 4F2hc/LAT2 produced after purification was not enough to crystallization requirements but adequate for microscopic techniques, as single particle-negative staining and 3D reconstruction.

3.1. The 3D model of the human 4F2hc/LAT2 heterodimer at a nanometric resolution.

The structural reconstruction from negative staining of single particles of purified human 4F2hc/LAT2 produced in *Pichia* cells resulted in the first structural model of a HAT at a nanometric resolution (19Å). The 4F2hc/LAT2 model shows two connected particles, being one smaller and where the atomic structure of the ectodomain of human 4F2hc (Fort *et al.* 2007) could be fitted (Figure 53). Thus, paradoxically the larger particle should correspond to the light subunit LAT2. Indeed, this larger particle has a central depression facing the smaller particle (see figures 51 and 52). This characteristic shape is reminiscent of the prokaryotic LAT2 homologues analyzed by Single Particle Negative staining, Stet (Ser/Thr exchanger from *Bacillus subtilis*) and AdiC (Arg/agmatine exchanger from *E.coli*) (Reig *et al*. 2007; Casagrande *et al*. 2008; Meury *et al.*

2011). This central depression might corresponds to a large vestibule like the one present in the outward-facing structure of AdiC (Gao *et al*. 2009 [PDB 3LRB]; Gao *et al*. 2010 [PDB 3L1L]; Fang *et al*. 2009 [PDB 3NCY]; Kowalczyk *et al.* 2011 [PDB 3OB6]). The protein fold of LAT2 (and SteT) is expected to be similar to that of AdiC and LeuT, the structural paradigm of the 5+5 inverted repeat fold (also called LeuT-fold) (Yamashita *et al*. 2005). Indeed, the membrane topology of human xCT (Gasol *et al*. 2003) a paralogue of LAT2, and the structure-function studies with SteT (Bartoccioni *et al*. 2010) support this concept. Interestingly, the central depression is facing the 4F2hc ectodomain suggesting that LAT2 is in an outward-facing conformation.

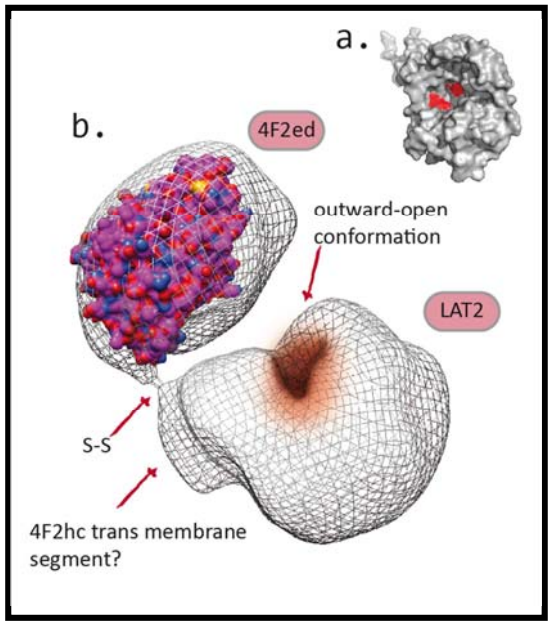

Figure 53. **4F2hc/LAT2 3D model. a)** Single AdiC subunit in outward-open conformation. View from the extracellular side showing locations of W293, an amino acid located into the translocation pathway (in red) (Fang *et al*. 2010). **b)** 4F2hc/LAT2 3D model. LAT2 shows a cavity which may indicate an outward-open conformation.

As mentioned above, the atomic structure of 4F2hc ectodomain fitted well within the small particle of 4F2hc/LAT2 model (Figue 53). Indeed, this small particle has a similar size (large, 65X wide, 55X high, 45 Å) than the atomic structure of human 4F2hc ectodomain (60X45X30 Å) (Fort *et al*. 2007). In contrast, the size of the protomer of the atomic structure of AdiC (45X50X45 Å) (Kowalczyk et al. 2011) is remarkably smaller than the large particle of the 4F2hc/LAT2 model (75X65X55 Å) (Figure 54). The high amount of detergent (DDM) sorrounding the hydrophobic surface of membrane proteins in negative-staining samples is the most probable cause for the enlargement of the LAT2 particle. Indeed, the estimated size of LAT2 in the 3D-model is very similar to that of their prokaryotic homologous analyzed by negative staining: (SteT, large, 70X wide, 60 Å) (Reig *et al*. 2007) and AdiC protomer (large, 60X wide, 75 Å) (Casagrande *et al*. 2008) (Table 5). Moreover, it should be taking into account that the large particle in the 3D model also contains the transmembrane domain of 4F2hc.

Protein	Method	Oligomeric State	Dim. (Å)	Publication
			large X wide x high	
SteT	SP-NS	Monomer	70X60	Reig *et al.* 2007
AdiC	SP-NS	Homodimer	120 X 75	Casagrande *et al.* 2008
AdiC	2D-crystallyzation (6Å)	Homodimer	95 X 55	Casagrande *et al.* 2008
AdiC	3D-crystallyzation (3.1Å)	Homodimer	90 X 50 X 45	Gao *et al.* 2009, Fang *et al.* 2010; Kowalczyk *et al.* 2011
4F2ed	SP-NS	Monomer	65 X 58	Data not shown
4F2ed	3D crystallyzation (2.1Å)	Monomer	60 X 45 X 30	Fort *et al.* 2007
4F2hc/LAT2	3D MODEL (19Å)			Present study (2012)
4F2hc		Heterodimer	65 X 55 X 45	
LAT2		Heterodimer	75 X 65 X 55	

Table 5. Prokaryotic homologues and eukaryotic transporters measurements (Å). The used methodology and the oligomeric state are indicated, the resolution is indicated between parenthesis. SP-NS Single particle –negative staining.

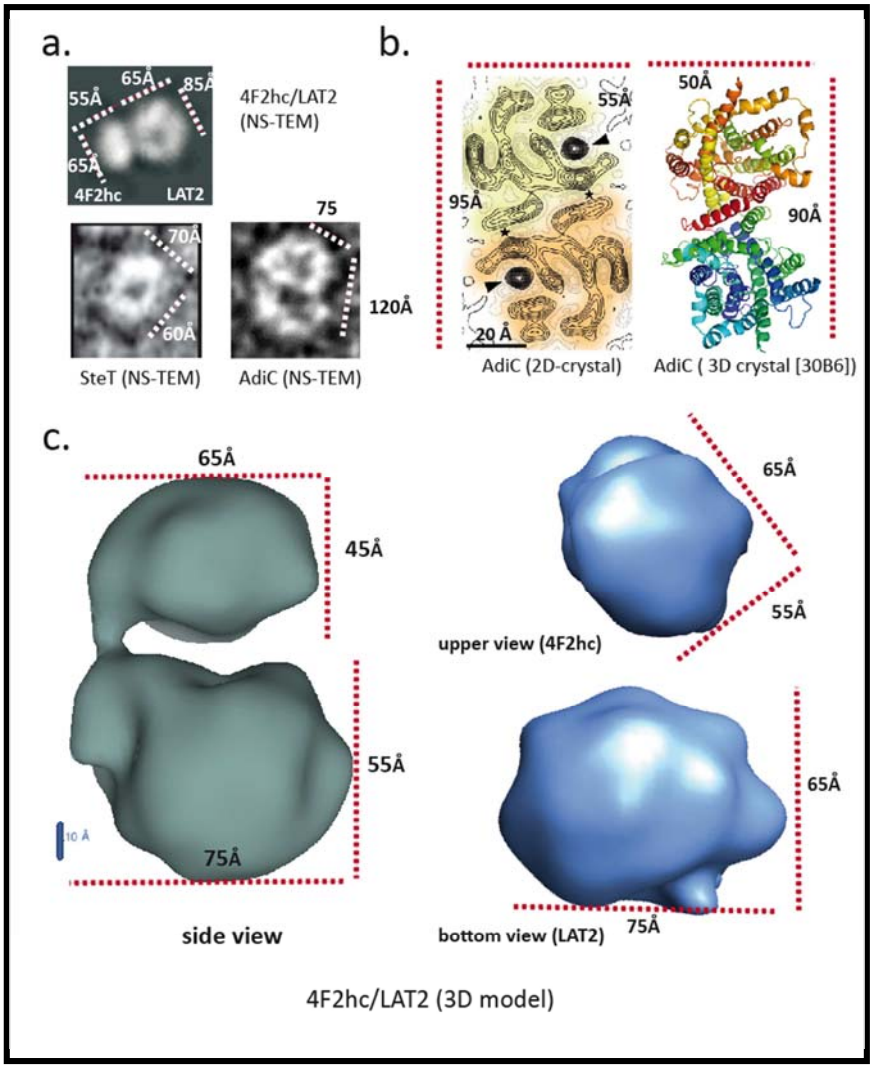

Figure 54. **Size dimensions of APC and HAT transporters estimated with different experimental approaches (Single particle-Negative staining [SP-NS], 2D-crystallization, 3D-crystallization and 3D modelling by single particle-negative staining [SP-NS]. (A) T**EM of negatively stained of 4F2hc/LAT2, SteT and AdiC-W293L (homodimer) particles. The measurements are displayed in the corresponding picture. **(B)** AdiC 2D projection structure and 3D crystal (upper view and showed as a homodimer in all the cases) both crystal structures (2D and 3D crystal) measurements coincide (90X55 Å), in contrast NS-TEM (a.) shows a bigger molecule (120X70 Å), probably due to the surrounding detergent (i.e. DDM) **(C)** 4F2hc/LAT2 heterodimer negative staining-TEM, 3D modelling structures in different views. SP-NS (a.) shows different measurements tan 3D modelling probably because of the view and the shadows in the electron micrograph.

3.2. 4F2hc/LAT2 modeling support

Fort and co-workers observed the presence of homodimers (4F2ed-4F2ed) in the 3D crystal structure preparations of the human 4F2hc ectodomain (Fort *et al*. 2007). This fact, could remember the oligomerization of rBAT/b^{0+}AT, which was found as a heterotetramer (i.e. dimer of heterodimers; rBAT/b^{0+}AT-rBAT/b^{0+}AT) in Blue Native and other supporting methods. Surprisingly, this oligomerization was independent of the integrity of the disulfide bond, suggesting other interactions between both heterodimers, being rBAT the main subunit implied in the oligomerization. Anyway, the single heterodimer was the functional unit suggesting that the oligomerization could provide a quality control step in the biogenesis pathway of the transporter. A similar analysis of the oligomerization for 4F2hc/xCT and 4F2hc/LAT2 revealed only heterodimers (Fernandez *et al*. 2006). According to these results, the new 4F2hc/LAT2 model is presented as a single functional heterodimer with no evidence of oligomerization in SP-NS after solubilization with DDM.

3.3. 4F2hc-ED on top of LAT2.

The atomic structure of 4F2ed-4F2ed homodimers allowed the construction of a model of a full 4F2hc homodimer in the membrane. This model was based on the Glycophorine A structure (Lemmon *et al*. 1994; MacKenzie *et al*. 1997), charges and hydrophobicity interactions (Fort *et al*. 2007). The model located the 4F2hc ectodomains lying on the cellular membrane suggesting an interaction with the negative-charged phospholipis (Introduction, Figure 10). In this model, the light subunit should be next to the ectodomain of 4F2hc allowing free movement of the light subunit to carry out with its transport function. This disposition may let the heavy subunit interact with other proteins (such as integrin β1 or galectin 3) to develop the role of 4F2hc as a multifunctional protein and allowing the functional transport of the light subunit without interferences. The new 4F2hc/LAT2 model proposes a particular disposition of

the heavy and the light subunits, were the ectodomain of 4F2hc is located on top of LAT2 (Figure 55).

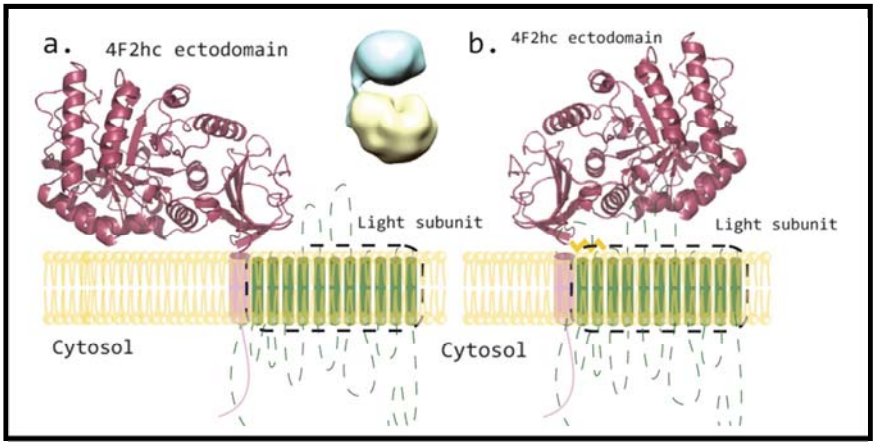

Figure 55. Previous and new heterodimer model. **a)** Proposed model for a HAT based in the crystallized 4F2hc ectodomain structure (Fort *et al*. 2007). **b)** New model based in the 3D model for 4F2hc/LAT2 (Present study).

3.4. Is 4F2hc a modulator of the transport activity of their light subunits?

In the new model, the separation between both subunits is ~16Å, which is fully compatible with the length of the longest external loops of LAT2 based on the atomic structure of AdiC. The longest loops, EL3 (external loop between TM5 and TM6) and EL4 (external loop between TM7 and TM8) are candidates to interact with the ectodomain of 4F2hc. EL3 contains ~23 residues (> 25 Å long) and shows high mobility in the AdiC atomic structures (Kowalczyk *et al*. 2011). The transition from the outward-facing apo conformation (Gao *et al.* 2009; Fang *et al*. 2009) to the outward-facing Arginine-bound occluded conformation (Gao *et al.* 2010) of AdiC implies a tilt of ~40^{o} of TM6 with the corresponding changes in EL3. Similarly, EL4 is expected to acts as a lid that closes the substrate cavity from the external medium in the inward-facing conformation (Krishnamurthy *et al*. 2012). A putative interaction of the ectodomain of 4F2hc with EL3 and EL4

might therefore interfere with the occlusion of the substrate from the external medium and the transition from outward to inward conformations (Figure 56). In other words, the location of 4F2hc ectodomain in top of LAT2 might modulate the transport activity of the light subunit.

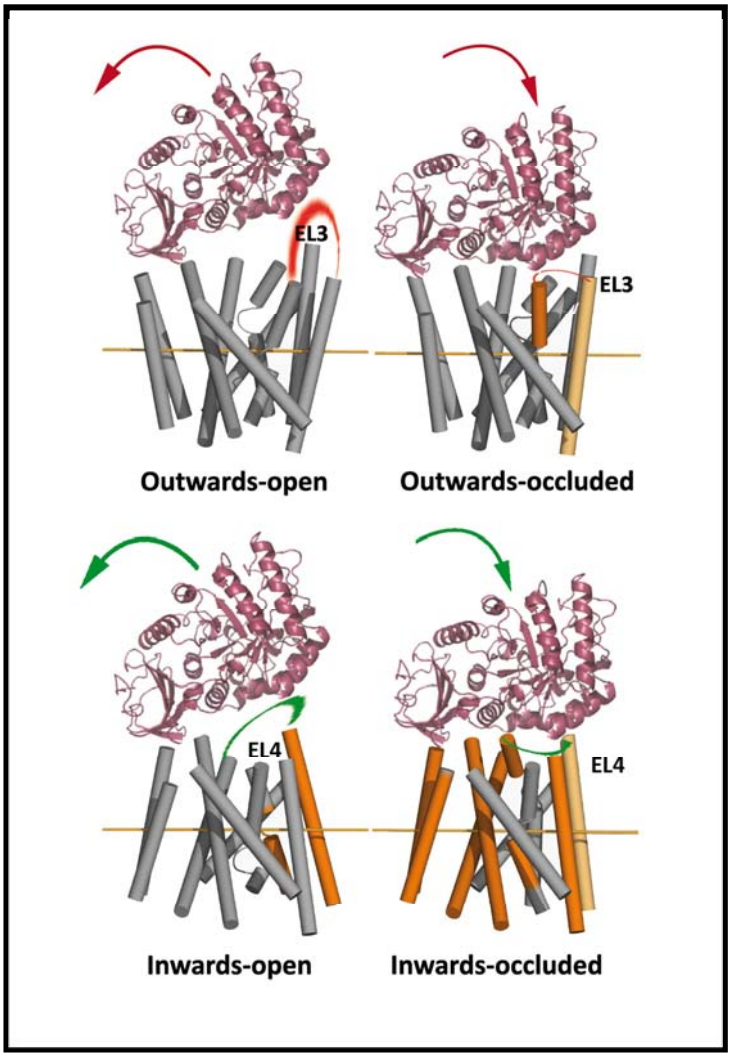

Figure 56. Position of the external loop 3 (EL3) in outward conformation and position of the external loop 4 (EL4) in inward conformation. In the figure is possible to observe the theoretical movement of EL3 when transmembrane 6 tilt 60^{o} from open to occluded state and EL4 in the same situation in the inward conformation (Image adapted from Kowalczik *et al*. 2011).

In line with the previous described hypothesis, 4F2hc-interacting proteins might modify the transport kinetics of the corresponding 4F2hc-associated light subunit. Several proteins with Ig-like ectodomain (i.e. ICAM1/2, EpCAM, CD147) interact with 4F2hc (Xu *et al*. 2005). As was explained in the introduction (see introduction, 6.4. "4F2hc bounds CD147"), Xu and Hemlet proposed that 4F2hc and CD147 are regulated in parallel in response to cell energetic needs. The functional co-regulation of cell surface 4F2hc/LAT1 and CD147/MCT protein complexes was consistent with their physical association and suggest a coordinated role on cellular metabolism. 4F2hc was found not only associated to CD147 and LAT1 but, also to the amino acid transporter ASCT2 and EpCAM (cell surface glycoprotein that is highly expressed in most malignant epithelial cells). A similar situation was observed for integrins β1/β3 (Feral *et al*. 2005; Feral *et al*. 2007), which needs 4F2hc to mediate their outside –to- inside signalling. Interestingly, all these proteins are related with cell growing and tumorigenic processes with high energetic requirements. The ectodomain of 4F2hc on top of LAT2 might facilitate the transference of information from the adhesion molecules to LAT2 transport activity. This fact may cause changes in the LAT2 transport activity. Indeed, ICAM1 crosslinking with antibodies modifies properties of 4F2hc/LAT2 in CACO-cells (Liu *et al.* 2003). In this way, 4F2hc might act as a "Key" molecule integrating cell adhesion (Feral *et al*. 2005; Liu *et al*. 2007), cell protein turnover (Nicklin *et al.* 2009), energetic requirements and cell growing (Xu *et al*. 2005) (Figure 57).

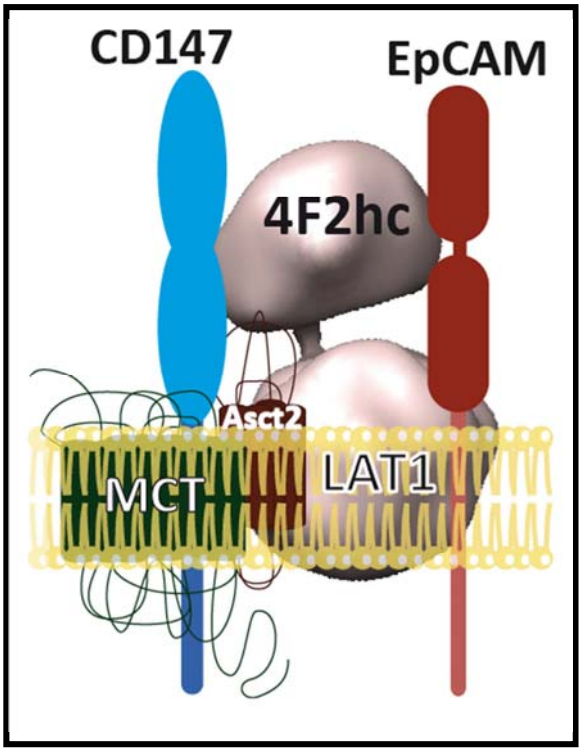

Figure 57. Model of the 4F2hc complex. Based in Xu and co-workers direct association between CD147, MCT, 4F2hc, LAT1, Asct2 and EpCAM a new view with 4F2hc/LAT2 model was performed. With the present data is impossible to know the heterodimer orientation in the cellular membrane. Figure adapted from Xu *et al*. 2005.

Conclusions

I. Co-expression of human 4F2hc and LAT2 results in the formation of disulfide-linked 4F2hc/LAT2 heterodimers, disulfide-linked 4F2hc homodimers and 4F2hc monomers in Pichia Pastoris. In contrast, 4F2hc expressed alone produces monomers and disulfide-linked homodimers, as reported in other expression systems. Expression of human LAT2 alone did not produce disulfide-linked heterodimers.

II. Pichia cells expressing 4F2hc/LAT2 or LAT2 alone acquired Na^+- independent L- Leucine uptake characteristic of the system L transport activity of the LAT2 subunit. Interestingly both transport activity had a similar KM for L-Leucine. This indicates that LAT2 in Pichia Pastoris is properly folded and traffics to the yeast plasma membrane in the absence of the heavy subunit 4F2hc.

III. 4F2hc, expressed in Pichia Pastoris is a relatively stable protein upon solubilization in DDM and purification. In contrast LAT2 expressed in Pichia Pastoris is an unstable protein with fast-aggregation upon solubilization in DDM and purification. Interestingly 4F2hc/LAT2 heterodimer is more stable than LAT2 alone upon solubilization and purification as revealed by size exclusion chromatography. This indicates than the complex with 4F2hc increases the stability of LAT2.

IV. 4F2hc/LAT2 heterodimers expressed in Pichia have been functional reconstituted in proteoliposomes upon solubilization in DDM. The reconstituted transport activity showed the typical overshoot of system L amino acid exchangers. In contrast, the fast aggregation of LAT2 expressed alone, precluded the incorporation of this protein in proteoliposomes.

V. Upon DDM solubilization, the sequential purification of 4F2hc and LAT2 in cells co-expressing both proteins yielded only in three protein species: 4F2hc/LAT2 heterodimer, 4F2hc monomers and LAT2 aggregates. The presence of only

one dimer in these preparations facilitated negative staining-single particle (NS-SP) analysis of 4F2hc/LAT2 heterodimers.

VI. 4F2hc/LAT2 heterodimers were revealed as two asymmetric particles, been the smaller brighter. 11,000 4F2hc/LAT2 particles were gathered for 3D-reconstruction, resulting, in the first low resolution (19 Å) model of a heteromeric amino acid transporter.

VII. The 3D model of human 4F2hc/LAT2 shows two connected particles connected by a lateral density. The atomic structure (PDB 2DH2) of the human 4F2hc ectodomain fits reasonable well into the small particle of the heterodimer 3D model. The light subunit particle is larger than expected for a light subunit, as compared with the monomer of the closes structural paradigm of this protein (AdiC PDB 3OB6). This suggests the presence of detergent surrounding the light subunit particle. The atomic structure of the present structural paradigm of HAT light subunits (PDB 3OB6) cannot be fitted in the large particle, indicating the presence of detergent The larger particle shows a cavity facing the smaller particle

VIII. Our first resolution model of human 4F2hc/LAT2 propose a particular disposition of the heavy and the light subunits, were the ectodomain of 4F2hc is located on top of LAT2. This suggests contacts between 4F2hc ectodomain and external loops of LAT2. This opens the possibility for a new hypothesis were changes in the interaction between the ectodomain of 4F2hc and the light subunits induced by 4F2hc interacting proteins (e.g., integrins) might modulate the activity of 4F2hc associated amino acid transporters.

Material and Methods

1. Molecular Biology

Polimerase Chain reaction (PCR)

This general molecular technic is explained in detailed in several handbooks, manuals (i.e. Molecular cloning, (Sambrook *et al*. 1989), and several thesis from our laboratory. The PCR consists in a DNA fragment amplification from a DNA template thanks to the DNA-polymerase enzyme. In the present study, the polymerase "Taq DNA polymerase" (without exonuclease activity 3´→5´ [1430-000; Roche]) and the "Expand High Fidelity Taq polymerase" (with exonuclease activity 3´→5´ [1732650; Roche]) were used depending on the needed characteristics.

Site-Directed Mutagenesis by PCR

The mutagenesis kit "QuikChangeTM Site-Directed Mutagenesis Kit" (Stratagene) let to get a fast mutated plasmid from a double stranded DNA. The basic procedure requires the synthesis of a DNA primer (around 25 nucleotides) containing in the middle of the sequence the single mutation. The used polymerase was "Pfu Turbo" which replicates both plasmid chains with the incorporated mutation. When the amplification is finished the endonuclease Dpn I is used (specific for methylated DNA) in order to digest the parental DNA. Thus, the double stranded molecule obtained is introduced into the host cells *E.Coli* XL1-Blue (supercompetents) and cloned. Finally, mutants are selected. The directed mutagenesis was used to eliminate the glycosylated sites in 4F2hc (Asn^{264}, Asn^{280}, Asn^{323} and Asn^{405}).

Sequencing

Sequencing was used in order to check if a mutation has been incorporated successfully in the DNA. In the present work the kit "ABI PRISM Dye Terminator Cycle Sequencing Ready Reaction" was fully used. The kit consists in a PCR reaction with fluorescent dinucleotides. These fluorescent dinucleotides are placed in the DNA during the amplification. The reactions for the present thesis

work were carried out by “Serveis Cientifico-Tecnics de la UB” in Parc Científic de Barcelona (PCB).

2. The methylotrophic yeast *Pichia pastoris*

The importance of *Pichia pastoris*

P. pastoris is one of the yeast species capable of metabolizing methanol. The methanol metabolic pathway involves a unique set of pathway enzymes being the first step of the oxidation of methanol to formaldehyde. The process is led by the enzyme alcohol oxidase (AOX) in the peroxisome generating hydrogen peroxide, a toxic compound expulsed away from the rest of the cell. The AOX gene and its promoter were isolated in 1980 by Salk Institute Biotechnology/Industrial Associate Inc. (SIBIA) who developed different vectors and strains to convert *Pichia pastoris* in a strong expression system under the control of this AOX promoter. Later two genes in *P. pastoris* that code for AOX (AOX1 and AOX2) were found, but the AOX1 gene is responsible for the vast majority of alcohol oxidase activity in the cell. Expression of the AOX1 gene is tightly regulated and induced essentially by methanol to high levels, controlled at the level of transcription (Courdec *et al*. 1980; Ellis *et al*. 1985; Cregg *et al*. 1989). Is important to remark that *Pichia pastoris* is useful with both, heterologous intracellular proteins or secreted proteins, which requires the presence of a signal sequence on the foreign protein to target it to the secretory pathway (For further information visit www. pichia.com).

Pichia pastoris expression strains

Three types of host strains derived of NRRL-Y 11430 (Northern Regional Research Laboratories, Peoria, Ill.) are available. These strains vary with regard to their ability to utilize methanol based in deletions in one or both *AOX* genes and all of them grown in complex media. To allow the selection, sometimes these strains have mutations in one or more auxotrophic genes like His4,

requiring a supplementation with histidine to grown on poor media (Cregg *et al*. 2009). The most common used strain is GS115 (His4) (also called GS115H); this strain is wild type for both genes, AOX1 and AOX2 and grows at the normal methanol rate. This strains are called Mut^+ phenotype (methanol utilization plus) consuming a large amount of methanol (from 5% to 30% of total media). The strains with deletions in one or both AOX genes are usually better producers of foreign proteins. In the present study the strain KM71H has been used, a strain with a large deletion in the gene AOX1 and replaced with the *S. cerevisiae* ARG4 gene. This strain is a Mut^s phenotype (or methanol utilization slow) due to the methanol metabolic pathway is regulated only by the weak gene AOX2 and is especially used when the fermentors are used and large amounts of methanol are required. The third, and less known host, MC100-3, is deleted for both AOX genes and is totally unable to grow on methanol (methanol utilization minus or Mut^- phenotype).

***Pichia pastoris* expression, vector pPICZ.**

Plasmid vectors designed for heterologous protein expression in *P. pastoris* have several common features. The chosen vector was pPICZ (EasySelect™ Pichia Expression Kit, Invitrogen). The vector allows high-level, methanol inducible expression of the gene of interest in *Pichia pastoris,* and can be used in any Pichia strain (Figure 58). The important elements in this vector are (i) the AOX promoters (AOX1 and AOX2) that are induced by methanol followed by one or more unique restriction sites for insertion of the foreign gene. (ii) The vector carries a resistance to Zeocin (Invitrogen) which can be used for selection in both, *Pichia* or *E.Coli*, and (iii) the original vector had a polyhistidine tag (6xHis), but it was modified by Dr. Rosell making it longer (10XHis), with the aim to increase the affinity in the future purification steps.

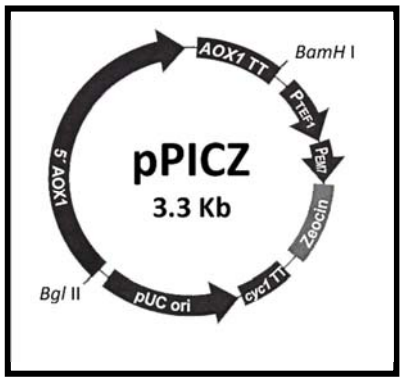

Figure 58. **Plasmid pPICZ** (This image is a modification from Invitrogen´s pPICZ image)

The ligation of the interest genes in pPICZ vector was carried out by Dr. Rosell previously to this study (for further information about pPICZ vector, consult the Invitrogen manual or www.Pichia.com).

3. Design of the recombinatinant proteins and cloning

Heavy subunits of HATS

The constructs were designed with a histidine tag (10XHis) in the N-terminus for the future purification steps (cobalt^{2+} or niquel^{2+} resin), the factor XA was designed as the cleavage site (Figure 59[a]). The construct and the strategy were developed by Dr.Rosell in our lab.

Light Subunit of HATS

The constructs were designed with a commercial short-tag call Streptag II in the N-terminus (Strep-tag II, IBA Strep-tag® Technology). This tag is composed by 8 specific amino acids, all the available information can be found in *www.iba-go.com*. Again, the cleavage site was the factor XA, as part of future purification strategies (Figure 59[b]). The construct and the strategy were developed by Dr.Rosell in our lab.

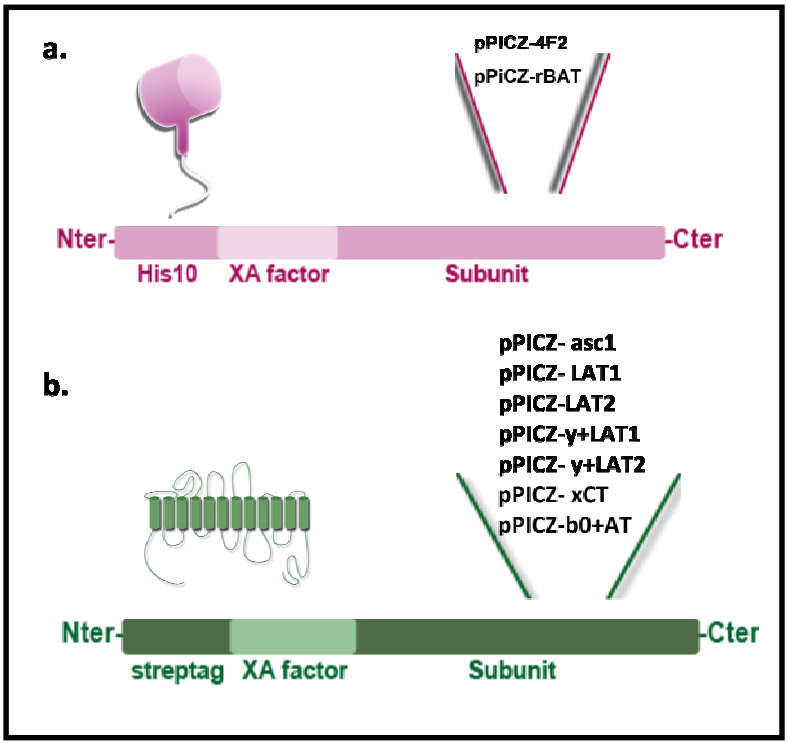

Figure 59. Design of the recombinatinant proteins a) The heavy subunits (i.e. 4F2hc and rBAT) constructs have a histidine tag in the N-terminus and the Factor XA as cleavage site. **b)** The light subunits (i.e. asc1, LAT1, LAT2, y+LAT1, y+LAT2, xCT and b^{0+}AT) have a strep-tag (IBA) and the Factor XA as cleavage site in N-terminus.

Heterodimers

The expression cassette corresponding with the light subunits was cut (BAMHI/BGLII) from the vector pPICZ and cloned in a new vector pPICZ. The expression cassette corresponding with the heavy subunits was cut (BAMHI) from the vector pPICZ and cloned in the same pPICZ where light subunit was cloned. The resulting construct showed both cDNAs (light and heavy subunits), each of them with its own promotor AOX1. This construct was used to transform the *Pichia pastoris* strain KMH71 in order to generate the different heterodimers (i.e. rBAT/b0+AT, 4F2hc/asc1, 4F2hc/LAT1, 4F2hc/LAT2). The production of a large number of clones was required in order to find a clone with a good and balanced expression of both subunits (i.e. heavy and light subunit) and the

consequent heterodimer formation. Construct and strategy was developed by Dr.Rosell in our lab.

3.1. Transformation into *E.coli* competents (XL Blue strain)

A first amplification in *E.coli* was required in order to generate a high amount of pPICZ vector with the gene of interest (heavy or light subunits or both). The transformation was carried out using hot temperatures with the consequently membrane destabilization (Heat shock method).

1. Take competent E.coli cells from –80ºC freezer and keep them at 4^{o}C until will be thawed.

2. Mixture of 80 µl of competent cells with 100 ng of DNA

3. Keep tubes on ice during 20 minutes.

4. Incubate the competents cells with the DNA into water bath at 42^{o}C for 90 seconds.

5. Incubate the sample on ice for 2 minutes.

6. Add 900 ml of LB (with no antibiotic added).

7. Incubation for 1 hour at 37^{o}C shaking at 900 rpm.

8. Centrifugate at max fast during 15 seconds and resuspend the pelled in 100 µg of LB.

9. Spread about 100 µl of the resulting culture on LB plates with Zeocine (25 µg/ml)

10) Incubate the plates overnight at 37^{o}C.

Next day the colonies will be prepared to be picked up. 6 different clones will be grown overnight in liquid LB adding zeocine (25 µl/ml) at 37^{o}C.

DNA Extraction

The clones were grown in a 500 ml culture to extract the DNA with a Maxiprep kit (Qiagen) under the owner recommendations. Both, Miniprep and Maxiprep kits are based in the cellular membrane lysis by a salt treatment and the DNA adsorption in a silica resin in presence of a high salt concentration buffer. The elution was done with a low salt concentration buffer or deionized water.

3.2 Transformation into *Pichia pastoris* cells.

Linearization of pPICZ constructs

To promote integration, the linearization of the vector is recommended, but not mandatory. The linearization is done within the 5′ AOX1 (Figure 60) region and the invitrogen protocol provides the list with the unique sites that may be used to linearize pPICZ prior to transformation. The cleavage sites are the same for all the versions of pPICZ. In our case the enzyme pmeI (New England Biolabs, the protocol is provided by the owner. Restriction site 414 bp) was chosen.

1. Digestion: ~10–25 µg of plasmid DNA digested with pmeI.

2. Check a small aliquot of your digest by agarose gel electrophoresis for a complete linearization.

3. If the vector is completely linearized, heat 65ºC during 15 minutes to inactivate the endonuclease.

4. Evaporate the buffer by a vacuum concentrator and resuspend in 10 µl sterile and deionized water.

5. Use immediately or store at –20°C.

Sometimes and depending on the construct, *pme*I was not working properly making the digestion unviable. In this case was necessary to increase the amount of DNA to 150 µg, evaporate the buffer and resuspend in 10 µl of deionized sterile water. If the DNA is half linearized, purify the lineal vector from an agarose gel, this should enrich the linearized plasmid and should make easy the future transformation.

***Generation of competent Pichia pastoris* cells**

25 ml cold (4°C) sterile sorbitol (1 M) (place on ice the day of the experiment), 30°C incubator, Electroporation device and 0.2 cm cuvettes (Gene Pulser® II electroporator: (Bio-Rad Laboratories), YPD-Agar plates containing Zeocin (100 µg/ml).

1. Grow a 5mL overnight culture of *Pichia pastoris* cells (KM71H strain) in YPD in a 30°C shaking incubator.

2. Dilute the overnight culture to 0.15–0.20 ($A_{bs600nm}$) in a volume of 50 mL YPD in a flask large enough to provide good aeration, which means 5 times initial volume.

3. Grow yeast to an absorbance of 0.8–1.0 ($A_{bs600nm}$) in a 30°C shaking incubator. It should take 4-5 hours.

4. Centrifuge the culture at 500×g for 5 min at room temperature and pour off the supernatant.

5. Resuspend the pellet in 9 mL of ice-cold supplemented BEDS solution with DTT 200 mM.

6. Incubate the cell suspension for 5 min at 100 rpm in the 30°C shaking incubator.

7. Centrifuge the culture again at 500×g for 5 min at room temperature and resuspend the cells in 1 mL of BEDS solution without DTT.

8. The competent cells are now ready for transformation. It is possible in that point, to freeze the cells slowly in small aliquots at -80°C. Do not store the cells more than 6 months.

***Pichia pastoris* transformation**

1. Mix approximately 10 µl of linearized plasmid DNA with 80 µl of competent cells in an electroporation cuvette (0.2 cm gap sterile electroporation cuvette, bio-Rad). Incubate for 2 min on ice.

2. Electroporate samples using the following parameters: Gene Pulser® II electroporator: (Bio-Rad Laboratories): cuvette gap, 2.0 mm; charging voltage, 1500 V; resistance, 200 Ω; capacitance, 25 µF.

3. Immediately after electroporation, resuspend in 0.5 mL 1.0 M sorbitol and 0.5 mL YPD, incubate in a 30°C shaker for 1 h-3h.

4. Plate on media containing zeocin (100 µg/mL).

Note: Increasing the zeocine concentration from 100 µg/ml to 1000 µg/ml is useful in the selection multicopy integrants.

4. Expression Screening of HATs in *Pichia pastoris*

4.1. Selecting Positive clones (Zeocin resistants)

A small-scale initial screening (50 ml conical polypropylene tubes, Nunc) is required to identify or confirm a recombinant *Pichia pastoris* clone that is expressing the inserted protein. It is recommended to perform the screening with 6-10 colonies.

Culture with YPD medium

Resuspend a single colony in 5ml of YPD autoclaved medium.

Grow at 30°C in a shaking incubator (250 rpm, for 16h). Inoculate 20 µl from the first YPD culture in 5 ml of YPD with Zeocin (50 µg/ml or 100 µg/ml). Grow at 30°C in a shaking incubator (250 rpm for 16h). The cultures growning in these conditions will be considered as putative positives.

Expressing protein in *Pichia pastoris*

1. Inoculate 15 µl from the YPD culture corresponding to the putative positives, in 15 ml of BMGY in a 50 ml conical polypropylene tube.

2. Grow at 30°C in a shaking incubator (250 rpm) until culture reaches an $A_{BS600nm}$ = 2–6 (approximately 16–18 hours).

3. Centrifuge the cells using sterile centrifuge tubes at 1500 g for 5 minutes at room temperature.

4. Decant the supernatant and resuspend cell pellet in 3 ml of BMMY medium to start induction. (To Scaling up, note than BMMY volume always is 5X less than BMGY).

5. Cover the tubes with 2 layers of sterile gauze and return to incubator.

6. Continue to grow at 30°C shaking 250 rpm.

7. Add 1% methanol every 24 hours (3 days as standard).

8. Centrifuge cells at 2500g for 5 minutes at room temperature.

9. Decant the supernatant and store the cell pellets at –80°C until ready to process.

5. Cellular lysis and membrane purification

In order to disrupt the *Pichia pastoris* strong membrane in small pieces, setting up different lysis strategies were required. Once the membranes were lysed, membrane purification was required in order to discard the soluble proteins and the large membrane pieces. Always protease inhibitors (Complete, EDTA-free; Roche) were added in the specified proportion (1 tablet each 25-50 ml).

Cellular disruption and membrane purification using Glass beads and FastPrep

The pelled from the putative positives was resuspended in 300 µl of Breaking Buffer. The same volume of glass beads was mixed with the sample in a special reinforced Fast-Prep tube.

The FastPrep (FP120A Instrument (120W), QBiogene), is an instrument to lyse up simultaneously 12 samples in special reinforced tubes (Kisker, 2ml tubes). Using resins or beads (glass beads, acid-washed 212-300 µm [Sigma-Aldrich]), is possible to pulverize the sample because of the vertical and angular motion.

The lysis protocol was: Power: 6.0 W, Time: 10 seconds, Cycles: 3

After this first lysis step centrifuge during 10 minutes at 4^{o}C, 600Xg, remove the supernatant and keep it in ice. Add 300 µl of Breaking Buffer in the FastPrep tube and resuspend the glass beads. Again, repeat the FastPrep cycle: Power: 6.0 W, Time: 10 seconds, Cycles: 3. Finally, to obtain the purified membranes ultracentrifuge the supernatant at 250,000xg, 4^{o}C for 1:15h. Remove the supernatant and resuspend the pellet in 300 µl of Tris 20mM/150 mM NaCl/ 5% glycerol. Frezze the purified membranes fastly in liquid N^2 and keep them at -80^{o}C. The amount of total membrane protein was evaluated by BCA Assay (Pierce). The protein expression will be analysed by western Blot (See Material and methods 7.2)

Scaling up the *Pichia pastoris* growing

The scaling up is necessary in order to produce enough amount of protein to carry out the crystallization assays once the positive clone for your recombinant

protein is detected. Depending on the protein expression amount, the growing volume will be calculated. In the present study, 1 liter of culture (BMMY) was enough for three small affinity purification trials. Starting with 5 liters of BMGY a final volume of 1 liter (BMMY) is produced (a reduction of 5X).

1. Inoculate 150-200 µl from the starter (YPD) in 1 liter of BMGY.

2. Grow at 30°C in a shaking incubator (250 rpm) until culture reaches an OD600 = 2–6 (approximately 16–18 hours).

3. Centrifuge the cells using sterile centrifuge tubes at 1500 g for 5 minutes at room temperature.

4. Decant the supernatant and resuspend cell pellet in 200 ml of BMMY medium to start induction.

5. Cover the tubes with 2 layers of sterile gauze and return to incubator.

6. Continue to grow at 30°C shaking 250 rpm.

7. Add 1% methanol every 24 hours (3 days as standard).

8. Centrifuge cells at 2500g for 5 minutes at room temperature.

9. Decant the supernatant and store the cell pellets at –80°C until ready to process.

Cellular lysis and membrane purification by Cell disruptor

This disruption method is based in acceleration cells from static to high velocity with the help of a pump through a very small jet orifice. The rapid acceleration causes the outer skin of the cell to rush into a jet. The mass of the cells internal content however take longer to achieve the same speed. The result is that the content of the cell fall out of the back of the cells outer skin.

Disruption head was surrounded by a cooling jacket, necessary for the 4^{o}C maintenance and avoid the protein degradation. To break *P.pastoris* membrane, only one cycle at the maximum pressure (40 KPSI) was enough, but in order to reduce the DNA density effect, a study of different cycle and pressures was required. At least the protocol was fixed in 1 cycle at 25 KPSI, 2 cycles at 30 KPSI and 1 final cycle at 40 KPSI. The cells were lysed in a final ratio of 0.2gr/ml in Breaking buffer.

Once the cellular lysis finished, the membrane purification started.

1. Centrifuge the broken cells during 15 minutes at 4ºC, 20000Xg

2. Remove the supernatant and keep it in a reinforced tube for ultracentrifuge.

3. Ultracentrifuge the supernatant at 250000xg, 4^{o}C during 1:15 h.

4. Remove the supernatant.

5. Resuspend the pellet in half of the starting volume of Tris 20mM/150 mM NaCl/ 5% glycerol, using an adequate syringe.

6. Ultracentrifuge at 250000xg, 4^{o}C during 1:15 h.

7. Resuspend the pellet in half of the initial volume of Tris 20mM/150 mM NaCl/ 5% glycerol, using an adequate syringe.

8. Frezze the purified membranes fastly in liquid N_2 and keep at -80^{o}C.

The amount of total membrane protein was evaluated by the BCA Assay (Pierce)

The protein expression will be analysed by western Blot (See Material and methods 7.2)

6. Media and buffers used in the *P.pastoris* protocols

Low Salt LB Medium (with Zeocin) (1 liter)

1. Dissolve 10 g Tryptone, 5 g NaCl and 5 g Yeast Extract in 950 ml of deionized water.

2. Adjust pH to 7.5 with 1N NaOH. Bring the volume up to 1 liter (For plates, add 15 g/L agar before autoclaving)

3. Autoclave (liquid cycle) for 20 minutes.

4. Allow the medium to cool to at least 55°C before adding Zeocin to 25 µg/ml final concentration.

5. Store plates at 4°C in the dark.

Plates containing Zeocin are stable for up to 2 weeks.

Yeast Extract Peptone Dextrose Medium (YPD) (1 liter)

1. Dissolve 10 g yeast extract and 20 g peptone in 900 ml deionized water (For plates, add 20 g of 2% agar at time with the yeast extract and the peptone and dissolve, adjust the pH to 7,5)

2. Autoclave for 20 minutes (liquid cycle)

3. Add 100 ml of 2% dextrose (200 g of dextrose [D-glucose] in 1000 ml of hot deionized water and autoclave for 20 minutes; filter-sterilize dextrose before use).

Zeocin (Invitrogen, 100mg/ml), is added in a final concentration of 100 μg/ml (25 μg/ml in *E.Coli* case) if necessary when the temperature down 55^{o}C (Plates containing Zeocin are stable for 1 or 2 weeks).

Special Buffers:

BEDS solution**:** 10 mM bicine-NaOH, pH 8.3, 3% (v/v) ethylene glycol, 5% (v/v) (dimethyl sulfoxide) DMSO, and 1 M sorbitol. Keep it at Room Temperature.

BEDS solution with DTT: BEDS adding DTT. Various concentrations were tried (from 50 to 250 mM) being 200 mM the most effective. Keep it cold.

Yeast Nitrogen Base (YNB) (10X) (1 liter)

1. Dissolve 134 g of yeast nitrogen base (YNB, Promega) in 1000 ml deionized water and filter.

2. Store at 4°C in a dark room. The shelf life of this solution is approximately one year.

Biotin 500x (0.02%)

1. Dissolve 20 mg biotin in 100 ml of deionized water and filter.

2. Store at 4°C (The shelf life of this solution is approximately one year).

Buffered Glycerol-complex medium (BMGY) / Buffered Methanol-complex medium (BMMY)

2% peptone, 100 mM potassium phosphate, pH 6.0, 1.34% YNB, 4 × 10-5% biotin, 1% glycerol / 0.5% methanol, 1% yeast extract

1. Dissolve 10 g of yeast extract, 20 g peptone in 700 ml deionized water.

2. Autoclave 20 minutes on liquid cycle.

3. Cool to room temperature, and then add the following and mix well (into the laminar hood):

100 ml potassium phosphate (1 M) buffer, pH 6.0

100 ml YNB (10X)

2 ml Biotin (500X)

100 ml Glycerol (10X)

4. For Methanol-complex medium, add 100 ml Methanol (10X)
instead of glycerol.

5. Store media at 4° (The shelf life of this solution is approximately two months)

Breaking Buffer (1 liter)

1. Dissolve 6 g sodium phosphate monobasic (50 mM sodium phosphate), 372 mg EDTA (1 mM EDTA), 50 ml glycerol (5% glycerol) into 900 ml deionized water

2. Adjust pH 7.4 and bring up the volume to 1 liter. Store at 4°C. The shelf life of this solution is approximately six months.

7. Protein analysis and detection

7.1. Electrophoresis in Sodium Dodecyl Sulphate PolyAcrylamide Gel Electrophoresis (SDS-PAGE)

The electrophoresis in polyacrylamide gel with SDS (SDS- PAGE) has been a method widely used to separate proteins according to their molecular weight (Laemmli, 1970). The method is based in two gels with a different acrylamide concentration. The upper gel (stacking) is a large pore (pH 6) gel meanwhile the below gel (running) is the separator gel. The proteins are concentrated during the first running in a thin starting zone. The second gel has higher polyacrylamide content and is in this step when the proteins separation takes place. All the westerns in the present study were done in gels of 10 x 8 cm and 1.5 mm (thickness) in the "miniprotein 3 kit (Bio-Rad)". The gels were composed by different acrylamide concentration in order to see different kind of bands: (i) the heavy subunits (~70 KDa, 4F2hc and rBAT), 7.5 % of acrylamide and (ii) the light subunits (~50 KDa, asc1, LAT1, LAT2, y+LAT1, y+LAT2, b^{0+}AT), 10 % of

acrylamide. In addition the herodimers were analysed in only one of these gels in order to detect the heavy/light subunit or both.

Sample preparation for SDS-PAGE.

Always 5 µg, of total protein from purified membranes was charged in each well. The total protein was mixed with loading sample buffer 2X (LSB, composition: Tris/HCl 50 mM, pH 6.8, DTT 10 mM, 2 % (w/v) SDS, glycerol 10 % and bromophenol blue 0.1 % (w/v)) in the same volume (1:1 v/v) and heated during 10 minutes in order to make easier the band detection. The heating temperatures changed depending on the protein, (i) the heavy subunits were heated at 95^{o}C and (ii) the light subunits and the heterodimers were heated at 60^{o}C. Only when it was required, DTT (dithiothreitol) was added in a concentration of 100 mM with the aim to reduce the disulfide linkages. Using DTT the single band of the heterodimer is detected as two different bands (i.e. one for the heavy subunit and another for the light subunit). The molecular weight marker was provided by Bio-Rad, the range as general moved from 30 KDa to 250 KDa with variations depending on the batch.

SDS-PAGE gel staining

The coomassie staining was performed as a sample purity control (all the present proteins in an amount of 0.5 µg should be stained). The SDS-PAGE was stained for 1 hour with the staining buffer (45 % methanol, 10 % acetic acid, 45 % distilled water and 0.1 % w/v Brilliant Blue R, Sigma). In this point all the proteins present in the gel should be visible. The gel was washed with a cleaning solution (7.5% acetic acid, 7.5% isopropanol and distilled water) until the background was almost transparent. On the other hand, the silver staining method was widely used in the present study because of its high sensitive rate, detecting until 0.25 ng of protein. The silver staining kit from Pierce was used following exactly the owner direction.

7.2. Western Blot Analysis

The resulting separated proteins by SDS-PAGE were transferred to a nitrocellulose membrane activated previously with methanol (5 minutes) and transferred during 1:30 h at 250 mA (miniprotein 3 kit; Bio-Rad). The heavy subunits and the light subunits followed different western blot protocols.

Heavy subunits

The membrane was blocked in PBS 1X, 5% milk for 1 hour at room temperature. After the blocking step the antibodies were added, (i) the heavy subunit 4F2hc, was incubated with anti-CD98 (H-300) (Santa Cruz Biotechnology) at 4^{o}C in a 1:1000 dilution overnight. The heavy subunit rBAT (ii) was incubated with anti-Histag antibody overnight at 4^{o}C in a 1:1000 dilution. The membranes were washed three times with PBS 1X, 0.5%-Tween during 10 minutes. The incubation with the secondary antibody was carried out (donkey antirabbit (4F2hc) or antimouse (rBAT) in a dilution of 1:25000) during 1 hour at room temperature.

Light subunits

The membrane was blocked in albumin 3%, Tween-0.5 % in PBS for 1 hour at room temperature. After the blocking step, the membrane was incubated with Strepmab-classic HRP conjugate (IBA) antibody, at room temperature for 1 hour (dilution 1:10000) in PBS 1X, Tween-0.5%. This antibody is conjugated with a peroxidase, thus the addition of a secondary antibody was not required. The same day the membranes were washed three times in PBS 1X, Tween-0.5% during 10 minutes. In both cases the membranes were prepared to be developed with ECL (Amersham-Pharmacia).

8. Solubilization trials

To extract the protein from the membrane the use of detergent was required. One of the most popular detergents is DDM, and was the most used during all this study. All the solubilization trials were done in small scale.

Solubilization buffer: 20 mM Tris/HCl, 150 mM NaCl, 10% glycerol and detergent in the desired concentration. Note: for the screenings different concentrations were tried (from 0.1-0.5% to 1%). 2% was used in the scaled up affinity purification trials.

The membranes were mixed with the solubilization buffer in a total membrane protein concentration of 3 mg/ml (different concentrations were tried, see Results Figures from 24 to 28), in a final volume of 500 µl. The membranes were solubilized during 1-2 hours at 4°C, gently agitated. After that, an ultracentrifugation at 250,000xg, 4°C was carried out during 1:15h. The supernatant was kept at 4°C (solubilized protein) and the pelled was resuspended in 500 µl of tris 20mM buffer (aggregated protein). Both, supernatant and pellet were quantified by BCA Assay (Pierce) and compared by western blot.

9. Protein purification

The 4F2hc protein had a 10Xhis tag which allows the purification step using cobalt or nickel resin. In the present study cobalt was used in order to get the maximum purity. Cobalt resin is based in the stable chelation charged with the Co^{2+} ion, which has a remarkable affinity and specificity for his-tagged proteins.

Equilibration buffer: 20 mM Tris/HCl, 150 mM NaCl, 10% glycerol, 5mM Imidazole, detergent in a low concentration (i.e. DDM 0.25% for 4F2hc)

Washing buffer: 20 mM Tris/HCl, 150 mM NaCl, 10% glycerol, 25mM Imidazole, DDM 0.25%.

Elution buffer: 20 mM Tris/HCl, 150 mM NaCl, 10% glycerol, 200mM Imidazole, detergent 1.5XCMC (0.15% of final DDM for 4F2hc)

The resin was previously equilibrated centrifuging (700 x g for 2 min), removing the supernatant and adding 10 bed volumes of Equilibration buffer. Three washes were enough to equilibrate the resin. Transfer the required amount of

resin suspension to a cold tube and keep it in ice. In the present study 2 ml of resin slurry were added for 50 mg of total membrane protein.

The binding was done generally by batch followed by a second gravity binding. This method combines the speed and convenience of a batch procedure with the higher purity of the gravity-flow column method. The solubilized protein and the equilibrated resin were gently agitated at 4°C for 2 hours on a platform shaker. Next, the resin was centrifuged at 700 x g for 5 min, and carefully the supernatant was kept in a tube. The resin was then packet in a column and the supernatant was passed through by gravity (4 ° C).

The resin was washed by gravity adding 10–20 bed volumes of Washing Buffer. In this step the detergent concentration (DDM) was decreased to 0.25% and the Imidazole concentration was increased to 25 mM.

Finally, the concentration of imidazole was increased to 200 mM. The Imidazole elutes the sample and the protein is collected in fractions of 500 µl in cold eppendorfs.

The LAT2 purification was based in the well-known binding of biotin to streptavidin (http://www.ibago.com /prottools/prot_i_story.html) and was done with the superflow prepacket columns from IBA (strep-tactin superflow, IBA), a friendly one step purification.

Equilibration buffer: 20 mM Tris/HCl, 150 mM NaCl, 10% glycerol, detergent in a low concentration (DDM 0.15%)

Washing buffer: 20 mM Tris/HCl, 150 mM NaCl, 10% glycerol, DDM 0.25%.

Elution buffer: 20 mM Tris/HCl, 150 mM NaCl, 10% glycerol, DDM 0.15%, 2.5 mM desthiobiotin.

The resin was previously equilibrated adding 10 bed volumes of equilibration buffer by gravity. The binding was done by gravity at 4°C. In this step the protein binds the resin. The resin was washed adding 5 bed volumes of Washing Buffer ç80.25% DDM). In the elution step the detergent concentration (DDM) was decreased to 0.15%. Desthiobiotin displaces Strep-tag II proteins at the biotin-binding site of Strep-Tactin in a competitive manner resulting in a mild elution of the protein. The eluate was collected in 500 µl fractions.

In the case of the heterodimer 4F2hc/LAT2) two tags were present (10XHis tag in the heavy subunit and Streptag II in the light subunit) having the possibility of a double round purification. The protocol is exactly the same explained for both resins (i.e. cobalt and streptactin), considering the eluted from the first purification the starting sample for the second one.

Considerations:

Cobalt resin is the best choice during the first purification round. StreptagII is more analytical and more useful in the second round purification. This is entirely explained in "Results 4.3 Heterodimers".

The timeline of the experiment was extremely long; with the consequent loss of protein. Thus, when the double round purification was not necessary, it was avoided, and the affinity purification was performed in only one round (cobalt).

10. Protein Concentration

After the protein purification step, a concentrator with a cut off of 100 KDa (millipore) was used to concentrate the sample, always keeping the temperature at 4^{o}C. During this step the detergent and the imidazole concentration were reduced if was required.

11. Size Exclusion Chromatography

Äkta purifier (GE healthcare) let the fast protein liquid chromatography (FPLC) purification for proteins or peptides. The Äkta purifier accepts protein amounts in order of μg-mg and measures at 280 nm as usual. This Äkta was used widely in the present study to comprove the aggregation state of the proteins (i.e. 4F2hc, LAT2 and 4F2hc/LAT2) always keeping the temperature at 4^{o}C and using the high resolution Superdex 200 10/300 GL column (GE healthcare). That resin (i.e. Superdex200) accepts ranges from 3,000 to 660,000 Daltons of molecular weight in a bed volume of 24 ml.

12. Functional characterization

Membrane proteins usually keep their functional activity only if they are in an adequate phospholipid environment. Thus, liposomes are widely used in functional studies and characterization of these proteins. The important parameters to be considered in reconstitution are (i) the stability of the protein complex in the detergent-solubilized state, (ii) the specific lipid requirement of the protein and the liposome type, and (iii) the specific protein-to-lipid ratio.

Phospholipids, detergents and cholesterol

The tendency of phospholipids to aggregate forming spontaneously circular vesicles in presence of water (Tanford *et al*. 1980) has been broadly used in different fields and specialities. The typical structure adopted in aqueous medium is the liposome. Liposomes are used in cancer therapies carrying drugs or cytotoxic metals (i.e. Cis-platinum) (Reviewed by Frezza *et al.* 2010), in cancer research non-toxic metals (i.e. erbium, gadolinium) are being irradiated in biomedical beamlines to destroy glyomas in rats (Regnard *et al*. 2008), melanoma or cancer breast (Costa *et al*. 2009), Fe^{2+}/Fe^{3+} magnetoliposomes are lead to tumours by using giant medical magnets (Fattahi *et al.* 2011; Wang *et al*. 2011; Alexiou *et al.* 2006). Liposomes can carry vitamins or other substances useful in nutrition or cosmetics (Papakostas *et al*. 2011). Liposomes are used in transport assays to characterize transporters (Reig *et al*. 2002) and, in the present study were used widely to reconstitute the heterodimer 4F2hc/LAT2 with the aim of both, to comprovate the functionality of the solubilized heterodimer, and investigate the role of the heavy subunit in the transport function.

Different kinds of liposomes are developed for these transport assays, but not all of them are used in the same context. Multilamellar Large Vesicles (i.e. MLV) formation is spontaneous by vortexing phospholipids in aqueous medium, these liposomes have a very small lumen with a high number of lamellas hidden inside. MLVs are saturated rapidly, and high amount of protein could be reconstituted in the hidden lamellas, because of that, are not the best option. When MLVs are

disaggregated by mechanical sound waves, oligolamellar liposomes (i.e. OLV) appear with a diameter in ranges of 80-700 nm. If these mechanical waves are prolonged, typically produce small unilamellar vesicles (SUV) with diameters in the range of 15-50nm (Lichtenberg *et al*. 1988; Weiner *et al*. 1994; Chandran *et al*. 1997; Mozafari. 2005; Samad *et al*. 2007). SUV´s are smaller than OLV´s and only with a single bilayer and are typically formed with a probe tip sonicator. Homogenous formation of SUV´s is highly complicated, remaining always large particles (OLV) that can be removed by low-speed centrifugation (1500 g) to yield a clear suspension of SUVs. When OLVs or MLVs are extruded, unilamellar large vesicles (i.e. ULV) appear (Figure 60). These liposomes are probably the most useful carrying drugs or other molecules, are the large size liposomes with only one lamella. The unilamellar large vesicles (ULVs) are normally controlled by size and number by Dynamic light scattering (DLS) or Small angle X-ray diffraction (SAXS) (Nawroth *et al*. 2011; Cocera *et al*. 2004; Kucerka *et al*. 2007) by linear or circular particles accelerators.

The liposomes in the present study were huge OLVs generated in a bath sonicator, with a homogeneus population of 900 nm (See results Figure 46).

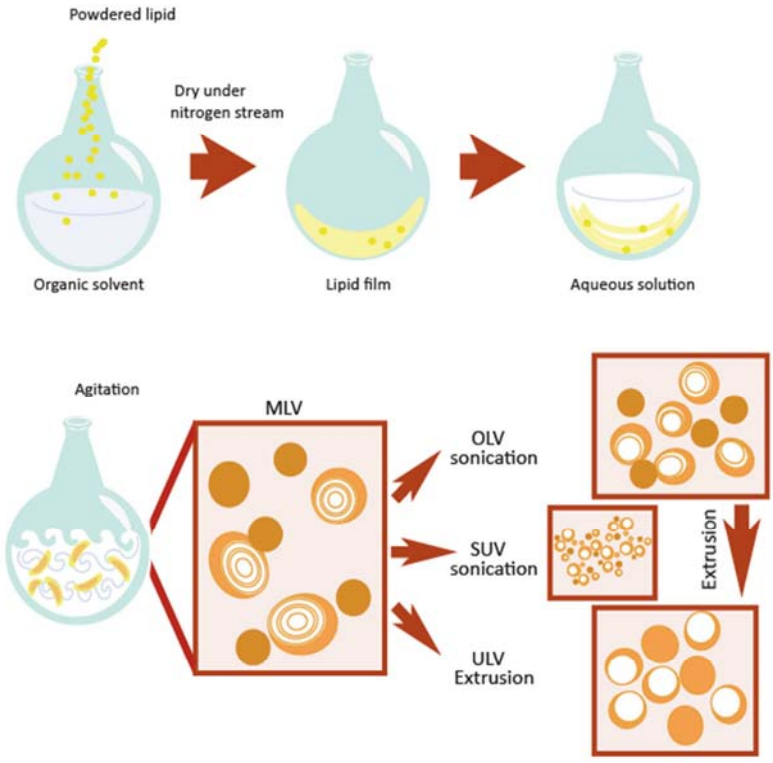

Figure 60. A general scheme of liposome formation. Lipids are solubilized in an organic solvent (i.e. chloroform) and dried under N2 gas forming the typical lipid film. Hydration with the desired polar solvent will form MLV by vortexing. Oligolamellar large vesicles (OLV), small unilamellar vesicles (SUV) or unilamellar large vesicles (ULV) could be formed depending on used method.

12.1. Reconstitution from solubilized protein

Liposomes formation (OLV´s)

For liposome preparation, soybean phospholipids (Asolectin, 40 mg/ml [Sigma-Aldrich] and purified pig brain lipids were both dissolved in chloroform in a specific ratio, 1:1 (v/v) (based in Reig *et al*. 2002). Lipids were dried slowly under a stream of nitrogen, and pumped under vacuum for at least 3h. The final lipid films were resuspended in reconstitution buffer (0.5 mM EDTA, 1 mM MgSO4, 5mM TrisSO4, pH 7.4, 1% Glycerol, 120 mM KPI, pH 7.4 and 4 mM L-amino acid or not) and vortexed for 15 minutes, resulting in a final concentration of

multilamellar vesicles (MLVs) of 40 mg/ml. The resulting MLVs were sonicated in a bath sonicator (4 cycles, 30 seconds) resulting in OLV´s (Figure 61).

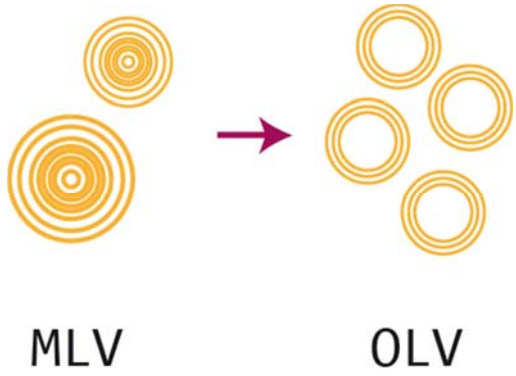

Figure 61. Schematic view of multilamellar large vesicles and oligolamellar large vesicles. OLVs have a medium encapsulate capacity and a medium number of hidden lamellas in constast with MLVs, which have a low encapsulate capacity and a high number of hidden lamellas.

Incorporation of protein with the liposomes

Based on Dr. Kanner protocol (Radian *et al*. 1985) and the consequent adaptation for the light subunit b^{0+}AT in our laboratory (Reig *et al.* 2002), a new protocol was performed for solubilized protein reconstitution in liposomes. The original protocol is specified in Dra.Reig´s dissertation (Reig *et al*. 2002), in order to make these phospholipids extremely pure. In the present study, a new reconstitution protocol from solubilized protein was adapted.

The proteins (4F2hc/LAT2 and 4F2hc) were solubilized with DDM 0.5% during 30 minutes at 4°C. The solubilized proteins were ultracentrifugated at 250,000xg, during 1 hour at 4°C. The liposomes and each solubilized protein were mix in a lipid protein ratio (LPR) (w/w) 50/1 during 10 minutes, vortexing twice during 2 seconds each. After the incubation, the detergent (i.e. DDM 0.5%) was adsorbed with polystyrene beads (Bio-Beads SM2 Adsorbent, Bio-Rad Laboratories) during

3 hours by three different additions at 4°C and the supernatant was collected by pipetting. Proteoliposomes were harvested by ultracentrifugation (250,000×g, 4°C, 1h) and the pellet was resuspended in half of the volume with reconstitution buffer. The incorporated protein in the harvested liposomes was analysed by a BCA assays, adding SDS 2% in order to avoid the liposomes scattering.

Liposomes characterization

The DLS (Dynamic light scattering [Zetasizer Nano S, Malvern]) is used to measure particle size and molecule size. This technique measures the diffusion of particles moving under Brownian motion, and converts this to size and a size distribution in relation with the scattering angle. The machine has a temperature regulator that keeps the sample at 4°C. In the present study, DLS was useful to check the different size populations in the liposomes sample and the corresponding diameter of the liposomes. Thus, the most homogenous sonicated liposomes made with Pig Brain Lipid and asolectine in different ratios was determined. The sample volume required was 50 µl in a dilution of 1:100 from a 20 mg/ml sample. The results were represented in bars graphic showing the volume (%) of each liposome population and the size diameter (nm).

Transport Assay in proteoliposomes

The same transport Assay protocol was performed for solubilized 4F2hc/LAT2 and for purified 4F2hc/LAT2.

Proteoliposomes (10 µl) were mixed with 180 µl of transport buffer (150 mM choline chloride, 10 mM Tris-HEPES, pH 7.4, 1mM MgCl2 and 1mM CaCl2, 0.5 µCi of radiolabeled L-amino acid and 10 µM of unlabelled L-amino acid; Radiolabeled compounds (American Radiolabeled Chemicals) l-[3H] Leucine, l-[3H] Isoleucine) and incubated at room temperature for different periods of time. Reactions were stopped by the addition of 850 µl of ice-cold stop buffer (150 mM choline chloride, 10 mM Tris-HEPES and 5 mM L-amino acid) and all the volume was filtrated through membrane filters (Sartorius; 0.45-µm pore

size). Filters were then washed three times with 2 ml of stop buffer and dried. The trapped radioactivity was counted in a Packard Tri-Carb Liquid Scintillation Counter. All experimental values were corrected by subtracting zero time values obtained by adding the stop solution before the proteoliposomes into the transport buffer.

12.2. Transport Assay in *Pichia pastoris* cells

The transport uptake was set up in the expression system *Pichia pastoris* expressing 4F2hc/LAT2, LAT2 and 4F2hc. The protocol was adapted from the paper of Doring *et al*. 1998 and any important change was done.

From a final volume culture of 6 ml (BMMY), cells were centrifuged (2,500×g, 10 min) and washed twice in 10 ml of amino acid-free transport buffer (150 mM choline chloride, 10 mM Tris-HEPES, pH 7.4, 1mM MgCl2 and 1mM CaCl2, with and without amino acid [0.5 µCi of radiolabeled L-Leucine and the desired concentration of unlabelled L-Leucine; American Radiolabeled Chemicals] in order to remove the rich culture medium. A third centrifugation round was done and the final pellet was resuspended to 1 OD ·10 μl^{-1} of transport buffer amino acid free (Doring *et al*. 1998). The uptake measurements were performed mixing 10 µl of cell suspension with 40 µl of transport buffer adding L-leucine at different concentrations and incubating at different periods of time. The reaction was stopped by the addiction of 3 ml of cold-stop transport buffer (150 mM choline chloride, 10 mM Tris-HEPES and 5 mM L-Leucine) and quantified filtering through membranes (Sartorius; 0.45-µm pore size). The filters were washed twice with 1-2 ml of ice-cold stop transport buffer. After dry, the radioactivity remaining in the filters was counted in a Packard Tri-Carb Liquid Scintillation Counter correcting all the counted values subtracting the zero time.

13. Negative Stain- Transmission Electron Microscopy (NS-TEM)

DDM-solubilized and purified 4F2hc/LAT2 protein was adsorbed for 10s to parlodion carbon-coated copper grids rendered hydrophilic by glow discharge at low pressure in air. Grids were washed with three drops of double-distilled water and stained with 2 drops of 0.75% uranyl formate. This washing step is to effectively removing the buffer solution and not adsorbed protein. The former, if not removed, can lead to precipitation of the uranyl salts with buffer components. Electron micrographs were recorded at a magnification of ×50,000 and an underfocus of 400 nm on Eastman Kodak Co. S0-163 sheet films with a Hitachi H-7000 electron microscope operated at 100 kV.

Bibliography

Adam Y, Edwards RH, Schuldiner S. *Expression and function of the rat vesicular monoamine transporter 2*. Am J Physiol Cell Physiol. 2008, 294(4):C1004-11

Albi JL, Canals P, Gallardo MA, Sánchez J.; Na(+)-independent L-alanine uptake by trout cells. Evidence for the existence of at least two functionally different acs systems. J Membr Biol. 1994 Jun;140(3):189-96.

Alexander BD, Perfect JR. Antifungal resistance trends towards the year 2000. Implications for therapy and new approaches. Drugs. 1997 Nov;54(5):657-78. Review.

Aller S.G, Yu J, Ward A, Weng Y, Chittaboina S, Zhuo R, Harrell P.M, Trinh Y.T, Zhang Q, Urbatsch I.L, Chang G. *Structure of P-glycoprotein reveals a molecular basis for poly-specific drug binding.* Science 2009

Anton E, Vidal F, Egozcue J, Blanco J.*Genetic reproductive risk in inversion carriers*. Fertil Steril. 2006 ;86(2):498

Asojo OA, Koski RA, Bonafé N. Structural studies of human glioma pathogenesis-related protein 1. Acta Crystallogr D Biol Crystallogr. 2011 Oct;67(Pt 10):847-55. Epub 2011 Sep 8.

Bailey CG, Ryan RM, Thoeng AD, Ng C, King K, Vanslambrouck JM, Auray-Blais C, Vandenberg RJ, Bröer S, Rasko JE.Loss-of-function mutations in the glutamate transporter SLC1A1 cause human dicarboxylic aminoaciduria. J Clin Invest. 2011 Jan;121(1):446-53. doi: 10.1172/JCI44474. Epub 2010 Dec 1.

Bartoccioni P, Del Rio C, Ratera M, Kowalczyk L, Baldwin JM, Zorzano A, Quick M, Baldwin SA, Vázquez-Ibar JL, Palacín M. *Role of transmembrane domain 8 in substrate selectivity and translocation of SteT, a member of the L-amino acid transporter (LAT) family.*J Biol Chem. 2010; Sep 10;285(37):28764-76

Bartoccioni P, Rius M, Zorzano A, Palacín M, Chillarón J. *Distinct classes of trafficking rBAT mutants cause the type I cystinuria phenotype*. Hum Mol Genet. 2008; Jun 15;17(12):1845-54

Bertran J, Magagnin S, Werner A, Markovich D, Biber J, Testar X, Zorzano A, Kühn LC, Palacin M, Murer H. *Stimulation of system y(+)-like amino acid transport by the heavy chain of human 4F2 surface antigen in Xenopus laevis oocytes.* Proc Natl Acad Sci U S A. 1992; Jun 15;89(12):5606-10

Bertran J, Werner A, Moore ML, Stange G, Markovich D, Biber J, Testar X, Zorzano A, Palacin M, Murer H.*Expression cloning of a cDNA from rabbit kidney cortex that induces a single transport system for cystine and dibasic and neutral amino acids*.Proc Natl Acad Sci U S A. 1992; Jun 15;89(12):5601-5.

Bertran J, Werner A, Stange G, Markovich D, Biber J, Testar X, Zorzano A, Palacin M, Murer H. *Expression of Na(+)-independent amino acid transport in Xenopus laevis oocytes by injection of rabbit kidney cortex mRNA*. Biochem J. 1992; 1;281 (Pt 3):717-23.

Betsuyaku T, Kadomatsu K, Griffin GL, Muramatsu T, Senior RM.

Increased basigin in bleomycin-induced lung injury. Am J Respir Cell Mol Biol. 2003 May;28(5):600-6

Bhatnagar RS, Gordon JI. Understanding covalent modifications of proteins by lipids: where cell biology and biophysics mingle. Trends Cell Biol. 1997 Jan;7(1):14-20.

Boado RJ.Brain-derived peptides increase blood-brain barrier GLUT1 glucose transporter gene expression via mRNA stabilization. Neurosci Lett. 1998 Oct 23;255(3):147-50.

Borsani G, Bassi MT, Sperandeo MP, De Grandi A, Buoninconti A, Riboni M, Manzoni M, Incerti B, Pepe A, Andria G, Ballabio A, Sebastio G. *SLC7A7, encoding a putative permease-related protein, is mutated in patients with lysinuric protein intolerance.*Nat Genet. 1999; Mar;21(3):297-301

Braun D, Wirth EK, Wohlgemuth F, Reix N, Klein MO, Grüters A, Köhrle J, Schweizer U. *Aminoaciduria, but normal thyroid hormone levels and signalling, in mice lacking the amino acid and thyroid hormone transporter Slc7a8.* Biochem J. 2011; 15;439(2):249-55

Bröer A, Wagner CA, Lang F, Bröer S. *The heterodimeric amino acid transporter 4F2hc/y+LAT2 mediates arginine efflux in exchange with glutamine*. Biochem J. 2000; Aug 1;349 Pt 3:787-95

Bröer A, Friedrich B, Wagner CA, Fillon S, Ganapathy V, Lang F, Bröer S. Association of 4F2hc with light chains LAT1, LAT2 or y+LAT2 requires different domains. Biochem J. 2001 May 1;355(Pt 3):725-31.

Bröer S, Bailey CG, Kowalczuk S, Ng C, Vanslambrouck JM, Rodgers H, Auray-Blais C, Cavanaugh JA, Bröer A, Rasko JE. Iminoglycinuria and hyperglycinuria are discrete human phenotypes resulting from complex mutations in proline and glycine transporters. J Clin Invest. 2008 Dec;118(12):3881-92. doi: 10.1172/JCI36625. Epub 2008 Nov 6.

Bröer S, Palacín M. T*he role of amino acid transporters in inherited and acquired diseases*. Biochem J. 2011; Jun 1;436(2):193-211

Boyd CA. Facts, fantasies and fun in epithelial physiology. Exp Physiol. 2008 Mar;93(3):303-14. Epub 2008 Jan 11.

Busch A, Waldegger S, Herzer T, Biber J, Markovich D, Hayes G, Murer H, Lang F. *Electrophysiological analysis of Na+/Pi cotransport mediated by a transporter cloned from rat kidney and expressed in Xenopus oocytes.*Proc Natl Acad Sci U S A. 1994; Aug 16;91(17):8205-8.

Caffrey M, Porter C. *Crystallizing membrane proteins for structure determination using lipidic mesophases*. J Vis Exp. 2010; Nov 21;(45). pii: 1712

Calonge MJ, Gasparini P, Chillarón J, Chillón M, Gallucci M, Rousaud F, Zelante L, Testar X, Dallapiccola B, Di Silverio F.Cystinuria caused by mutations in rBAT, a gene involved in the transport of cystine. Nat Genet. 1994 Apr;6(4):420-5

Cantor J, Browne CD, Ruppert R, Féral CC, Fässler R, Rickert RC, Ginsberg MH. *CD98hc facilitates B cell proliferation and adaptive humoral immunity*. Nat Immunol. 2009; Apr;10(4):412-9.

Casagrande F, Ratera M, Schenk AD, Chami M, Valencia E, Lopez JM, Torrents D, Engel A, Palacin M, Fotiadis D. *Projection structure of a member of the amino acid/polyamine/organocation transporter superfamily*. J Biol Chem. 2008 ; Nov 28;283(48):33240-8

Conte MR, Matthews S. Retroviral matrix proteins: a structural perspective. Virology. 1998 Jul 5;246(2):191-8.

Current Protocols in Molecular Biology. (2001) editorial Coligan

Cregg JM. *Introduction: distinctions between Pichia pastoris and other expression systems.* Methods Mol Biol. 2007; 389:1-10.

Chairoungdua A, Segawa H, Kim JY, Miyamoto K, Haga H, Fukui Y, Mizoguchi K, Ito H, Takeda E, Endou H, Kanai Y. Identification of an amino acid transporter associated with the cystinuria-related type II membrane glycoprotein. J Biol Chem. 1999 Oct 8;274(41):28845-8.

Chillarón J, Estévez R, Mora C, Wagner CA, Suessbrich H, Lang F, Gelpí JL, Testar X, Busch AE, Zorzano A, Palacín M. *Obligatory amino acid exchange via systems bo,+-like and y+L-like. A tertiary active transport mechanism for renal reabsorption of cystine and dibasic amino acids.*J Biol Chem. 1996 ; ;271(30):17761-70.

Chillarón J, Estévez R, Samarzija I, Waldegger S, Testar X, Lang F, Zorzano A, Busch A, Palacín M. *An intracellular trafficking defect in type I cystinuria rBAT mutants M467T and M467K*. J Biol Chem. 1997; 4;272(14):9543-9

Chillarón J, Roca R, Valencia A, Zorzano A, Palacín M. *Heteromeric amino acid transporters: biochemistry, genetics, and physiology.* Am J Physiol Renal Physiol. 2001; Dec;281(6):F995-1018

Chillarón J, Font-Llitjós M, Fort J, Zorzano A, Goldfarb DS, Nunes V, Palacín M. Pathophysiology and treatment of cystinuria. Nat Rev Nephrol. 2010 Jul;6(7):424-34. Epub 2010 Jun 1.

Christensen ND, Kreider JW. *Antibody-mediated neutralization in vivo of infectious papillomaviruses.* J Virol. 1990; Jul;64(7):3151-6.

Christensen,H.N. *Role of amino acid transport and countertransport in nutrition and metabolism*. Physiol Rev. 1990.

Cocera M, Gelen Rodrıguez, Laia Rubio, Lucyanna Barbosa-Barros,Nuria Benseny-Cases, Josep Cladera, Manel Sabes, Francois Fauth,Alfonso de la Maza and Olga Lopeza Characterisation of skin states by non-crystalline diffraction *Soft Matter*

Costa M, N.Benseny-Cases, C.V. Teixeira , M.Alsina , J.Cladera, O.Lopez, M.Fernandez and M.Sabés Diagnosisi applications of non-crystalline diffraction

of collagen fibres: Breast Cancer and Skin diseases Applications of Synchrotron Light to Non-Crystalline Diffraction in Materials and Life Sciences (2009)

Daghastanli KR, Ferreira RB, Thedei G Jr, Maggio B, Ciancaglini P. *Lipid composition-dependent incorporation of multiple membrane proteins into liposomes.* Colloids Surf B Biointerfaces. 2004 ; Aug 1;36(3-4):127-37.

Dalton P, Christian HC, Redman CW, Sargent IL, Boyd CA. *Membrane trafficking of CD98 and its ligand galectin 3 in BeWo cells--implication for placental cell fusion*. FEBS J. 2007; Jun;274(11):2715-27.

De la Ballina, thesis dissertation, 2011

Deora AB, Ghosh RN, Tate SS. *Progressive C-terminal deletions of the renal cystine transporter, NBAT, reveal a novel bimodal pattern of functional expression.* J Biol Chem. 1998; Dec 4;273(49):32980-7.

Desjeux JF, Simell RO, Dumontier AM, Perheentupa J. *Lysine fluxes across the jejunal epithelium in lysinuric protein intolerance.* J Clin Invest. 1980 ; Jun;65(6):1382-7.

Devés R, Chavez P, Boyd CA. *Identification of a new transport system (y+L) in human erythrocytes that recognizes lysine and leucine with high affinity.* J Physiol. 1992; Aug;454:491-501.

Dietz AB, Bulur PA, Knutson GJ, Matasić R, Vuk-Pavlović S. Saturation of human monocyte-derived dendritic cells studied by microarray hybridization. Biochem Biophys Res Commun. 2000 Sep 7;275(3):731-8.

Döring F, Klapper M, Theis S, Daniel H. *Use of the glyceraldehyde-3-phosphate dehydrogenase promoter for production of functional mammalian membrane transport proteins in the yeast Pichia pastoris.* Biochem Biophys Res Commun. 1998 ; Sep 18;250(2):531-5.

Döring F, Michel T, Rösel A, Nickolaus M, Daniel H. *Expression of the mammalian renal peptide transporter PEPT2 in the yeast Pichia pastoris and applications of the yeast system for functional analysis.* Mol Membr Biol. 1998; Apr-Jun;15(2):79-88.

Döring F, Theis S, Daniel H. *Expression and functional characterization of the mammalian intestinal peptide transporter PepT1 in the methylotropic yeast Pichia pastoris*. Biochem Biophys Res Commun. 1997; Mar 27;232(3):656-62.

Drew D, Newstead S, Sonoda Y, Kim H, von Heijne G, Iwata S. *GFP-based optimization scheme for the overexpression and purification of eukaryotic membrane proteins in Saccharomyces cerevisiae.* Nat Protoc. 2008; ;3(5):784-98.

Drew D, Simon Newstead, Yo Sonoda, Hyun Kim, Gunnar von Heijne, So Iwata. *GFP-based optimization scheme for the overexpression and purification of eukaryotic membrane proteins in Saccharomyces cerevisiae.* Nature, 2008; 3(5):784-98.

Duret G, Van Renterghem C, Weng Y, Prevost M, Moraga-Cid G, Huon C,

Sonner JM, Corringer PJ. *Functional prokaryotic-eukaryotic chimera from the pentameric ligand-gated ion channel family*.Proc Natl Acad Sci U S A. 2011; Jul 19;108(29):12143-8.

Eleno N, Devés R, Boyd CA. *Membrane potential dependence of the kinetics of cationic amino acid transport systems in human placenta.* J Physiol. 1994; Sep 1;479 (Pt 2):291-300

Ellory JC, Jones SE, Young JD.; Glycine transport in human erythrocytes, J Physiol. 1981 Nov;320:403-22.

Fang Y, Jayaram H, Shane T, Kolmakova-Partensky L, Wu F, Williams C, Xiong Y, Miller C. *Structure of a prokaryotic virtual proton pump at 3.2 A resolution.*Nature. 2009; Aug 20;460(7258):1040-3

Feliubadaló L, Arbonés ML, Mañas S, Chillarón J, Visa J, Rodés M, Rousaud F, Zorzano A, Palacín M, Nunes V. *Slc7a9-deficient mice develop cystinuria non-l and cystine urolithiasis*.Hum Mol Genet. 2003 ; Sep 1;12(17):2097-108

Feliubadaló L, Font M, Purroy J, Rousaud F, Estivill X, Nunes V, Golomb E, Centola M, Aksentijevich I, Kreiss Y, Goldman B, Pras M, Kastner DL, Pras E, Gasparini P, Bisceglia L, Beccia E, Gallucci M, de Sanctis L, Ponzone A, Rizzoni GF, Zelante L, Bassi MT, George AL Jr, Manzoni M, De Grandi A, Riboni M, Endsley JK, Ballabio A, Borsani G, Reig N, Fernández E, Estévez R, Pineda M, Torrents D, Camps M, Lloberas J, Zorzano A, Palacín M; *International Cystinuria Consortium.Non-type I cystinuria caused by mutations in SLC7A9, encoding a subunit (bo,+AT) of rBAT*.Nat Genet. 1999; Sep;23(1):52-7.

Fenczik CA, Zent R, Dellos M, Calderwood DA, Satriano J, Kelly C, Ginsberg MH. *Distinct domains of CD98hc regulate integrins and amino acid transport.* J Biol Chem. 2001; Mar 23;276(12):8746-52

Féral CC, Nishiya N, Fenczik CA, Stuhlmann H, Slepak M, Ginsberg MH. *CD98hc (SLC3A2) mediates integrin signaling.* Proc Natl Acad Sci U S A. 2005 ; Jan 11;102(2):355-60

Féral CC, Zijlstra A, Tkachenko E, Prager G, Gardel ML, Slepak M, Ginsberg MH. *CD98hc (SLC3A2) participates in fibronectin matrix assembly by mediating integrin signaling.* J Cell Biol. 2007 ; Aug 13;178(4):701-11

Fernández E, Jiménez-Vidal M, Calvo M, Zorzano A, Tebar F, Palacín M, Chillarón J. The structural and functional units of heteromeric amino acid transporters. The heavy subunit rBAT dictates oligomerization of the heteromeric amino acid transporters. J Biol Chem. 2006 Sep 8;281(36):26552-61. Epub 2006 Jul 6.

Fischer G, Kosinska-Eriksson U, Aponte-Santamaria C, Palmgren M, Geijer C, Hedfalk K, Hohmann S, De Groot B.L, Neutze R, Lindkvist-Petersson K. C*rystal Structure of a Yeast Aquaporin at 1.15 A Reveals a Novel Gating Mechanism.1.15 A. Plos Biol. 2009*

Fogelstrand P, Féral CC, Zargham R, Ginsberg MH. *Dependence of proliferative vascular smooth muscle cells on CD98hc (4F2hc, SLC3A2).* J Exp Med. 2009 ; Oct 26;206(11):2397-406

Fort J, de la Ballina LR, Burghardt HE, Ferrer-Costa C, Turnay J, Ferrer-Orta C, Usón I, Zorzano A, Fernández-Recio J, Orozco M, Lizarbe MA, Fita I, Palacín M. *The structure of human 4F2hc ectodomain provides a model for homodimerization and electrostatic interaction with plasma membrane.* J Biol Chem. 2007; Oct 26;282(43):31444-52

Franca R, Veljkovic E, Walter S, Wagner CA, Verrey F. *Heterodimeric amino acid transporter glycoprotein domains determining functional subunit association.* Biochem J. 2005; Jun 1;388(Pt 2):435-43.

Fukasawa Y , Segawa H , Kim JY , Chairoungdua A , Kim DK , Matsuo H , Cha SH , Endou H , Kanai Y. *Identification and characterization of a Na(+)-independent neutral amino acid transporter that associates with the 4F2 heavy chain and exhibits substrate selectivity for small neutral D- and L-amino acids*. J Biol Chem 2000; Mar 31;275(13):9690-8.

Furriols M, Chillarón J, Mora C, Castelló A, Bertran J, Camps M, Testar X, Vilaró S, Zorzano A, Palacín M. *rBAT, related to L-cysteine transport, is localized to the microvilli of proximal straight tubules, and its expression is regulated in kidney by development.* Biol Chem. 1993 ; Dec 25;268(36):27060-8.

Gabrisko M, Janecek S. *Looking for the ancestry of the heavy-chain subunits of heteromeric amino acid transporters rBAT and 4F2hc within the GH13 alpha-amylase family.* FEBS J. 2009; Dec;276(24):7265-78

Gao X, Lu F, Zhou L, Dang S, Sun L, Li X, Wang J, Shi Y.*Structure and mechanism of an amino acid antiporter.* Science. 2009; Jun 19;324(5934):1565-

Gao X, Zhou L, Jiao X, Lu F, Yan C, Zeng X, Wang J, Shi Y. *Mechanism of substrate recognition and transport by an amino acid antiporter.*Nature. 2010 ; Feb 11;463(7282):828-32.

Gasol E, Jiménez-Vidal M, Chillarón J, Zorzano A, Palacín M. *Membrane topology of system xc- light subunit reveals a re-entrant loop with substrate-restricted accessibility*.J Biol Chem. 2004; Jul 23;279(30):31228-36

Geertsma ER, Nik Mahmood NA, Schuurman-Wolters GK, Poolman B. *Membrane reconstitution of ABC transporters and assays of translocator function.*Nat Protoc. 2008; 3(2):256-66.

Halestrap AP, Meredith D. The SLC16 gene family-from monocarboxylate transporters (MCTs) to aromatic amino acid transporters and beyond. Pflugers Arch. 2004 Feb;447(5):619-28. Epub 2003 May 9.

Hansen S.B, Tao X, Mackinnon R. Structural basis of PIP(2) activation of the

classical inward rectifier K(+) channel Kir2.2. Nature 2011

Haviv H, Cohen E, Lifshitz Y, Tal DM, Goldshleger R, Karlish SJ. *Stabilization of Na(+),K(+)-ATPase purified from Pichia pastoris membranes by specific interactions with lipids*.Biochemistry. 2007; Nov 6;46(44):12855-67

Haynes BF, Hemler ME, Mann DL, Eisenbarth GS, Shelhamer J, Mostowski HS, Thomas CA, Strominger JL, Fauci AS. *Characterization of a monoclonal antibody (4F2) that binds to human monocytes and to a subset of activated lymphocytes*.J Immunol. 1981; Apr;126(4):1409-14.

Ho J.D, Yeh R, Sandstrom A, Chorny I, Harries W.E, Robbins R.A, Miercke L.J, Stroud R.M. *Crystal structure of human aquaporin 4 at 1.8 A and its mechanism of conductance . Proc.Natl.Acad.Sci.USA 2009*

Horsefield R, Norden K, Fellert M, Backmark A, Tornroth-Horsefield S, Terwisscha van Scheltinga A.C, Kvassman J, Kjellbom P, Johanson U, Neutze R. *High-resolution x-ray structure of human aquaporin 5.* Proc.Natl.Acad.Sci.Usa 2008

Kaira K, Oriuchi N, Imai H, Shimizu K, Yanagitani N, Sunaga N, Hisada T, Kawashima O, Iijima H, Ishizuka T, Kanai Y, Endou H, Nakajima T, Mori M. Expression of L-type amino acid transporter 1 (LAT1) in neuroendocrine tumors of the lung. Pathol Res Pract. 2008;204(8):553-61. Epub 2008 Apr 28

Kaleeba JA, Berger EA. *Kaposi's sarcoma-associated herpesvirus fusion-entry receptor: cystine transporter xCT*. Science. 2006; Mar 31;311(5769):1921-4.

Kanai Y, Segawa H, Chairoungdua A, Kim JY, Kim DK, Matsuo H, Cha SH, Endou H. *Amino acid transporters: molecular structure and physiological roles.* Nephrol Dial Transplant. 2000; 15 Suppl 6:9-10.

Kanai Y, Segawa H, Miyamoto K, Uchino H, Takeda E and Endou H. *Expression cloning and characterization of a transporter for large neutral amino acids activated by the heavy chain of 4F2 antigen (CD98).* J Biol Chem 1998; Sep 11;273(37):23629-32

Karpusas M, Cachero T.G, Qian F, Boriack-Sjodin A, Mullen C, Strauch K, Hsu YM, Kalled S.L. *Crystal structure of extracellular human BAFF, a TNF family member that stimulates B lymphocytes.* J.Mol.Biol 2002

Kirk P, Wilson MC, Heddle C, Brown MH, Barclay AN, Halestrap AP. CD147 is tightly associated with lactate transporters MCT1 and MCT4 and facilitates their cell surface expression. EMBO J. 2000 Aug 1;19(15):3896-904.

Kleemola M, Toivonen M, Mykkänen J, Simell O, Huoponen K, Heiskanen KM. *Heterodimerization of y(+)LAT-1 and 4F2hc visualized by acceptor photobleaching FRET microscopy.*Biochim Biophys Acta. 2007 ; Oct;1768(10):2345-54.

Kleta R, Romeo E, Ristic Z, Ohura T, Stuart C, Arcos-Burgos M, Dave MH,

Wagner CA, Camargo SR, Inoue S, Matsuura N, Helip-Wooley A, Bockenhauer D, Warth R, Bernardini I, Visser G, Eggermann T, Lee P, Chairoungdua A, Jutabha P, Babu E, Nilwarangkoon S, Anzai N, Kanai Y, Verrey F, Gahl WA, Koizumi A. Mutations in SLC6A19, encoding B0AT1, cause Hartnup disorder.Nat Genet. 2004 Sep;36(9):999-1002. Epub 2004 Aug 1.

Koch C, Staffler G, Hüttinger R, Hilgert I, Prager E, Cerný J, Steinlein P, Majdic O, Horejsí V, Stockinger H. T cell activation-associated epitopes of CD147 in regulation of the T cell response, and their definition by antibody affinity and antigen density. Int Immunol. 1999 May;11(5):777-86.

Kolesnikova TV, Mannion BA, Berditchevski F, Hemler ME. Beta1 integrins show specific association with CD98 protein in low density membranes. BMC Biochem. 2001;2:10. Epub 2001 Oct 15.

Kowalczyk L, Ratera M, Paladino A, Bartoccioni P, Errasti-Murugarren E, Valencia E, Portella G, Bial S, Zorzano A, Fita I, Orozco M, Carpena X, Vázquez-Ibar JL, Palacín M. *Molecular basis of substrate-induced permeation by an amino acid antiporter.* Proc Natl Acad Sci U S A. 2011; Mar 8;108(10):3935-40

Krishnamurthy H, Gouaux E.; X-ray structures of LeuT in substrate-free outward-open and apo inward-open states. Nature. 2012 Jan 9;481(7382):469-74. doi: 10.1038/nature10737.

Kurayama R, Ito N, Nishibori Y, Fukuhara D, Akimoto Y, Higashihara E, Ishigaki Y, Sai Y, Miyamoto K, Endou H, Kanai Y, Yan K. *Role of amino acid transporter LAT2 in the activation of mTORC1 pathway and the pathogenesis of crescentic glomerulonephritis*. Lab Invest. 2011 ; Jul;91(7):992-1006

Laemmli U.K. *Cleavage of structural proteins during the assembly of the head of bacteriophage T4*. Nature 1970

Lash LH, Putt DA, Xu F, Matherly LH. *Role of rat organic anion transporter 3 (Oat3) in the renal basolateral transport of glutathione*.Chem Biol Interact. 2007 ; Nov 20;170(2):124-34

Lemmon MA, Treutlein HR, Adams PD, Brünger AT, Engelman DM. *A dimerization motif for transmembrane alpha-helices*. Nat Struct Biol. 1994; Mar;1(3):157-63.

Lin-Cereghino J, Wong WW, Xiong S, Giang W, Luong LT, Vu J, Johnson SD, Lin-Cereghino GP. *Condensed protocol for competent cell preparation and transformation of the methylotrophic yeast Pichia pastoris.* Biotechniques 2005; Jan;38(1):44, 46, 48.

Liu X, Charrier L, Gewirtz A, Sitaraman S, Merlin D. CD98 and intracellular adhesion molecule I regulate the activity of amino acid transporter LAT-2 in polarized intestinal epithelia.J Biol Chem. 2003 ; Jun 27;278(26):23672-7.

Long SB, Campbell EB, Mackinnon R. Crystal structure of a mammalian voltage-dependent Shaker family K+ channel. Science. 2005 Aug

5;309(5736):897-903. Epub 2005 Jul 7.

Long SB, Campbell EB, Mackinnon R, Voltage sensor of Kv1.2: structural basis of electromechanical coupling. Science. 2005 Aug 5;309(5736):903-8. Epub 2005 Jul 7.

Long SB, Tao X, Campbell EB, MacKinnon R. Atomic structure of a voltage-dependent K+ channel in a lipid membrane-like environment. Nature. 2007 Nov 15;450(7168):376-82.

Lumadue JA, Glick AB, Ruddle FH. *Cloning, sequence analysis, and expression of the large subunit of the human lymphocyte activation antigen 4F2*.Proc Natl Acad Sci U S A. 1987; Dec;84(24):9204-8.

McLaughlin S, Aderem A. The myristoyl-electrostatic switch: a modulator of reversible protein-membrane interactions. Trends Biochem Sci. 1995 Jul;20(7):272-6.

MacKenzie KR, Prestegard JH, Engelman DM. *A transmembrane helix dimer: structure and implications*. Science 1997; Apr 4;276(5309):131-3.

MacKinnon AC, Farnworth SL, Hodkinson PS, Henderson NC, Atkinson KM, Leffler H, Nilsson UJ, Haslett C, Forbes SJ, Sethi T. *Regulation of alternative macrophage activation by galectin-3*.J Immunol. 2008; Feb 15;180(4):2650-8.

Mackinnon R. Structural biology. *Membrane protein insertion and stability.* Science. 2005; Mar 4;307(5714):1425-6.

Martinez Molina D, Wetterholm A, Kohl A, Mccarthy AA, Niegowski D, Ohlson E, Hammarberg T, Eshaghi S, Haeggstrom JZ, Nordlund P Structural basis for synthesis of inflammatory mediators by human leukotriene c4 synthase. Nature (2007) 448 p.613

Mastroberardino L, Spindler B, Pfeiffer R, Skelly PJ, Loffing J, Shoemaker CB, Verrey F. *Amino-acid transport by heterodimers of 4F2hc/CD98 and members of a permease family.* Nature. 1998; Sep 17;395(6699):288-91.

Meury M, Harder D, Ucurum Z, Boggavarapu R, Jeckelmann JM, Fotiadis D. Structure determination of channel and transport proteins by high-resolution microscopy techniques Biol Chem. 2011 Jan;392(1-2):143-50.

Miyamoto K, Segawa H, Tatsumi S, Katai K, Yamamoto H, Taketani Y, Haga H, Morita K, Takeda E. *Effects of truncation of the COOH-terminal region of a Na+-independent neutral and basic amino acid transporter on amino acid transport in Xenopus oocytes*. J Biol Chem. 1996 ; Jul 12;271(28):16758-63.

Naranjo D, Latorre R, Cherbavaz D, McGill P, Schumaker MF. A *simple model for surface charge on ion channel proteins.*Biophys J. 1994 ; Jan;66(1):59-70

Nehme CL, Fayos BE, Bartles JR. Distribution of the integral plasma membrane glycoprotein CE9 (MRC OX-47) among rat tissues and its induction by diverse stimuli of metabolic activation. Biochem J. 1995 Sep 1;310 (Pt 2):693-8.

Nicklin P, Bergman P, Zhang B, Triantafellow E, Wang H, Nyfeler B, Yang H,

Hild M, Kung C, Wilson C, Myer VE, MacKeigan JP, Porter JA, Wang YK, Cantley LC, Finan PM, Murphy LO. *Bidirectional transport of amino acids regulates mTOR and autophagy.*Cell. 2009 ; Feb 6;136(3):521-34.

Ohno H, Nakatsu Y, Sakoda H, Kushiyama A, Ono H, Fujishiro M, Otani Y, Okubo H, Yoneda M, Fukushima T, Tsuchiya Y, Kamata H, Nishimura F, Kurihara H, Katagiri H, Oka Y, Asano T. *4F2hc stabilizes GLUT1 protein and increases glucose transport activity*.Am J Physiol Cell Physiol. 2011 ; May;300(5):C1047-54

Palacín M, Estévez R, Bertran J, Zorzano A. *Molecular biology of mammalian plasma membrane amino acid transporters.*Physiol Rev. 1998 ; Oct;78(4):969-1054.

Palacin M, Fernández E, Chillarón J, Zorzano A. T*he amino acid transport system b(o,+) and cystinuria.The amino acid transport system b(o,+) and cystinuria.*Mol Membr Biol. 2001 ; Jan-Mar;18(1):21-6.

Palacín M, Kanai Y. *The ancillary proteins of HATs: SLC3 family of amino acid transporters*.Pflugers Arch. 2004 ; Feb;447(5):490-4.

Palacín M, Nunes V, Font-Llitjós M, Jiménez-Vidal M, Fort J, Gasol E, Pineda M, Feliubadaló L, Chillarón J, Zorzano A. *The genetics of heteromeric amino acid transporters.*Physiology (Bethesda). 2005 ; Apr;20:112-24.

Ohno H, Nakatsu Y, Sakoda H, Kushiyama A, Ono H, Fujishiro M, Otani Y, Okubo H, Yoneda M, Fukushima T, Tsuchiya Y, Kamata H, Nishimura F, Kurihara H, Katagiri H, Oka Y, Asano T. *4F2hc stabilizes GLUT1 protein and increases glucose transport activity*.Am J Physiol Cell Physiol. 2011

Parmacek MS, Karpinski BA, Gottesdiener KM, Thompson CB, Leiden JM. Structure, expression and regulation of the murine 4F2 heavy chain.Nucleic Acids Res. 1989 Mar 11;17(5):1915-31.

Peters T, Thaete C, Wolf S, Popp A, Sedlmeier R, Grosse J, Nehls MC, Russ A, Schlueter V. A mouse model for cystinuria type I. Hum Mol Genet. 2003 Sep 1;12(17):2109-20.

Pfeiffer M, Rink T, Gerwert K, Oesterhelt D, Steinhoff HJ. Site-directed spin-labeling reveals the orientation of the amino acid side-chains in the E-F loop of bacteriorhodopsin.J Mol Biol. 1999 Mar 19;287(1):163-71

Pfeifer M, Muders F, Luchner A, Blumberg F, Riegger GA, Elsner D. *Leukotriene receptor blockade in experimental heart failure*. Res Exp Med (Berl). 1997; 197(4):177-87.

Pineda M, Fernández E, Torrents D, Estévez R, López C, Camps M, Lloberas J, Zorzano A, Palacín M. *Identification of a membrane protein, LAT-2, that Co-expresses with 4F2 heavy chain, an L-type amino acid transport activity with broad specificity for small and large zwitterionic amino acids*.J Biol Chem. 1999 ; Jul 9;274(28):19738-44.

Pineda M, Wagner CA, Bröer A, Stehberger PA, Kaltenbach S, Gelpí JL, Martín Del Río R, Zorzano A, Palacín M, Lang F, Bröer S. *Cystinuria-specific rBAT(R365W) mutation reveals two translocation pathways in the amino acid transporter rBAT-b0,+AT*. Biochem J. 2004; Feb 1;377(Pt 3):665-74.

Prager G, Feral C, Kim C, Han J, Ginsberg M. *CD98hc (SLC3A2) Interaction with the Integrin Subunit Cytoplasmic Domain Mediates Adhesive Signaling.* THE JOURNAL OF BIOLOGICAL CHEMISTRY 2007; Aug 17;282(33):24477-84

Prager GW, Féral CC, Kim C, Han J, Ginsberg MH. *CD98hc (SLC3A2) interaction with the integrin beta subunit cytoplasmic domain mediates adhesive signaling.* J Biol Chem. 2007 ; Aug 17;282(33):24477-84

Pushkarsky T, Zybarth G, Dubrovsky L, Yurchenko V, Tang H, Guo H, Toole B, Sherry B, Bukrinsky M CD147 facilitates HIV-1 infection by interacting with virus-associated cyclophilin A. Proc Natl Acad Sci U S A. 2001 May 22;98(11):6360-5. Epub 2001 May 15.

Quackenbush E, Clabby M, Gottesdiener KM, Barbosa J, Jones NH, Strominger JL, Speck S, Leiden JM. *Molecular cloning of complementary DNAs encoding the heavy chain of the human 4F2 cell-surface antigen: a type II membrane glycoprotein involved in normal and neoplastic cell growth.* Proc Natl Acad Sci U S A. 1987; Sep;84(18):6526-30.

Qin JM, Li F, Tan XH, Guo SX, Wang XB, Zhang WJ, Xie JX, Huang J, Pu XM, Rui DS, Yang L. A case-control study on risk factor of Kaposi's sarcoma in Xinjiang. Zhonghua Liu Xing Bing Xue Za Zhi. 2005 Sep;26(9):673-5.

Radian R, Kanner BI. *Reconstitution and purification of the sodium- and chloride-coupled gamma-aminobutyric acid transporter from rat brain*. J Biol Chem. 1985; Nov 25;261(33):15437-41.

Radian R, Kanner BI. *Reconstitution and purification of the sodium- and chloride-coupled gamma-aminobutyric acid transporter from rat brain*. J Biol Chem. 1985.

Rajantie J, Simell O, Perheentupa J. *Lysinuric protein intolerance. Basolateral transport defect in renal tubuli*.J Clin Invest. 1981; Apr;67(4):1078-82.

Regnard P, Le Duc G, Bräuer-Krisch E, Troprès I, Siegbahn EA, Kusak A, Clair C, Bernard H, Dallery D, Laissue JA, Bravin A. *Irradiation of intracerebral 9L gliosarcoma by a single array of microplanar x-ray beams from a synchrotron: balance between curing and sparing.*Phys Med Biol. 2008; Feb 21;53(4):861-78

Reig N, Chillarón J, Bartoccioni P, Fernández E, Bendahan A, Zorzano A, Kanner B, Palacín M, Bertran J. *The light subunit of system b(o,+) is fully functional in the absence of the heavy subunit.*EMBO J. 2002 ; Sep 16;21(18):4906-14.

Reig N, del Rio C, Casagrande F, Ratera M, Gelpí JL, Torrents D, Henderson

PJ, Xie H, Baldwin SA, Zorzano A, Fotiadis D, Palacín M. *Functional and structural characterization of the first prokaryotic member of the L-amino acid transporter (LAT) family: a model for APC transporters.*J Biol Chem. 2007; May 4;282(18):13270-81

Rigaud JL. M*embrane proteins: functional and structural studies using reconstituted proteoliposomes and 2-D crystals*.Braz J Med Biol Res. 2002 ; Jul;35(7):753-66

Rius M, Chillaron J, The carrier subunit of a plasma membrane transporter is required for the oxidative folding of its helper subunit. J Biol Chem. 2012 Apr 9. [Epub ahead of print]

Rotoli BM, Dall'asta V, Barilli A, D'Ippolito R, Tipa A, Olivieri D, Gazzola GC, Bussolati O. *Alveolar macrophages from normal subjects lack the NOS-related system y+ for arginine transport.* Am J Respir Cell Mol Biol. 2007; Jul;37(1):105-12.

Sambrook. *Molecular cloning. A laboratory Manual*. (1989) editorial Sambrock

Segawa H, Fukasawa Y, Miyamoto K, Takeda E, Endou H, Kanai Y. *Identification and functional characterization of a Na+-independent neutral amino acid transporter with broad substrate selectivity.* J Biol Chem 1999; Jul 9;274(28):19745-51.

Shaffer PL, Goehring A, Shankaranarayanan A, Gouaux E. *Structure and mechanism of a Na+-independent amino acid transporter.*Science. 2009 ; Aug 21;325(5943):1010-4.

Shoji Y, Noguchi A, Shoji Y, Matsumori M, Takasago Y, Takayanagi M, Yoshida Y, Ihara K, Hara T, Yamaguchi S, Yoshino M, Kaji M, Yamamoto S, Nakai A, Koizumi A, Hokezu Y, Nagamatsu K, Mikami H, Kitajima I, Takada G. *Five novel SLC7A7 variants and y+L gene-expression pattern in cultured lymphoblasts from Japanese patients with lysinuric protein intolerance*.Hum Mutat. 2002; Nov;20(5):375-81.

Smith DW, Scriver CR, Tenenhouse HS, Simell O. *Lysinuric protein intolerance mutation is expressed in the plasma membrane of cultured skin fibroblasts.*Proc Natl Acad Sci U S A. 1987; Nov;84(21):7711-5.

Suga K, Katagiri K, Kinashi T, Harazaki M, Iizuka T, Hattori M, Minato N. *CD98 induces LFA-1-mediated cell adhesion in lymphoid cells via activation of Rap1.*FEBS Lett. 2001

Tan W, Gou DM, Tai E, Zhao YZ, Chow LM. *Functional reconstitution of purified chloroquine resistance membrane transporter expressed in yeast*. Arch Biochem Biophys. 2006 ; Aug 15;452(2):119-28.

Tao X, Avalos J.L, Chen J, MacKinnon R. *Crystal structure of the eukaryotic strong inward-rectifier K+ channel Kir2.2 at 3.1 A resolution*. Science 2009

Tao X, Lee A, Limapichat W, Dougherty D.A, MacKinnon R. *A gating charge transfer center in voltage sensors.* Science 2010

Tate SS, Yan N, Udenfriend S. *Expression cloning of a Na(+)-independent neutral amino acid transporter from rat kidney.* Proc Natl Acad Sci U S A. 1992; Jan 1;89(1):1-5.

Teixeira S, Di Grandi S, Kühn LC. *Primary structure of the human 4F2 antigen heavy chain predicts a transmembrane protein with a cytoplasmic NH2 terminus.* J Biol Chem. 1987; Jul 15;262(20):9574-80.

Theis S, Knutter I, Hartrodt B, Brandsch M, Kottra G, Neubert K, Daniel H. *Synthesis and characterization of high affinity inhibitors of the H+/peptide transporter PEPT2.* J Biol Chem. 2002 ; Mar 1;277(9):7287-92

Toole BP. Emmprin (CD147), a cell surface regulator of matrix metalloproteinase production and function. Curr Top Dev Biol. 2003;54:371-89

Tornroth-Horsefield S, Wang Y, Hedfalk K, Johanson U, Karlsson M, Tajkhorshid E, Neutze R, Kjellbom P. *Structural mechanism of plant aquaporin gating*. Nature2006

Torrents D, Estévez R, Pineda M, Fernández E, Lloberas J, Shi YB, Zorzano A, Palacín M. I*dentification and characterization of a membrane protein (y+L amino acid transporter-1) that associates with 4F2hc to encode the amino acid transport activity y+L. A candidate gene for lysinuric protein intolerance.*J Biol Chem. 1998; Dec 4;273(49):32437-45

Torrents D, Mykkänen J, Pineda M, Feliubadaló L, Estévez R, de Cid R, Sanjurjo P, Zorzano A, Nunes V, Huoponen K, Reinikainen A, Simell O, Savontaus ML, Aula P, Palacín M. Identification of SLC7A7, encoding y+LAT-1, as the lysinuric protein intolerance gene.Nat Genet. 1999 Mar;21(3):293-6.

Tsumura H, Suzuki N, Saito H, Kawano M, Otake S, Kozuka Y, Komada H, Tsurudome M, Ito Y. *The targeted disruption of the CD98 gene results in embryonic lethality.* Biochem Biophys Res Commun. 2003; Sep 5;308(4):847-51.

Turnay J, Fort J, Olmo N, Santiago-Gómez A, Palacín M, Lizarbe MA. Structural characterization and unfolding mechanism of human 4F2hc ectodomain. Biochim Biophys Acta. 2011 May;1814(5):536-44. Epub 2011 Feb 23.

Van Winkle LJ, Campione AL, Gorman JM. Na+-independent transport of basic and zwitterionic amino acids in mouse blastocysts by a shared system and by processes which distinguish between these substrates. J Biol Chem. 1988 Mar 5;263(7):3150-63.

Verrey F, Closs EI, Wagner CA, Palacin M, Endou H, Kanai Y. *CATs and HATs: the SLC7 family of amino acid transporters*.Pflugers Arch. 2004; Feb;447(5):532-42.

Verrey F, Meier C, Rossier G, Kühn LC. *Glycoprotein-associated amino acid*

exchangers: broadening the range of transport specificity. Pflugers Arch. 2000; Aug;440(4):503-12.

Wagner CA, Lang F, Bröer S. *Function and structure of heterodimeric amino acid transporters*. Am J Physiol Cell Physiol. 2001; Oct;281(4):C1077-93.

Wells RG, Hediger MA. *Cloning of a rat kidney cDNA that stimulates dibasic and neutral amino acid transport and has sequence similarity to glucosidases.*Proc Natl Acad Sci U S A. 1992; Jun 15;89(12):5596-600.

Wells RG, Lee WS, Kanai Y, Leiden JM, Hediger MA.*The 4F2 antigen heavy chain induces uptake of neutral and dibasic amino acids in Xenopus oocytes.*J Biol Chem. 1992 ; Aug 5;267(22):15285-8

Wiener MC. *A pedestrian guide to membrane protein crystallization*.Methods. 2004 Nov;34(3):364-72.

Wood M.J, Sampoli-Benitez B.A, Komives E.A. *Solution structure of the smallest cofactor-active fragment of thrombomodulin.* Nat.Struct.Biol. 2000

Xu D, Hemler ME. *Metabolic activation-related CD147-CD98 complex*. Mol Cell Proteomics. 2005

Xu D, Hemler ME. *Metabolic activation-related CD147-CD98 complex*. Mol Cell Proteomics. 2005; Aug;4(8):1061-71

Yamamoto A, Akanuma S, Tachikawa M, Hosoya K. *Involvement of LAT1 and LAT2 in the high- and low-affinity transport of L-leucine in human retinal pigment epithelial cells (ARPE-19 cells).* J Pharm Sci. 2010; May;99(5):2475-82.

Yamashita A, Singh SK, Kawate T, Jin Y, Gouaux E. *Crystal structure of a bacterial homologue of Na+/Cl--dependent neurotransmitter transporters.*Nature. 2005 ; Sep 8;437(7056):215-23

Yanagida O, Kanai Y, Chairoungdua A, Kim DK, Segawa H, Nii T, Cha SH, Matsuo H, Fukushima J, Fukasawa Y, Tani Y, Taketani Y, Uchino H, Kim JY, Inatomi J, Okayasu I, Miyamoto K, Takeda E, Goya T, Endou H. Human L-type amino acid transporter 1 (LAT1): characterization of function and expression in tumor cell lines. Biochim Biophys Acta. 2001 Oct 1;1514(2):291-302.

Yang G, Liu T, Peng W, Sun X, Zhang H, Wu C, Shen D. *Expression and localization of recombinant human EDG-1 receptors in Pichia pastoris.* Biotechnol Lett. 2006; Oct;28(19):1581-6.

Resumen

Introducción

Los transportadores heteroméricos de aminoácidos (HATs) están compuestos por una subunidad pesada (rBAT o 4F2hc), y una subunidad ligera ($b^{0,+}$ AT; asc1, LAT1; LAT2; y^+LAT1; y^+LAT2 y xCT), unidas ambas mediante un puente disulfuro (Chillarón *et al.* 2001). rBAT y 4F2hc son glicoproteínas de membrana de tipo II (N-terminal citoplasmático). Ambas presentan un único segmento transmembrana, una cola N-terminal intracelular y un dominio extracelular (ectodominio). Hasta lo que se sabe, la función de las subunidades pesadas es facilitar el tránsito de la subunidad ligera a la membrana plasmática. Las subunidades ligeras son proteínas politópicas no glicosiladas, con 12 segmentos transmembrana, y los extremos N- y C- terminal intracelulares. La subunidad ligera es la subunidad catalíticamente activa del holotransportador, definiendo el tipo de sistema de transporte para cada heterodímero (Reig *et al.* 2002). Así, es esta subunidad la que confiere al heterodímero especificidad respecto al sistema de transporte: LAT1 y LAT2 para el sistema L; y^+LAT1 y y^+LAT2 para el sistema y^+L; asc1 para el sistema asc; xCT para el sistema Xc-; y $b^{0,+}$AT para el sistema $b^{0,+}$ (Chillarón *et al.* 2001).

Junto al Dr.Rosell, la sobreexpresión de todas estas proteínas de humano, se llevó a cabo usando de sistema de expresión huésped la levadura metilotrófica *Pichia pastoris*, basado en un trabajo de Mackinnon y colaboradores (Long *et al*. 2005) donde mostraba la cristalización de un canal de potasio de mamífero. En el trabajo

quedaba patente la utilidad y las ventajas de esta levadura para la expresión heteróloga de proteínas de membrana eucariota. Así, se decidió expresar las dos subunidades pesadas de los transportadores heteroméricos de aminoácidos (4F2 y rBAT), las diferentes subunidades ligeras (asc1, LAT1, LAT2, y^+LAT1, y^+LAT2, xCT y $b^{0,+}$AT), y los diferentes heterodímeros (4F2hc/asc1, 4F2hc/LAT1, 4F2hc/LAT2 y 4F2/xCT) de humano.

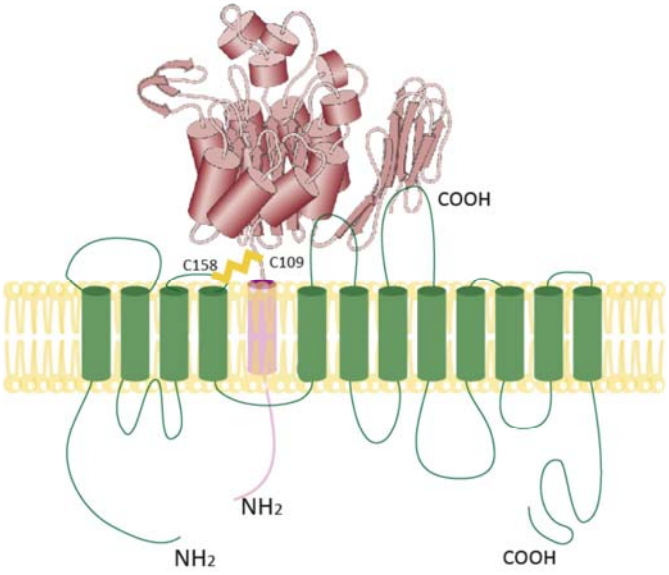

Figura 1. Esquema de un transportador de aminoácidos heteromérico de membrana (HAT). La subunidad pesada (rosa) y la subunidad ligera (verde) se unen por un puente disulfuro (amarillo) (cisteína 158 en la subunidad ligera xCT de humano y la cisteína 109 en la subunidad pesada 4F2hc de humano) (Gasol *et al*. 2004)

El objetivo final era conseguir suficiente proteína a un elevado nivel de pureza para intentar su cristalización 3D y/o 2D y comprobar su función mediante ensayos de transporte.

Las diferentes subunidades ligeras así como las dos subunidades pesadas fueron clonadas en el vector de expresión pPICZ (Invitrogen). Para conseguir la expresión en *Pichia* de los diferentes heterodímeros se clonaron en un mismo vector de expresión, rBAT junto con $b^{0,+}$AT; y 4F2hc con cada una de sus subunidades ligeras. Para facilitar la purificación de las diferentes proteínas, se introdujo por PCR en el extremo N-terminal de las subunidades pesadas un clúster de 10 histidinas seguido de una diana para la proteasa Factor Xa. En el extremo N-terminal de las subunidades ligeras en cambio, se añadió mediante PCR el StrepTagII (tag comercial de IBA) seguido también de una diana para el Factor Xa.

Se transformó la cepa de *Pichia pastoris* KM71H con los diferentes constructos mediante electroporación y se realizaron los primeros ensayos de expresión a pequeña escala, utilizando 6-8 transformantes por constructo, y se seleccionaron aquellos clones que ofrecían unos mejores niveles de expresión. Como resultado se obtuvo la expresión en *Pichia pastoris* de 4F2hc y rBAT para las subunidades pesadas, y+LAT2, LAT2 para las subunidades ligeras y 4F2hc/LAT2 para los heterodímeros en una concentración suficiente para continuar con la experimentación. Los otros candidatos, aunque en su mayoría se expresaban no lo hicieron en suficiente cantidad.

4F2hc es una glicoproteína con 4 posibles dianas de glicosilación. Las glicosilaciones confieren heterogeneidad a la proteína, dificultando así su cristalización. Al comprobar que tanto 4F2hc como alguno de sus heterodímeros se expresaban en *Pichia*, las dianas de glicosilación fueron eliminadas mediante mutagénesis dirigida. Estos mutantes se expresaron a muy buenos niveles. 4F2hc se purificó y se mantuvo estable con éxito (analizado por gel filtración) pero al no ser la subunidad catalítica del transportador su estudió se detuvo en este punto.

Así se procedió a la extracción de las subunidades ligeras y del heterodímero 4F2hc/LAT2 de la membrana celular y para ello se optimizó un proceso de solubilización. La mejor condición fue Tris 20 mM, NaCl 150 mM, glicerol 10%, DDM 2 %, pH 8, a 4ºC durante 1 hora. De todos los candidatos solo se solubilizaron en suficiente cantidad la subunidad ligera LAT2 y el heterodímero 4F2hc/LAT2.

Resultados

Subunidad ligera LAT2

Con el objetivo de obtener la mayor cantidad de proteína posible se realizó la expresión de LAT2 mediante fermentador. Para ello se estableció una colaboración con el "Grupo de biotecnología de levaduras e ingeniería de procesos" dirigido por el Dr. Francisco Valero de la Universidad Autónoma de Barcelona. Como resultado, y aunque la proteína se expresaba en igual concentración aún después de varias optimizaciones, se disponía de un volumen

mucho mayor. La subunidad ligera LAT2, fue purificada con éxito usando su tag comercial (streptagII, de IBA), sin embargo al ser analizada mediante gel filtración mostró un claro perfil de agregación, siendo desestimada la posibilidad de continuar con su cristalización.

Heterodímero 4F2hc/LAT2

También se consiguió optimizar la purificación del heterodímero 4F2hc/LAT2 y llevarla a cabo con éxito, esta proteína resultó mantenerse estable después del análisis por gel filtración. Así el heterodímero era notablemente más estable que la subunidad ligera sola, lo cual nos llevó a hacer una importante afirmación.

Las subunidades catalíticas de los transportadores de aminoácidos humanos necesitan de su subunidad pesada para aumentar su estabilidad, actuando así la subunidad pesada como una chaperona en el caso de 4F2hc.

Esta afirmación contrastaba con los resultados de la Dra. Bartoccioni en nuestro mismo laboratorio (Bartoccioni *et al*. 2008). En sus estudios de pulso y caza con el heterodímero rBAT/b^{0+}AT expresado en oocitos de *Xenopus laevis,* encontró justo el caso contrario. rBAT, la subunidad pesada, no era estable si no se encontraba en unida a su acompañante, la subunidad ligera b^{0+}AT, siendo esta vez la subunidad ligera la que actuaba de chaperona. Otra importante cuestión deriva de esta afirmación, si 4F2hc actúa de chaperona aumentando la estabilidad de la subunidad ligera, podría actuar también como catalizador, aumentando la funcionalidad del transportador. O en otras palabras, podría ser

que la subunidad ligera LAT2 fuera funcionalmente más eficiente acompañado de su subunidad pesada, 4F2hc. Para comprobarlo se llevaron a cabo varios estudios de función.

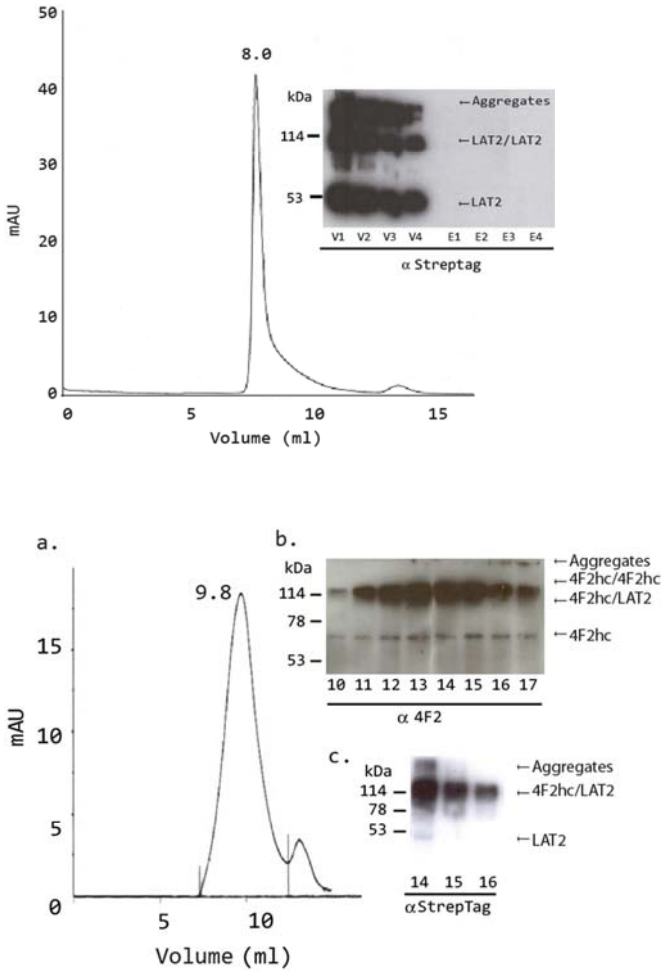

Figura 2. Cromatogramas de la purificaión por exclusión de la subunidad ligera LAT2 (arriba) y del heterodímero 4F2hc/LAT2 (abajo). Se observa claramente como el perfil de la subunidad ligera sola muestra una clara tendencia a agregar mientras que el heterodímero continua soluble.

Estudios de función con el heterodímero humano 4F2hc/LAT2

Se comprobó, en primer lugar, que el heterodímero 4F2hc/LAT2 era funcional en la membrana de la misma *P.pastoris*. Tanto el heterodímero como la subunidad ligera en estado monomérico (LAT2) resultaron ser funcionales, significando un correcto plegamiento de ambas a nivel de expresión. A partir de aquí se optimizaron los experimentos de funcionalidad siendo las condiciones finales de tampón: 150 mM cloruro de colina, 10 mM Tris-HEPES, pH 7.4, 1mM MgCl2 y 1mM CaCl2, 0,5 μCi de L-aminoácido marcado radioactivamente con tritio (L-Leucina) y varias concentraciones (en el rango de μM) de L-aminoácido no marcado. Se calculó la constante de afinidad por sustrato (KM) por el ajuste de Eadie-Hofftee, y se comprobó que no variaba, siendo la KM de la subunidad ligera en estado monomérico y la KM del heterodímero muy parecidas (~150 μM). Por lo tanto concluimos que:

la presencia de la subunidad pesada 4F2hc no afecta directamente la funcionalidad de transporte llevada a cabo por la subunidad catalítica LAT2.

En todos los experimentos, el control fue la proteína 4F2hc expresada como monómero en *P.pastoris*.

Estudios estructurales

Para llevar a cabo el estudio estructural y dada la dificultad para mantener el heterodímero 4F2hc/LAT2 estable durante largo tiempo, se decidió llevar acabo la técnica de Single particle

negative stainning (SP-NS), en el laboratorio del Dr. Fotiadis en la universidad de Berna (Suiza). La técnica de modelado 3D a partir de una tinción negativa de "single particle" en microscopía electrónica es relativamente nueva y se ha impuesto para proteínas de membrana de mamífero, ya que permite análisis estructurales con relativamente poca concentración y cantidad de proteína. El mayor problema de esta técnica es la baja resolución que da, ya que oscila entre 16 y 25 amstrongs, resolución a la cual no es posible ver las hélices alfa ni las estructuras beta de las proteínas. Una vez establecida la colaboración y ya en el laboratorio del Dr. Fotiadis se optimizó de nuevo la purificación del heterodímero, ya que se detectó que después de la segunda purificación, el puente disulfuro tendía a romperse, dejando las dos subunidades en estado monomérico y dando heterogeneidad a la muestra. Este problema se solventó parcialmente asumiendo la presencia de una disulfuro isomerasa y añadiendo un competidor, el glutatión, que también posee un puente disulfuro, a una concentración optimizada de 2 mM. Esto permitió llevar a cabo los experimentos de single particle. El heterodímero puro, se inmovilizó en rejillas para microscopía electrónica a una concentración de 2 μg/ml. Se aplicó entonces una tinción negativa de formiato de uranilo al 0,75% (optimizado a dos gotas durante 1 segundo, lavado con agua) y seguidamente se obtuvieron las imágenes por microscopía electrónica de transmisión (TEM). Gracias a las proyecciones de las diferentes orientaciones que 4F2hc/LAT2 tomó en las rejillas se calculó una serie de

orientaciones mediante un software especializado creando así una librería de proteínas separadas. El número mínimo de imágenes que se necesitaron para llegar a este punto fue de 11000 imágenes, no presentando variaciones ya desde las 6000 imágenes, lo cual demuestra una homogeneidad y una alta calidad de la muestra. La técnica de single particle y tinción negativa solo es posible con una muestra robusta que no presenta variaciones ni un alto background. Gracias a esa librería de orientaciones se hizo la reconstrucción 3D de esta proteína. La reconstrucción 3D, de 19 amstrongs de resolución, mostró la orientación de la subunidad pesada respecto a la ligera, además de permitir la superposición del cristal 3D del ectodomínio de 4F2hc. (Fort *et al*. 2007).

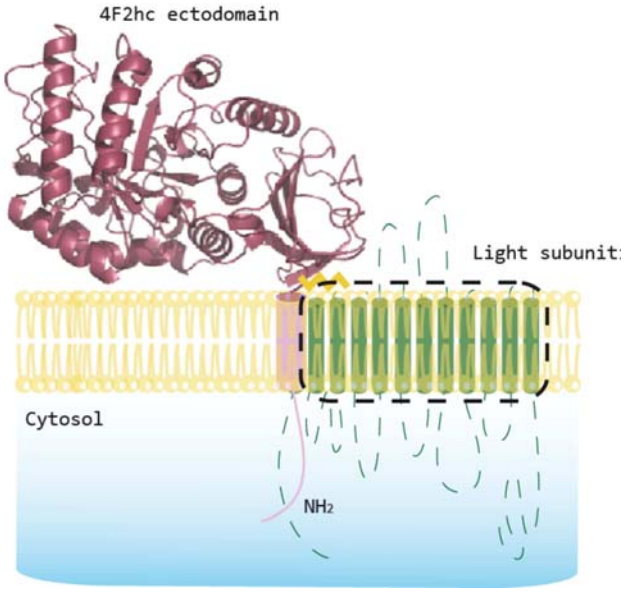

Figura 3. Modelo propuesto del heterodímero 4F2hc/LAT2 a partir de la estructura atómica del homodímero del ectodominio humano 4F2hc/4F2hc (Fort *et al*. 2007)

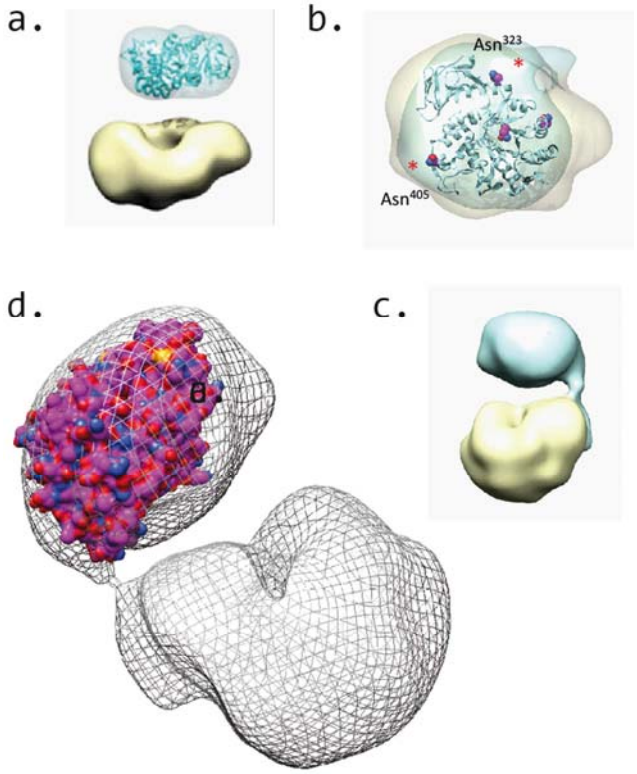

Figura 4. Modelo propuesto en el presente estudio del heterodímero 4F2hc/LAT2 a partir de evidencias mostradas por microscopía electrónica y tinción negativa.

Discusión

Como conclusión se observó que la subunidad pesada se sitúa encima de su subunidad ligera LAT2 y no como se había supuesto a un lado de la misma y en contacto con la membrana celular. En cuanto a las medidas, la subunidad pesada coincide con el cristal 3D ya existente pudiendo encajarla con bastante precisión, siempre asumiendo la presencia del segmento transmembrana no existente en el cristal 3D del ectodominio. Por el contrario, y

posiblemente debido a la gran cantidad de detergente existente en el modelo 3D, la subunidad ligera no se pudo encajar con el cristal de AdiC (Kowalczyk *et al.* 2011), un homólogo procariota de la subfamilia APA (también de la familia APC) recientemente cristalizado (Gao *et al.* 2009; Fang *et al*. 2009; Kowalczyk *et al.* 2011).

El modelo que se presenta en este trabajo explicaría estudios de interacción con integrinas (Feral *et al*. 2005; Feral *et al.* 2007) y otras proteínas de membranas involucradas en crecimiento celular, como ICAMI y/o sobreexpresadas en tumores, como CD147 (Liu *et al.* 2007; Xu *et al.* 2005 respectivamente). A parte la subunidad pesada 4F2hc podría modular la actividad de transporte de LAT2 al encontrarse en unida a otras proteínas de membrana formando un supercomplejo proteico (Liu *et al.* 2003).

Nuevas evidencias

Recientemente el modelo de heterodímero 4F2hc/LAT2 en el cual la subunidad pesada se sitúa justo encima de la ligera ha sido corroborado por cross-linking por la Srta. Elena Álvarez en nuestro laboratorio. Siendo esto un hecho, nos permitimos imaginar la gran probabilidad que tendría algunos loops externos de la subunidad ligera (LAT2) de interaccionar con la subunidad pesada haciendo así la asociación entre los dos componentes del holotransportador mucho más estrecha y colaborativa. Gracias a la estructura subatómica de AdiC, sabemos que el loop externo 3 es uno de los más largos y con más libertad en el espacio extracelular

de la membrana plasmática. En el caso de los heterodímeros es uno de los candidatos inmediatos a interaccionar con 4F2hc, la subunidad pesada. El loop externo 4 también tiene una longitud considerable, sin embargo se transforma de suelo del bolsillo de unión a sustrato en la conformación "inward-facing" del transportador, dejando con menos grados de libertad al susodicho loop externo.

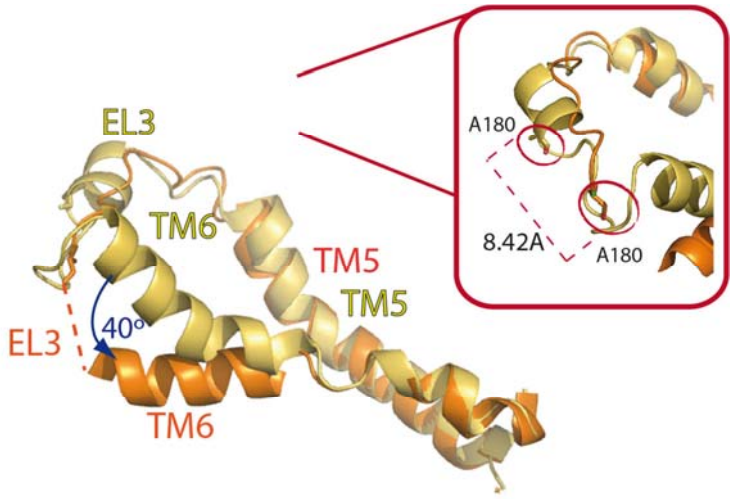

Figura 5. Representación de la hélice transmembrana 6 en el proceso de paso de conformación "open" (naranja) a conformación "closed" (amarillo). Se observa como el "loop" externo 3 se somete a un estrés extra en este paso causado por el gran giro de 40° que realiza el transmembrana 6. La Alanina 180 (A180) se mueve 8,40 Å en este proceso, como se indica en el cuadro de la izquierda.

Esto no evitaría la posible unión, dando así más posibilidades de que la subunidad ligera se viera regulada por movimientos de los

loops externos enganchados a la subunidad pesada. Haremos hincapié en que 4F2hc es una proteína multifuncional que parece unirse a proteínas implicadas en crecimiento celular y cáncer, hechos que necesitan un suplemento extra de aminoácidos.

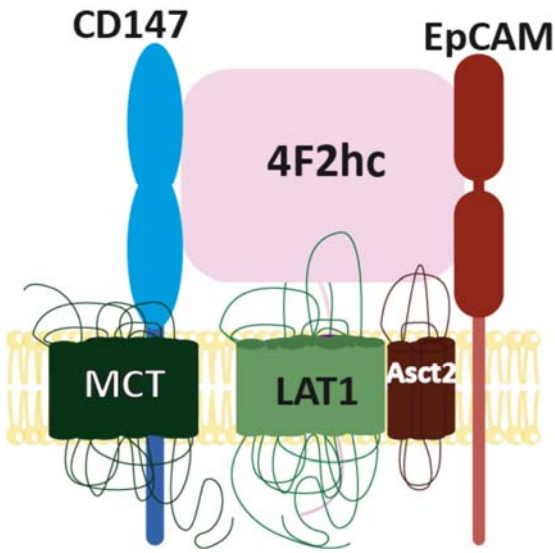

Figura 6. Esquema del supercomplejo proteico propuesto por Xu y colaboradores. Ellos sugieren la asociación entre CD147 y 4F2hc (Xu *et al*. 2005)